Earth-Science Reviews 182 (2018) 102–140

Contents lists available at ScienceDirect

Earth-Science Reviews

journal homepage: www.elsevier.com/locate/earscirev

Juxtaposed sequence stratigraphy, temporal-spatial variations of sedimentation and development of modern-forming forearc Lichi Mélange in North Luzon Trough forearc basin onshore and offshore eastern Taiwan: An overview

Chi-Yue Huang[a,b,*], Wen-Huang Chen[c], Ming-Huei Wang[d], Chiou-Ting Lin[b,e], Shengxiong Yang[f], Xuejie Li[f], Mengming Yu[c], XiXi Zhao[a], Kenn-Ming Yang[b], Char-Shine Liu[g], Yu-Huan Hsieh[g], Ron Harris[h]

[a] School of Ocean and Earth Science, Tongji University, Shanghai 200092, China
[b] Department of Earth Sciences, National Cheng Kung University, Tainan 701, Taiwan
[c] Key Laboratory of Marginal Sea Geology, Guangzhou Institute of Geochemistry, Chinese Academy of Sciences, Guangzhou 510640, China
[d] Exploration and Development Research Institute, CPC Corporation, Miaoli 36042, Taiwan
[e] Center of Deep Sea Research, Institute of Oceanography, Chinese Academy of Sciences, Qingdao 266071, China
[f] Guangzhou Marine Geological Survey, Guangzhou 51076, China
[g] Institute of Oceanography, National Taiwan University, Taipei 10617, Taiwan
[h] Department of Geological Sciences, Brigham Young University, Provo, UT, USA

ARTICLE INFO

Keywords:
Juxtaposed forearc sequences
Bivergent thrusting
syn-Sedimentation deformation
Oblique collision
Lichi Mélange

ABSTRACT

The South China Sea oceanic lithosphere has been subducting eastward beneath the Huatung Basin/Philippine Sea Plate since the Early Miocene (~18 Ma). The subduction is followed by the oblique collision between the Luzon arc and the subducting Eurasian plate from 6.5 Ma. The North Luzon Trough forearc strata and the Luzon arc are then obducted northwestward as the Coastal Range, eastern Taiwan, in the last 1 Ma. The collision propagates southward and is presently active in the region offshore SE Taiwan. Integrating seismic surveys offshore and a detailed forearc stratigraphy study onshore the Coastal Range, this paper overviews the characteristics of forearc deformation, dynamic sequence stratigraphy, temporal-spatial variations of forearc sedimentation and stratigraphic correlation onshore and offshore forearc sequences in response to the oblique convergent tectonics north of 20°N. Combining onshore and offshore forearc geology together allows us to reconstruct a structural evolution of the North Luzon Trough forearc basin from subduction through collision to obduction, and to discuss the mechanism and processes responsible for developments of the modern-forming forearc Lichi Mélange during the active Taiwan orogeny.

Seismic surveys offshore show that forearc deformation in the subduction zone is primarily caused by increase of rear prism slope and west-vergent thrusting of forearc strata along the prism top since the early forearc sedimentation. East-vergent backthrusting occurs during the late forearc sedimentation and propagates arcward when the volcanic arc collides with the accretionary prism in the collision zone. Bivergent thrusting leads to a development of the forearc Huatung Ridge popup as a bathymetric high which further controls the sedimentation of the younger forearc sequence in the collision zone. In response to the *syn*-sedimentation deformation, forearc depocenter shifts progressively eastward. Forearc stratigraphy thus changes from two mega-sequences bounded by an unconformity in the subduction zone to three mega-sequences juxtaposed from west to east unconformably in the collision zone. As a consequence, the forearc deformation and stratigraphy in the oblique collision zone off SE Taiwan show a characteristic temporal-spatial pattern that the lowest mega-sequence with the most intensive deformation occurs restrictedly in the west, whiles the middle and the upper mega-sequences with mild deformation crop out in the center and the eastern part of the forearc basin, respectively.

Detailed biostratigraphy study using planktonic foraminifera and calcareous nannoplanktons indicates that the forearc strata onshore the Coastal Range are also composed of three sequences (lower unit S-1: 6.5–5.8 Ma; middle unit S-2: 5.8–3.0 Ma; and upper unit S-3: < 3.0–1 Ma). They were previously mapped as lithostratigraphy

* Corresponding author at: School of Ocean and Earth Science, Tongji University, Shanghai 200092, China.
E-mail address: huangcy@mail.ncku.eu.tw (C.-Y. Huang).

https://doi.org/10.1016/j.earscirev.2018.01.015
Received 7 March 2017; Received in revised form 31 December 2017; Accepted 22 January 2018
Available online 14 May 2018
0012-8252/

units of the Lichi Mélange (6.5–3.0 Ma) in the west and the coherent flysch sequences of the Fanshuliao Formation (5.8–3.0 Ma) and the Paliwan Formation (< 3.0–1 Ma) in the east. However, the young coherent forearc sequences in the east thrust westward ubiquitously over the old and highly deformed Lichi Mélange in the west along the listric east-dipping Tuluanshan fault during the obduction. Detailed biostratigraphy study reveals that the lower sequence unit S-1 exposes restrictedly in the Lichi Mélange west of the Tuluanshan fault, whereas the middle sequence unit S-2 are either mapped as part of the Lichi Mélange or the coherent Fanshuliao Formation in both sides of the Tuluanshan fault, respectively. The upper sequence unit S-3 exposes exclusively east of middle sequence unit S-2 in the eastern Coastal Range. Stratigraphy and sedimentology study also reveals a temporal-spatial sedimentation variation of the upper sequence unit S-3 owing to deformation of the sequence units S-1 and S-2 together as a Pliocene Forearc Ridge at ~3 Ma, a scenario analog to development of the modern Huatung Ridge at ~1 Ma in active collision zone offshore. Temporal-spatial pattern of forearc sequences onshore the Coastal Range suggests that these three sequence units are juxtaposed from west to east and are bounded by two unconformities analog to what occur today in the collision zone offshore SE Taiwan. The characteristic deformation and an eastward-youngling trend of strata distribution onshore the Coastal Range all indicate Syn-sedimentation deformation during the oblique collision in 6.5–1 Ma. Furthermore, along the N-S orogenic strike, events of the forearc sedimentation and bivergent thrusting occur earlier onshore the obduction zone in the north than the modern collision zone offshore in the south. Across the orogenic strike forearc strata get older and deformation gets intensive from east to west onshore the Coastal Range, a scenario analog to what observed in the oblique convergent region offshore SE Taiwan.

A structure reconstruction reveals that the North Luzon Trough forearc strata have experienced multiple stages of thrust deformation from subduction through collision to obduction. These deformations account for the mechanism and processes to develop the modern-forming highly sheared SSZ-bearing forearc Lichi Mélange tectonically in the western Coastal Range during the last 1 Ma.

1. Introduction

In worldwide oblique plate convergent orogens like Sumatra-Java and Lesser Antilles or the oblique collision orogens like the continent-continent collision in Tibet and the arc-continent collisions in Timor and Taiwan, strain partitioning commonly results in developments of the bivergent thrusting to accommodate a space shorting (Reed et al., 1986, 1992; Silver and Reed, 1988; Torrini and Speed, 1989; Harris, 1991, 2011; Willet et al., 1993; Beaumont et al., 1996; Susilohadi et al., 2005; Wang et al., 2008; Brink et al., 2009; Sarkarinejad and Alizadeh, 2009). In these oblique convergent regions, bivergent thrusting includes trench-ward thrusting in the accretionary prism and arcward backthrusting over the arc backstop or in a backarc basin. Despite this well-known bivergent thrusting in the accretionary prism - backarc basin area, bivergent thrusting structures are rarely documented in ancient and modern forearc basins. Consequently, details of deformation processes of bivergent thrusting structure and the role of sedimentation of bivergent thrusting in forearc basin are hitherto unknown. Neither modern marine investigations offshore nor stratigraphic records onshore oblique subduction-collision belts have ever documented that bivergent thrusting would cause *syn*-sedimentation deformation to develop a juxtaposed forearc stratigraphy and to cause temporal-spatial variations of forearc sedimentation. For example, in the continent-continent collision of Tibet, Cretaceous-Eocene Xigaze forearc strata thrust southward over the Higher Himalaya accretionary prism and backthrust northward over the backstop of the Gangdese Arc (Wang et al., 2011). However, the sedimentation role of these bivergent structures in the Xigaze forearc basin during the suturing processes of subduction-collisional-obduction is generally unknown. In the Timor region, oblique subduction-collision along the Timor Trough leads to development of a southward thrusting in the accretionary prism and a northward backthrusting either in the forearc or backarc basin (Reed et al., 1986). Nevertheless, the details of forearc sedimentation in response to such a bivergent thrusting in the Timor region are ambiguous.

On the other hand, marine investigations in the modern arc-continent collision regions offshore show a similar tectonic role of bivergent thrusting to develop the Bobonaro Mélange in the Timor accretionary prism and the forearc Lichi Mélange in the Coastal Range, eastern Taiwan (Fig. 1; Harris et al., 1998; Chang et al., 2000; Huang et al., 2000, 2008; Harris and Huang, 2008; Huang, 2008). However, in the Timor oblique collision region forearc stratigraphy is poorly constrained and mostly has not been exposed yet onshore the Timor Island (Harris et al., 1998; Harris, 2011). Consequently, forearc stratigraphy and sedimentation features are not known in detail in the oblique subduction-collision Timor region. In contrast, Late Miocene-Pleistocene deep-sea forearc strata in the Taiwan oblique collision region are well exposed onshore the Coastal Range (Hsu, 1956, 1976) due to the obduction tectonics in the last 1 Ma (Huang et al., 2000). Geological characters of the Coastal Range are also well constrained by detailed studies on sedimentology, biostratigraphy and structure (Chang, 1967b, 1968, 1969; Chi et al., 1981; Huang and Yuan, 1994; Huang et al., 1995, 2000, 2006, 2008; Dorsey and Lundberg, 1988; Lin et al., 1999; Horng and Shea, 1996; Chang et al., 2000; Lin, YC, 2011b; Lin, CT, 2011a; Chen et al., 2015, 2017). Besides, due to a southward propagation of the oblique collision (Suppe, 1984), geodynamic processes operating today offshore SE Taiwan play as a modern analog for understanding what has happened prior to suturing the Coastal Range (Fig. 1; Huang et al., 1992, 1995, 2000; Chang et al., 2001). Therefore, the Coastal Range and its offshore extension provide the unique region to study the details of forearc deformation, dynamic stratigraphy and sedimentation in response to bivergent thrusting during the oblique convergent tectonics.

Three main tectonic processes, from south to north, of subduction, collision and obduction are operating simultaneously today in the Taiwan region (Figs. 1 and 2; Huang et al., 1997, 2000). South of 21°10′N, the Eurasian Continent-South China Sea oceanic lithosphere of the Eurasian Plate subducts eastward along the Manila Trench beneath the northwest-moving Huatung Basin/Philippine Sea Plate (Fig. 1; Tsai, 1986). In the Taiwan segment, the subduction starts from Late Early Miocene (~18 Ma, see Section 8.2) and develops, from west to east, the Hengchun Ridge accretionary prism, the North Luzon Trough forearc basin and the Lutao-Lanyu-Batan-Babuyuan volcanic island chain (from north to south) of the North Luzon Arc between Taiwan and Luzon Islands (Fig. 1; Huang et al., 1992, 1997; Liu et al., 1998). The Hengchun Ridge accretionary prism extends northward as the Hengchun Peninsula - Central Range onshore Central Taiwan, whereas the North

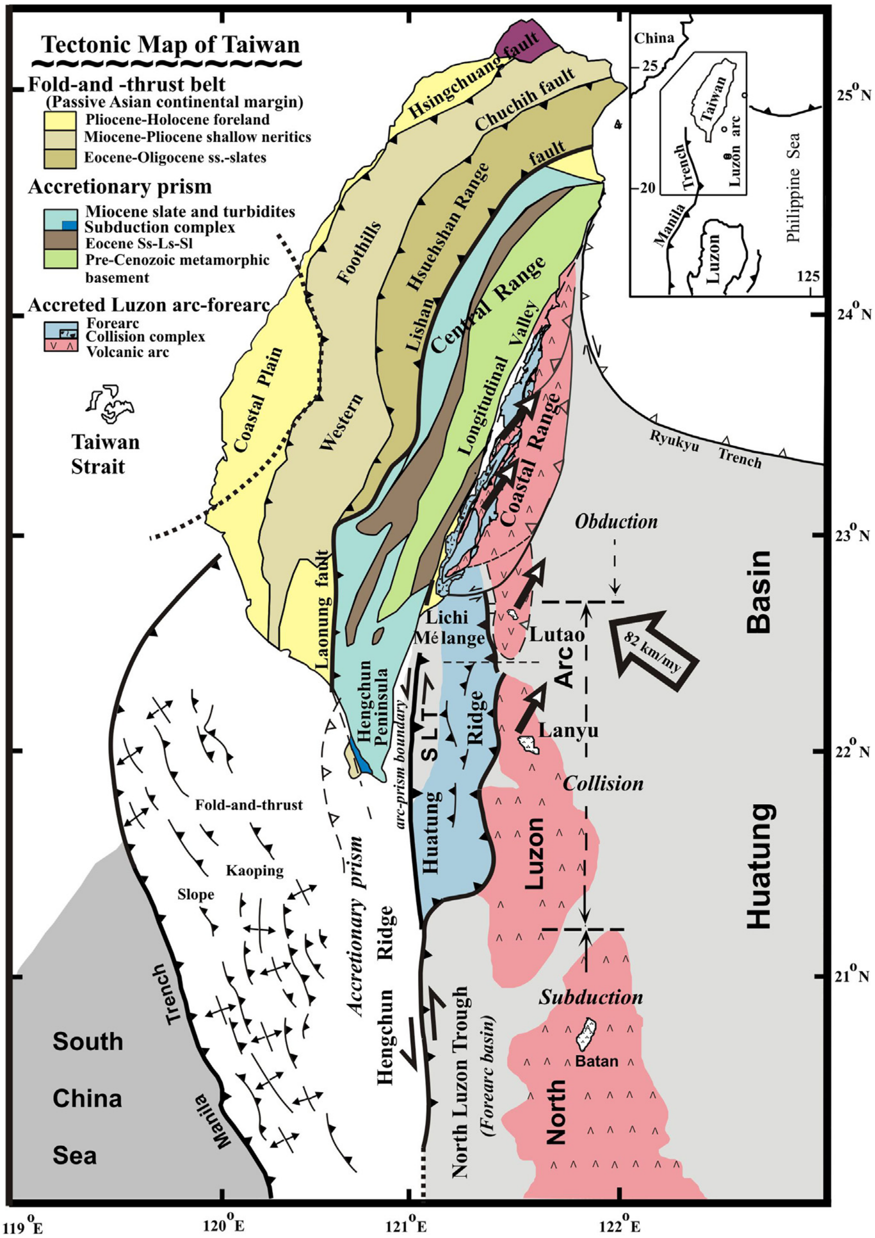

Fig. 1. Tectonic map of Taiwan showing bivergent thrusting to develop the forearc Huatung Ridge and tectonics of subduction, collision and obduction operating simultaneously in the Taiwan region (modified from Huang et al., 2000). Open arrows: clockwise rotation of the Luzon volcanic islands onshore and offshore eastern Taiwan (data compiled from Lee, 1991; Yang et al., 1983; Zhao et al., 2016); SLT: collisional suture basin of the Southern Longitudinal Trough.

Luzon Trough forearc basin and the North Luzon arc are obducted as the Coastal Range in eastern Taiwan (Fig. 1). Along the orogenic strike, the intra-oceanic subduction domain changes progressively northward to the oblique collision domain between 21°10′N and 24°N (Figs. 1 and 2; Huang et al., 1997). North of 21°10′N (or 21°20′N in Huang et al., 2000) the Luzon Arc on the NW-moving Huatung Basin/Philippine Sea Plate (81 mm/year in 305°; Yu et al., 1997) collides obliquely with the subducting Eurasian continent (060°). Multiple evidences show that the oblique collision started from ~6.5 Ma simultaneously with the last volcanism event at 6.6 Ma of the North Luzon Arc segment in eastern Taiwan (Lo et al., 1994) and exposures of the Hengchun Peninsula - Central Range accretionary prism above sea level (Huang et al., 2000). The exposed accretionary prism provides sediments transporting eastward into the North Luzon Trough forearc basin and westward into the foreland basin (Huang et al., 1997, 2000, 2006; Lin et al., 2003; Chen et al., 2017). On the basis of geophysical, geochemical features and thrusting vergence, the collisional domain can be further subdivided into an initial collision offshore (21°10′N–22°40′N) and an obduction (or advanced collision) onshore the Coastal Range (22°40′N–24°00′N; Fig. 1; Huang et al., 1997, 2000).

2. Coastal Range in eastern Taiwan

2.1. General geology and volcanic arc stratigraphy

The Coastal Range (Fig. 3; 15 km wide × 130 km long between 22°40′ and 24°00′N) in the obduction zone, eastern Taiwan, is primarily composed of volcanic arc and forearc strata (Figs. 4 and 5). The Coastal Range is thrusting westward over the Central Range accretionary prism along the Longitudinal Valley in the last 1 Ma (Fig. 3; Hsu, 1956, 1976). The Longitudinal Valley represents a collision suture and extends southward to the modern collision suture basin of the Southern Longitudinal Trough between the Hengchun Ridge-Central Range accretionary prism and the deformed forearc Huatung Ridge offshore (Fig. 1;

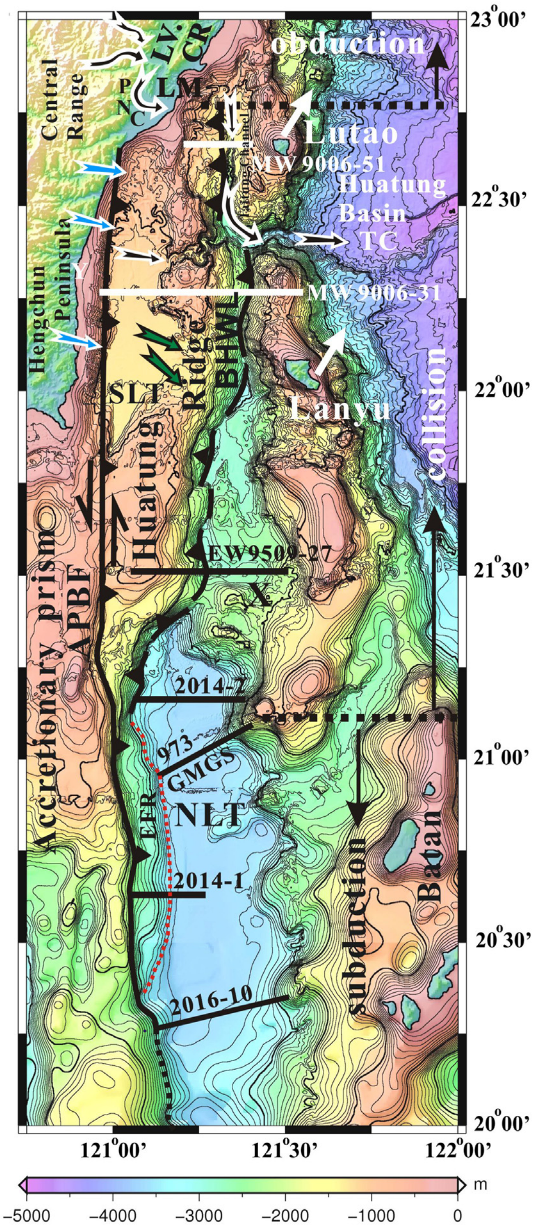

Fig. 2. Bathymetric map and transporting routes of modern sediments (mega-sequence unit M-C) into remnant forearc trough east of the Huatung Ridge, showing also locations of seven study seismic profiles in the oblique subduction-collision zones offshore SE Taiwan. Various colored arrows mark the different transporting routes of modern sediments from the Central Range into the North Luzon Trough forearc basin. White arrow: clockwise rotation of volcanic islands; BHWL: bathymetric high of the deformed Huatung Ridge west of Lanyu volcanic island; CR: Coastal Range onshore eastern Taiwan; EFR: East-dipping forearc ridge deformed by west-vergent thrusting in subduction zone; LV: Longitudinal Valley; LM: Lichi Mélange; NLT: North Luzon Trough forearc basin; PNC: Pinanta-Chi (River); SLT: collision suture basin of the Southern Longitudinal Trough; TC: Taitung Canyon; X: under-fill remnant forearc trough south of 'BHWL'; Y: topographic bend point of accretionary prism.

Huang, 1993; Huang et al., 1992, 1997, 2000).

Litho-stratigraphy of the Coastal Range is composed of Miocene-Pliocene volcanic arc basement of agglomerates (the Tuluanshan Formation) in the lower part overlain unconformably by Late Miocene-Pleistocene deep-sea flysch sequences in the upper part (Figs. 3, 4 and 5; Hsu, 1956). The Tuluanshan Formation (> 2 km thick) includes eruptive volcanics of agglomerates, tuffs and intrusive dikes. They are of andesitic compositions, representing the accreted North Luzon Arc.

Parts of the Tuluanshan Formation are capped by two independent fringing reefs. They differ from each other temporally and spatially (Fig. 3; the Kangkou Limestone 5.2 Ma in the north and the Tungho Limestone 2.9 Ma in the south; Chang, 1967b; Huang et al., 1988; Huang and Yuan, 1994; Huang et al., 1995). Various geological features, including continuity of volcanic ridge, Nd isotopic values (Chen et al., 1990), last volcanism ages (Lo et al., 1994) and temporal-spatial distributions of these two independent fringing reefs, reveal that two volcanic islands of the North Luzon arc (Chimei Volcanic Island in the north and the Chengkuangao Volcanic Island in the south; Fig. 4) were accreted onto the Coastal Range by westward thrusting during the obduction (Huang et al., 1995). Because of forearc deformation during the obduction, the volcanic Tuluanshan Formation exposes as two pairs of topographical ridges running in N-S to NE-SW directions throughout the Coastal Range (Fig. 3). The Yuehmeishan ridge - Takangshan ridge pair constitutes the Chimei Volcanic Island in the north, whereas the Liushihshihshan ridge - Chengkuangaoshan ridge pair gives to the Chengkuangao Volcanic Island in the south (Fig. 4). The majority of these two volcanic islands are still preserved offshore east off the Coastal Range (Fig. 1; Shyu and Chen, 1991).

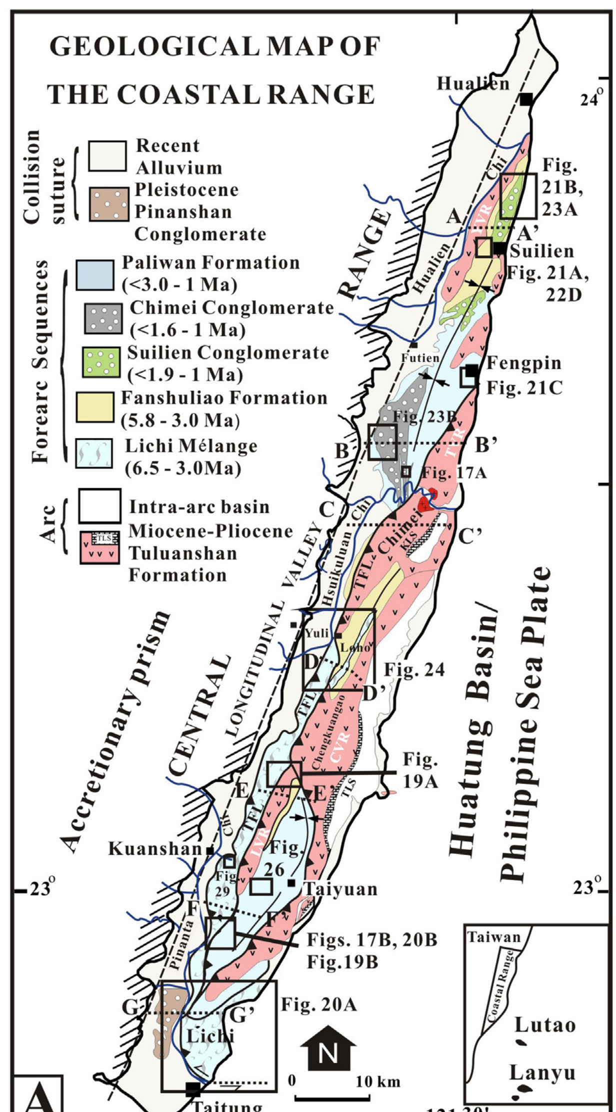

Fig. 3. (A) Geological map of the Coastal Range, eastern Taiwan (modified from Huang et al., 2000) showing also figure locations; (B) cross sections of the Coastal Range. LV: Longitudinal Valley; RFT: remnant forearc trough east of the Lichi Mélange; TFL: Tuluanshan fault (*s.l.*).

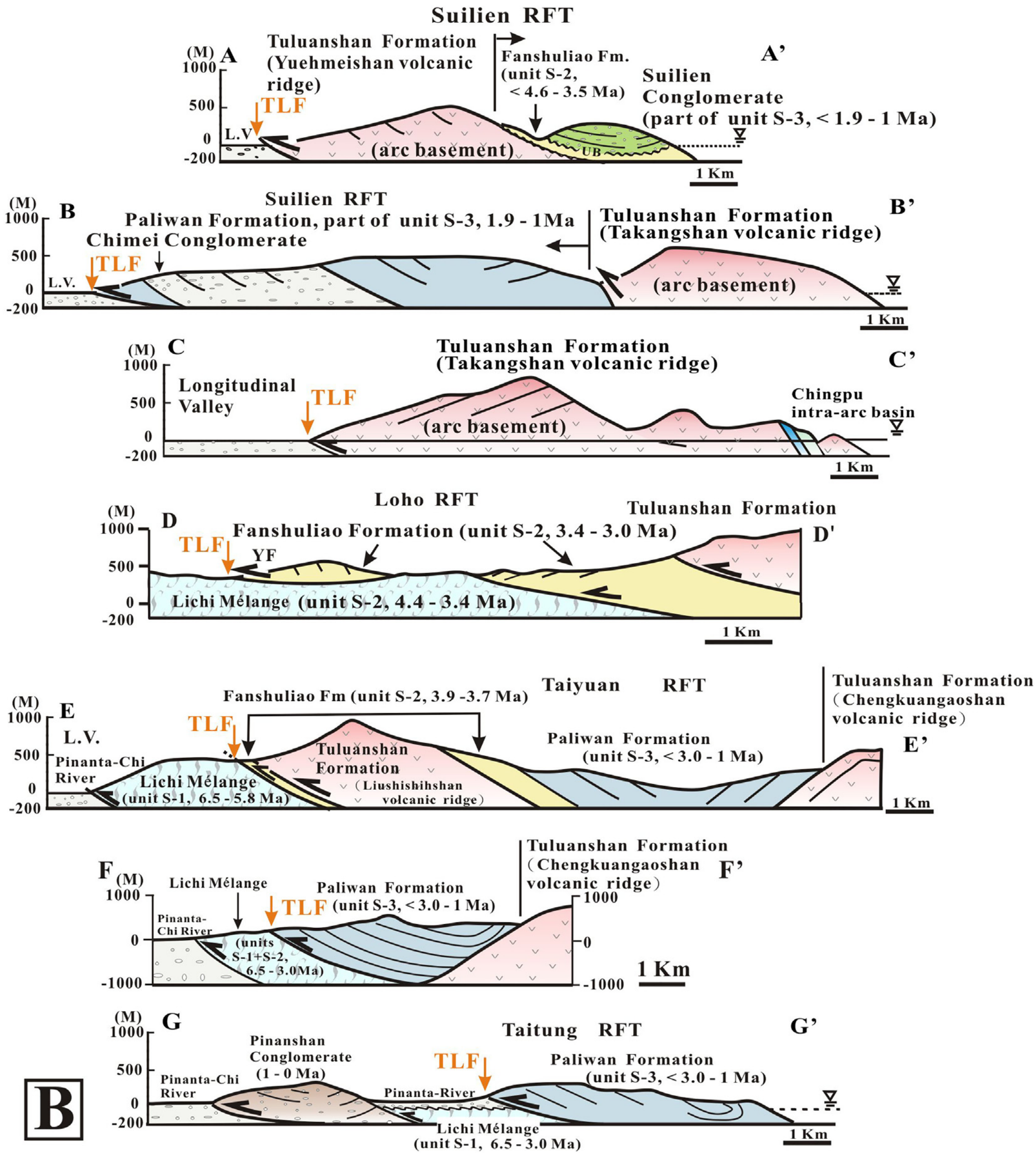

Fig. 3. (*continued*)

Shallow-marine Kangkou Limestone and Tungho Limestone caps unconformably on the Chimei and Chengkuangao volcanic island, respectively (Fig. 4). These shallow-marine reef limestones are, in turn, covered disconformably by coherent deep-sea flysch sequences (Fig. 5). The sequences record two independent tectonic subsidence events of the volcanic islands by pull-apart strike-slip faulting due to the oblique collision between 5.2 and 3.5 Ma in the north and between 2.9 Ma and < 1.8 Ma in the south (Huang, 1988; Huang et al., 1995). The arc-subsidence events lead to developments of the Chingpu intra-arc basin on the subsided Chimei Volcanic Island and the Chenkung intra-arc basin on the subsided Chengkuangao Volcanic Island (Fig. 4), a scenario similar to developments of modern intra-arc basins on the Lutao and Lanyu Volcanic Islands, respectively, in the modern oblique collision zone offshore SE Taiwan (Huang et al., 1995).

2.2. Previous study on forearc stratigraphy of the Coastal Range

In addition to the relatively thin deep-sea sediments (1–2 km thick) in two intra-arc basins on the subsided volcanic islands, Late Miocene-Pleistocene siliciclastic coherent flysch sequences (> 5 km thick) in the upper part of the Coastal Range are filled in the North Luzon Trough forearc basin between the Central Range accretionary prism in the west and the North Luzon arc in the east. Unlike two intra-arc basins are positioned east of main volcanic ridges on the subsided arc, the forearc basin is located west of the main volcanic ridges (Fig. 4). Forearc stratigraphy onshore the Coastal Range has been intensively studied in the last six decades (Hsu, 1956, 1976; Chang, 1967a, 1967b, 1968, 1969; Teng, 1979; Chi et al., 1981; Huang and Yuan, 1994; Huang et al., 1988, 1995; Horng and Shea, 1996; Chen et al., 2015, 2017). Most of these previous studies were primarily focused on biostratigraphy of planktonic foraminifera and/or calcareous nannofossils for age determination, whiles others studied the sediment provenance and depositional environment (Wang and Chen, 1966; Teng, 1979; Dorsey, 1988; Dorsey and Lundberg, 1988). Prior to 1995, these studies, however, considered the entire sedimentary sequences in the Coastal Range were deposited in a single, non-deformed North Luzon Trough forearc basin during their sedimentations. Besides, the Lichi Mélange in the western Coastal Range was even considered as a subduction complex in the accretionary prism (Teng and Wang, 1981), whereas the Longitudinal Valley was interpreted as the setting of the former Manila Trench (Tsai et al., 1981). In effect, neither dynamic forearc stratigraphy nor temporal-spatial variations of the North Luzon Trough

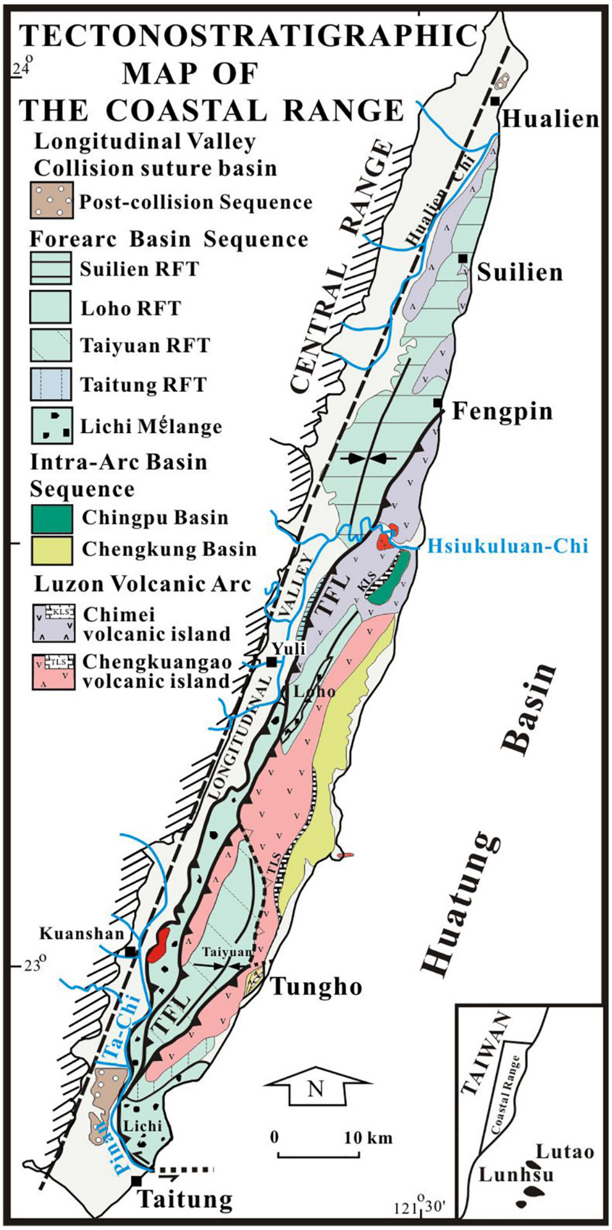

Fig. 4. Tectono-stratigraphic map of the Coastal Range (After Huang et al., 2008). Abbreviations are same as previous ones.

forearc sedimentation was thoroughly explored before.

Detailed stratigraphy study in the last decade showed that the thickness, depositional environment and age of the coherent flysch sequences in four remnant forearc troughs east of the Lichi Mélange onshore the Coastal Range are highly variable (Fig. 5). For example, comparing to the Suilien remnant forearc trough in the north and the Taiyuan remnant forearc trough in the south, the Loho remnant forearc trough in the middle Coastal Range differs from them by a relatively small basin size (15 km × 4 km), limited stratigraphy age (3.4–3.0 Ma), absence of Latest Pliocene-Pleistocene strata and exposure of the Lichi Mélange in the trough center (Figs. 3 and 5; Lin, YC, 2011b; Chen et al., 2015). There are > 2000-m-thick conglomerates in the Suilien remnant forearc trough in the north, but almost deprived in the other three remnant forearc troughs in the south (Figs. 3 and 5). Moreover, thick conglomerates in the Suilien remnant forearc trough were deposited in two independent fan systems via different transportation routes (see Section 6.5). Although the Lichi Mélange exposes continuously for > 50 km long from Taitung City to Yuli town in the western side of the southern Coastal Range (Fig. 3), it also locally exposes in the Loho remnant forearc trough center and in the eastern part of the Suilien remnant forearc trough along a fault south of Fengpin town in the northern Coastal Range (Hsu, 1976; Wang and Chen, 1993).

Geological significances of these temporal-spatial variations of the forearc stratigraphy and structures in the Coastal Range were ignored notably in previous studies because of: (1) lacks of detailed study on modern forearc stratigraphy and sedimentation in the active convergent region offshore SE Taiwan for an analog comparison between onshore and offshore forearc geology in eastern Taiwan, (2) configuring all of sedimentary sequences, including intra-arc sequences, into a simple non-deformed forearc basin during the sedimentation, and (3) controversial interpretations of ages and mechanisms responsible for the development of the Lichi Mélange onshore the Coastal Range. Neither marine investigations in active subduction-collision zone offshore, nor forearc stratigraphy studies onshore the Coastal Range, had addressed that the forearc sedimentation and stratigraphy were dynamically variable not only in the E-W direction across the orogenic strike, but also in the N-S direction along the orogenic strike from offshore collision zone to onshore obduction zone in eastern Taiwan. Moreover, throughout the Coastal Range there is an un-usual deformation character that the young coherent flysch sequences in the east thrust westward over the old and highly sheared Lichi Mélange in the west along the Tuluanshan fault (*s.l.*) (Fig. 3B). Significance of this special deformation character has never been explored before due to lacks of precise age determinations of the forearc strata.

3. Purposes and contents of this study

The purposes of this study are to review the fundamental characters of the modern North Luzon Trough forearc geology onshore and offshore, and to discuss the main factors that control stratigraphy, sedimentation and deformation in the forearc basin in the oblique subduction-collision zones offshore SE Taiwan by using seismic and bathymetric survey data (Fig. 2; Huang et al., 2018). The results obtained from marine surveys offshore are then used to compare with the geological characters of the Late Miocene-Pleistocene forearc strata obducted onshore the Coastal Range to investigate whether similar geological characters and control factors had operated before. Should the geological features be similar and comparable onshore and offshore, we would reconstruct a workable model of forearc stratigraphy, sedimentation and deformation, especially the mechanism and processes responsible for formation of a collisional forearc mélange, during the oblique subduction-collision for the orogenic belts worldwide with the same tectonics reported herein.

4. Study methods

Modern marine geological features obtained from geophysical surveys in the last 25 years are integrated for understanding how modern sediments are filled and deformed in the North Luzon Trough forearc basin in response to the active oblique subduction-collision tectonics offshore SE Taiwan today (Chen and Juang, 1986; Huang and Yin, 1990; Reed et al., 1992; Huang et al., 1992, 1997; Lundberg et al., 1997; Lallemand et al., 1997; Liu et al., 1998; Malavieille et al., 2002; Malavieille and Trullenique, 2009; Chi et al., 2003, 2014; Yen and Lundberg, 2006; Hirtzel et al., 2009; Lehu et al., 2015; Huang et al., 2017). The used geophysical data include swath bathymetry survey and seismic profiling (Fig. 2). For the seismic profiles used in this study, Lines MW9006-51 and 9006-31 are 6-channel migrated profiles collected by *R/V Moana Wave* of the University of Hawaii (Reed et al., 1992; Lundberg et al., 1992), whiles Line EW9509-27 (132-channel) was obtained by *R/V Maurice Ewing* of the Columbia University (Hirtzel et al., 2009). In addition, Lines 2014-1, 2014-2 and 973 GMGS are 480-channel profiles conducted by *R/V Tanbao* of the Guangzhou Marine Geological Survey, China (Huang et al., 2018). Based on these marine

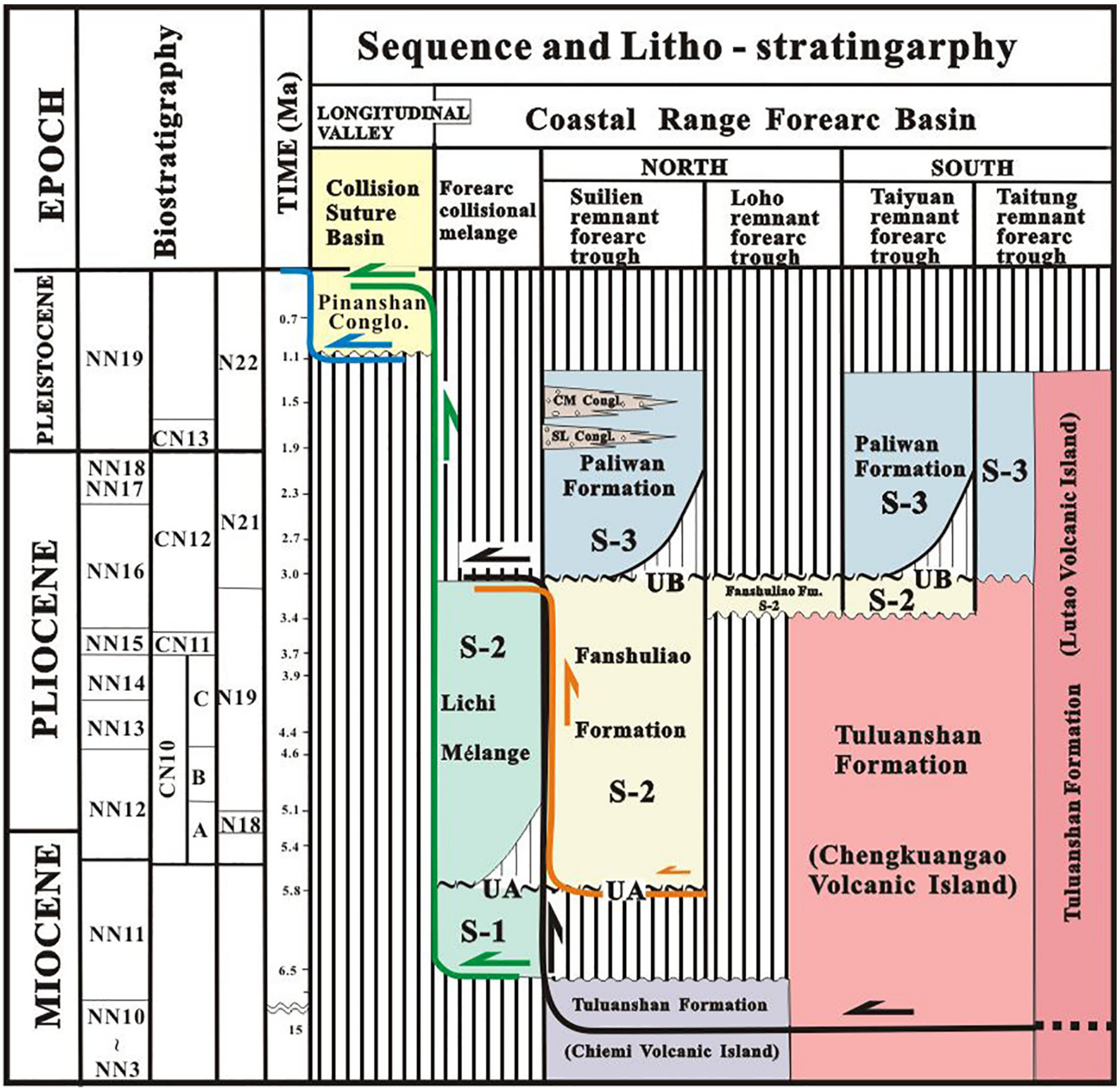

Fig. 5. Forearc lithostratigraphy and sequence stratigraphy of the Coastal Range (modified from Huang et al., 1995, 2006) showing also west-propagating thrust structures developed during obduction in the last 1 Ma. The Lichi Mélange in the west includes sequence units S-1 and S-2 separated by the unconformity UA at 5.8 Ma. Coherent flysch sequences in four remnant forearc troughs east of the Lichi Mélange include the Fanshuliao Formation (sequence unit S-2) and the Paliwan Formations (sequence unit S-3) bounded by the unconformity UB in ~3–2 Ma; SL: Suilien Conglomerate; CM: Chimei Conglomerate. Stratigraphy of two intra-arc basins is not shown here.

seismic images, we are able to establish the modern forearc seismic sequence stratigraphy of the North Luzon Trough and to document the characteristics of *syn*-sedimentation deformation in the active oblique subduction-collision region offshore SE Taiwan.

In the last decade we also conducted detailed field surveys onshore Coastal Range, eastern Taiwan, and re-studied the biostratigraphy of the Lichi Mélange and coherent flysch sequences in four remnant forearc troughs exposed along some key sections (Fig. 3; Huang et al., 2008; Lin, YC, 2011b; Lin, CT, 2011a; Chen et al., 2015, 2017). Field surveys focused on deposition ages, deformation and temporal-spatial variations of thick conglomerate depositions in the coherent flysch sequences. For the Lichi Mélange we emphasized depositional ages of argillaceous matrices and various states of strata disruptions, shearing and mixing of various SSZ rock types in the highly sheared argillaceous matrices. Results of age dating on two SSZ mafic blocks in the Lichi Mélange are also highlighted in this study (see Section 8). Depositional ages of the forearc stratigraphy are dated precisely by integrating micropaleontological study on both planktonic foraminifera and calcareous nannofossils (Fig. 6) in rock samples (200 g of sediments for foraminiferal study, planktonic foraminifera in residual sediments > 150 μm are identified) collected along key sections across structures. Results of detailed stratigraphic distributions of micro-planktons in the coherent lower flysch sequences in the Suilien remnant forearc trough are documented in this paper, whiles results of other sections were published in Lin, YC (2011b), Lin, CT (2011a) and Chen et al. (2015, 2017). Only their synthesized ages are shown herein. Biostratigraphic data published previously are also integrated (Chang, 1967b, 1968, 1969; Chang and Chen, 1970; Chi et al., 1981; Horng and Shea, 1996). We follow planktonic foraminiferal biostratigraphy of Blow (1969), Berggren et al. (1995) and biochronology of key planktons documented in Wade et al. (2011) (Fig. 6) to assign the depositional ages of the study sections. However, if planktonic foraminifera are rare, calcareous nannofossil ages are used to constrain the depositional time range (Martini, 1971; Raffi et al., 2006; Anthonissen and Ogg, 2012). The following age datum planes of planktonic foraminifera and calcareous nannofossils established previously from low-latitude areas are followed in this study (Fig. 6): First Occurrence (FO) of *Globorotalia plesiotumida* at 8.5 Ma, *Globorotalia tumida* at 5.5 Ma, *Spheroidinella*

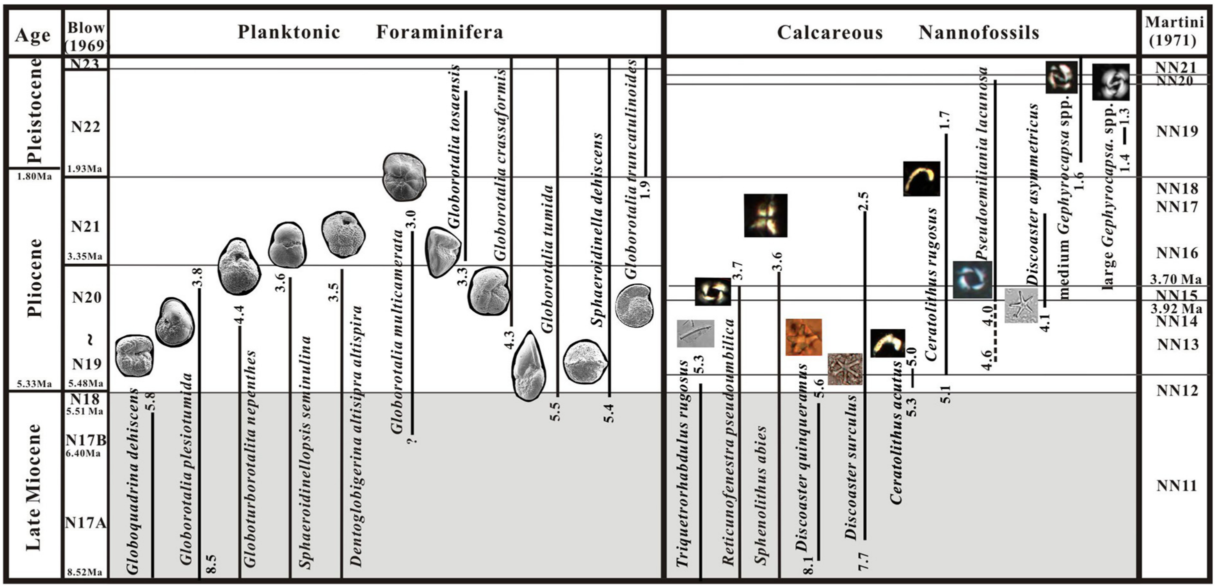

Fig. 6. Biostratigraphy of planktonic foraminifera and calcareous nannoplanktons used in this study. Biochronology of datum planes follow Wade et al. (2011) for planktonic foraminifera and Anthonissen and Ogg (2012) for calcareous nannofossils.

dehiscens at 5.4 Ma, *Ceratolithus rugosus* at 5.1 Ma, *Globorotalia crassaformis* at 4.3 Ma, *Discoaster asymmetricus* at 4.1 Ma, *Globorotalia tosaensis* at 3.3 Ma and *Globorotalia truncatulinoides* at 1.9 Ma; and Last Occurrences (LO) of *Globoquadrina dehiscens* at 5.8 Ma; *Discoaster quinqueramus* at 5.6 Ma, *Globoturborotalita nepenthes* at 4.4 Ma, *Sphaeroidinellopsis seminulina* at 3.6 Ma (in the Pacific region), *Dentoglobigerina altispira* at 3.5 Ma (in the Pacific region), *Globorotalia multicamerata* at 3.0 Ma, *Reticulofenestra pseudoumbilica* at 3.7 Ma, *Sphenolithus abies* at 3.6 Ma and *Discoaster surculus* at 2.5 Ma.

In the following sections, we first review the fundamental characters of the modern forearc deformation, dynamic sequence stratigraphy and transporting routes in the modern oblique convergent region north of 20°N off shore SE Taiwan using seismic profiles (Section 5). The marine geology plays as a modern analog for understanding the deformation characters and stratigraphy obducted onshore the Coastal Range, eastern Taiwan (Section 6). Integrating forearc geology offshore and offshore, we then construct an evolution model for forearc deformation and dynamic stratigraphy of the North Luzon Trough in 2-D profiles and map views from subduction through collision to obduction in the last 6.5 Ma (Section 7), and finally present and discuss the mechanism and processes responsible for development of the modern-forming Lichi Mélange in the Coastal Range (Sections 8).

5. Marine geology of the North Luzon Trough offshore SE Taiwan

5.1. Characteristics of the North Luzon Trough forearc geology

The most characteristic North Luzon Trough forearc geology in the oblique collision zone offshore SE Taiwan is the development of the Huatung Ridge by bivergent thrusting (Figs. 1 and 2; Huang and Yin, 1990; Reed et al., 1992; Huang et al., 1992, 2017). The bivergent deformation is still active today as indicated by occurrence of two high seismicity zones following bivergent thrust fault zones: the Longitudinal Valley Seismic Zone (LVSZ) on the west and the arc-parallel seismic zone (APSZ) on the east, respectively (Fig. 7; Cheng and Wang, 2001). Focal mechanism studies indicated that the earthquakes of these two high seismicity zones are thrust faults with a significant strike-slipping component (Lewis et al., 2015). However, seismicity gets less active south of 21°10′N (Fig. 7) consistent with a much simple and less active of forearc deformation in the subduction zone in the south.

The North Luzon Trough forearc basin in the subduction zone south of 20°10′N is wide (Fig. 2; 35–45 km), deep (> 3000 m), open and non-deformed except a narrow belt (east-dipping forearc ridge; EFR in Fig. 2) east of the arc-prism boundary. However, in the collision zone the forearc basins is highly deformed northward from 21°10′N. The deformation leads to a semi-closure of the gate for deep water exchanges between the Western Pacific Ocean and the South China Sea (Fig. 2; Lundberg et al., 1997; Tian et al., 2006; Huang et al., 2012; Chen et al., 2015) and controls of transportation routes of the modern young sediments east of the Huatung Trough (see Section 5.4).

Seismic profiles across the North Luzon Trough from the subduction zone northward to the collision zone delineate details of the processes of bivergent deformation in the modern forearc basin and the dynamic stratigraphy in response to *syn*-sedimentation deformation offshore SE Taiwan (Huang et al., 2018).

5.2. Forearc stratigraphy and deformation in the subduction zone south of 21°10′N

Forearc strata in the subduction zone south of 21°10′N are composed of ~10 seismic sequences of cyclic turbidite sedimentations (Figs. 8, 9 and 10). The sequences can be further grouped into two mega-sequence units M-A and M-B bounded by a mega-sequence boundary (MSB) unconformably (Figs. 8, 9 and 10). The lower mega-sequence unit M-A has fairly constant strata thickness with parallel to subparallel reflections, whiles the upper mega-sequence unit M-B shows divergent reflection lapping westward upon the lower mega-sequence unit M-A and a lateral thinning of strata toward the accretionary prism. Similar westward onlapping features with lateral thinning toward accretionary prism are frequently found onshore the Coastal Range (Fig. 17A).

The seismic configuration in the southern subduction zone (Line 2016-10) south of 20°30′N shows a down-warping feature, especially the lower mega-sequence unit M-A below MSB, probably due to an increase of east-dipping slope angle of the rear prism (Fig. 8) by frontal accretions of new sediments into the Hengchun Ridge accretionary prism in the subduction zone (Wang and Davis, 1996). A mild west-vergent thrusting occurs during the late sedimentation of the upper mega-sequence unit M-B in Line 2016-10 across the southern subduction zone (Fig. 8h–j).

However, approaching to the collision zone between 20°30′N and 21°10′N the seismic reflections become convex upward in the western

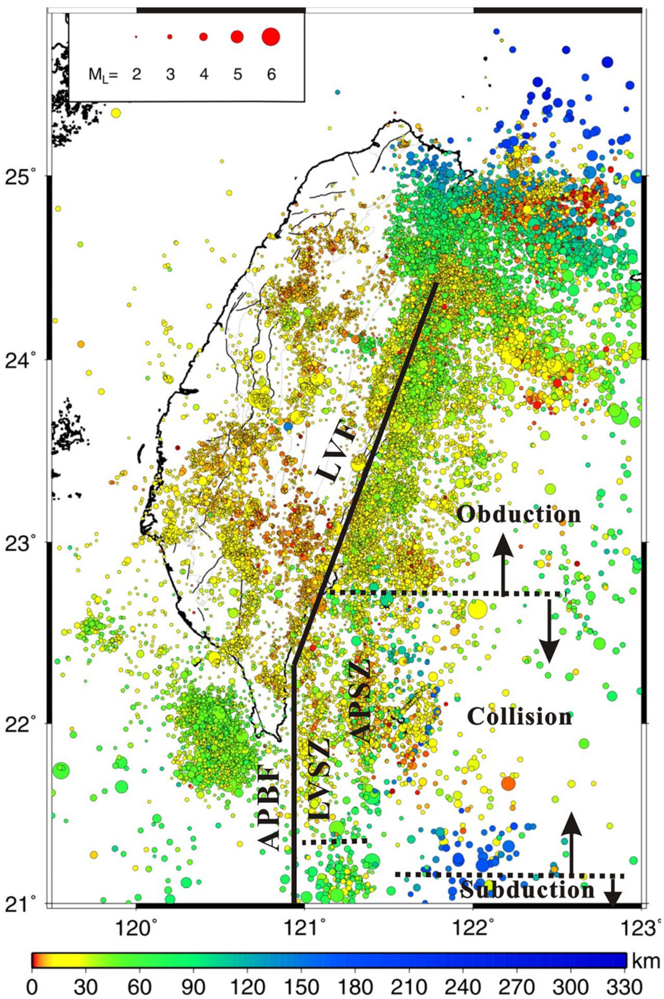

Fig. 7. Seismicity in the Taiwan region (after the Central Weather Bureau, Taiwan). Bivergent faults in both sides of the Huatung Ridge match well with two high seismicity zones of LVSZ on the west and APSZ on the east (Cheng and Wang, 2001). APBF: arc-prism boundary fault; LVF: Longitudinal Valley fault.

forearc basin (Fig. 9; Lines 2014-1 and 973GMGS), suggesting a compression primarily by west-vergent thrusting of forearc sequences over the accretionary prism along arc-prism boundary (Figs. 9 and 10). Detailed restoration of the seismic profiles indicates that west-vergent thrusting structures occur as early as the sedimentation of the lower mega-sequence unit M-A and continue until today to rise the seismic reflection as an east-dipping forearc ridge in the western forearc basin (Figs. 9 and 10f; EFR in Fig. 2). Consequently, in the subduction zone west-vergent thrusting occurs early in the north and late in the south in consistent with a southward propagating of the convergent tectonics in the Taiwan region.

The west-vergent thrusting structures developed in the western forearc basin of the subduction zone could have act later as main conduits of mud diapirs east of the arc-prism boundary (md in Fig. 9). Today, mud volcanos follows the footwall of the Longitudinal Valley fault, the northern extension of the arc-prism boundary fault offshore, in the western Coastal Range (Fig. 17B; Yang et al., 2004).

In response to *syn*-sedimentation deformation in the western forearc basin, forearc depocenter shifts eastward (dash line in Fig. 10) from D-I during the sedimentation of the lower mega-sequence unit M-A to D-II during the sedimentation of the overlying the mega-sequence unit M-B progressively (Fig. 10; Hirtzel et al., 2009; Huang et al., 2018).

5.3. Forearc sequence stratigraphy and deformation in the collision zone north of 21°10′N

The most characteristic features of marine geology of the North Luzon Trough in the collision zone between 21°10′N and 22°40′N are: (a) occurrences of backthrust structures propagating eastward toward volcanic arc (Line 2014-2; Fig. 11) to develop the Huatung Ridge (Fig. 12), (b) three seismic mega-sequences separated by two unconformities (MSB and U-HTR; Fig. 12), and (c) clockwise rotation of the Lutao and Lanyu volcanic islands of the northern Luzon arc (Figs. 1 and 2; Zhao et al., 2016).

In addition to west-vergent thrusting along the prism top, east-vergent backthrust structure occurs in the oblique collision zone to accommodate a space shorting by the collision between the northern Luzon volcanic arc and the accretionary prism north of 21°10′N (Fig. 2). Line 2014-2 across the southernmost collision zone shows that backthrust faults extend form the lower mega-sequence unit M-A upward cutting into the overlying mega-sequence unit M-B. Backthrusting propagates from the western forearc basin eastward (Fig. 11). When more parts of the mega-sequence unit M-B are involved into backthrusting, the east-dipping forearc ridge develops larger progressively as a growing Huatung Ridge (Fig. 11b). When the whole forearc sequences were bivergent thrust, a mature Huatung Ridge develops in the collision zone north of 21°20′N (Figs. 12 and 13) and uplifted the forearc basin floor and arc basement for ~900 m high (Hirtzel et al., 2009). In response to bivergent thrusting, forearc depocenter jumps eastward from D-II of the mega-sequence unit M-B to a new depressed trough between the uplifted Huatung Ridge and the west-dipping arc basement (D-III in Fig. 14). D-III is then filled by the youngest mega-sequence unit M-C overlapping the backthrust mega-sequence unit M-B of the Huatung Ridge unconformably (U-HTR; Figs. 12 and 14). The forearc stratigraphy in the oblique collision zone is thus composed of three mega-sequences juxtaposed from west to east (Fig. 14). Consequently, there is a characteristic temporal-spatial pattern of forearc deformation and the stratigraphy in the oblique collision zone (Fig. 14): The oldest mega-sequence unit M-A with the most intensive deformation occurs restrictedly in the western forearc basin, whiles the middle mega-sequence unit M-B and the youngest mega-sequence unit M-C with mild deformation crop up in the center and the eastern forearc basin, respectively (Fig. 14).

This characteristics of temporal-spatial distribution pattern of forearc deformation and stratigraphic in the oblique collision zone is fundamentally responsible for the mechanism and occurrence of the modern-forming collision forearc Lichi Mélange in the Coastal Range (details see Sections 7 and 8; Huang et al., 2008).

5.4. Different transportation routes of modern sediments of mega-sequence unit M-C in remnant forearc troughs east of the Huatung Ridge

Seismic reflections of the mega-sequence unit M-C unconformable overlying the Huatung Ridge are flat (Lines MW9006-51 and EW9509-27 in Fig. 12A and 12E; see also Fig. 5b of Lundberg et al., 1997, and Fig. 4 of Lehu et al., 2015). This suggests no intensive deformation post bivergent thrusting of the Huatung Ridge. However, no mega-sequence unit M-C is observed in the seismic profile of Line MW9006-31 (Fig. 12C; see also MW9006-30 in Fig. 5a of Lundberg et al., 1997). This discrepancy suggests that the Lines MW9006-31and MW9006-30 could transect over a bathymetric high west of Lanyu volcanic island ("BHWL" in Figs. 2 and 13) that no modern sediment of the mega-sequence unit M-C can be deposited on the bathymetric high. Swath bathymetry surveys incorporated with sediment coring in the active collision zone revealed that there were different routes to transport the modern sediments (mega-sequence unit M-C) into the remnant forearc trough (D-III) north and south of this bathymetric high, respectively (Fig. 2; Huang and Yin, 1990; Huang et al., 1992; Yen and Lundberg, 2006). Modern forearc sediments are eroded predominantly from the

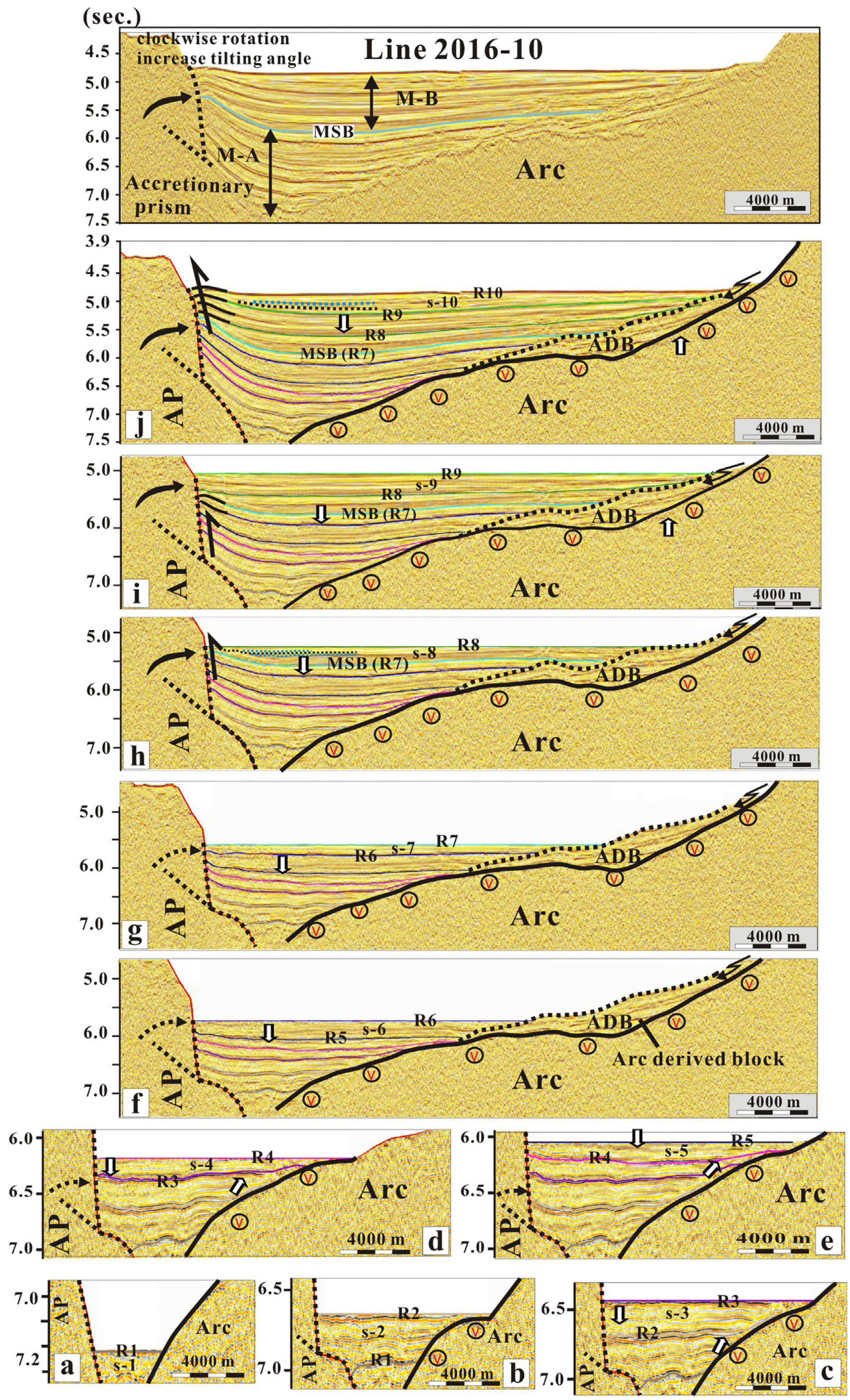

Fig. 8. Seismic profile (uppermost) and (a–j) sequential restorations of seismic reflections of each sequence in Line 2016-10 across the oblique subduction zone off SE Taiwan (after Huang et al., 2018). The forearc strata in the subduction zone south of 20°30′N are composed of mega-sequence units M-A and M-B bounded by the mega-sequence boundary (MSB). West-vergent thrusting along the prism top (or arc-prism boundary) starts from early sedimentation (sequence s-8; panel h) of the lower mega-sequence unit M-B. AP: accretionary prism; ADB: arc-derived block. Location of seismic line is shown in Fig. 2.

exhumed accretionary wedge (the Central Range - Hengchun Peninsula) with minor portion derived from the Coastal Range via two main different routes (Fig. 2).

North of Taitung City in the southern Coastal Range, eastern Taiwan, the Pinanta-Chi River is the major route for transporting sediments into the modern remnant forearc trough between the Huatung Ridge and the Lutao Volcanic Island (Figs. 2 and 13). The Pinanta-Chi River develops from the eastern slope of the Central Range. It first runs eastward and then veers southward into the N-S-trending collisional suture of the Longitudinal Valley between the Central Range and the Coastal Range (Fig. 2). However, as the river approaching to Taitung City it detours sharply eastward along the E-W-trending left-lateral strike slip fault line in the southernmost Coastal Range (Fig. 13). This left-lateral strike slip fault line marks the boundary between the active oblique collision zone offshore and the obduction zone onshore the Coastal Range (Figs. 2 and 13). The Pinanta-Chi River further runs

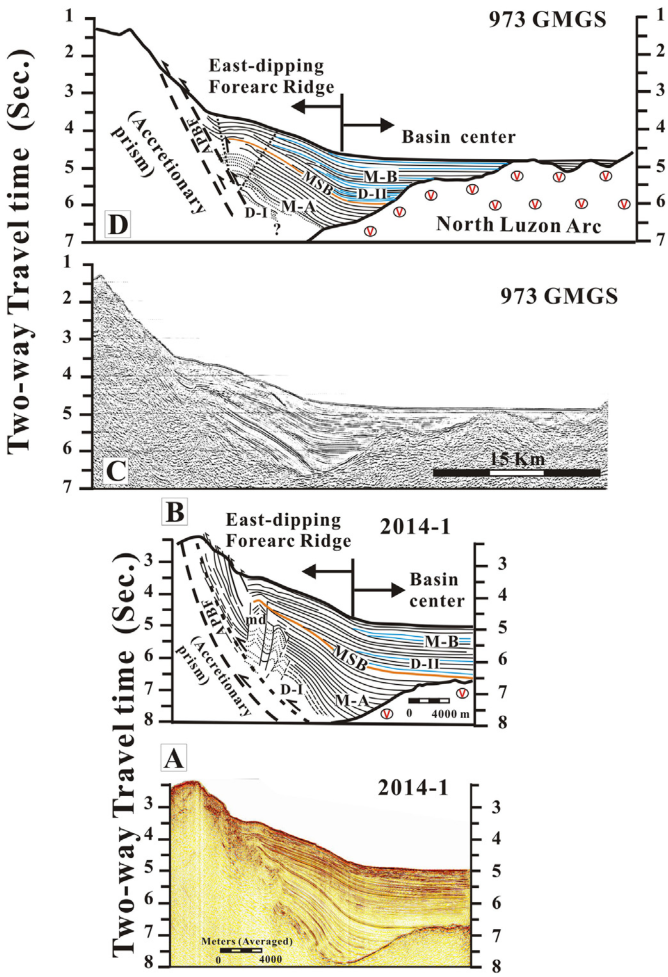

Fig. 9. Seismic profiles and interpretations of Line 2014-1 (A, B) and Line 973GMGS (C, D) in the subduction/collision transition region. Abbreviations are similar to Fig. 8; D-I and D-II: forearc depocenter during sedimentation of the mega-sequence unit M-A and unit M-B, respectively (after Huang et al., 2018). Blue lines in the mega-sequence unit M-B mark west-lapping sequences. Locations of seismic lines are shown in Fig. 2.

through a river mouth shallow-marine fan delta on the narrow continental shelf (< 200 m water depth) off the southern Coastal Range, then turns southward to the remnant forearc trough between the Huatung Ridge and the Lutao volcanic island via the N-S-trending submarine deep Taitung Channel (water depth: −1000 to −2500 m; Figs. 2 and 13). The basement of the river mouth fan delta is part of the deformed forearc Huatung Ridge. The submarine Taitung Channel (Fig. 12f) cuts through the Huatung Ridge and transports cobbles to fine-grained debris flow deposits of metamorphic rocks southward (Fig. 2; Huang and Yin, 1990; Huang et al., 1992). They are finally dumped in the over-fill remnant forearc trough north of the 'BHWL' bathymetric high (Fig. 2).

However, south of Taitung City, similar metamorphics dominant sediments eroded from the southern Central Range - Hengchun Peninsula are directly transported eastward into the Southern Longitudinal Trough via some other short rivers during typhoon seasons (light blue arrows with white board in Fig. 2; Huang and Yin, 1990; Huang et al., 1992; Malavieille et al., 2002). When this suture basin has been filled up, finer-grained sediments of these metamorphics dominant debris flow deposits are further transported eastward into a temporally starved under-fill remnant forearc trough (marked as X in Fig. 2) south of the 'BHWL' bathymetric high via several small submarine channels (deep green arrows in Fig. 13) bypassing over the pop-up Huatung Ridge (Fig. 2).

Current paleomagnetic surveys demonstrated that the Lutao and Lanyu volcanic islands offshore active oblique collision zone have been clockwise rotated for, at least, 30 degrees (Figs. 1 and 13; Zhao et al., 2016). This implies that the volcanic arc basements could have been involved into deformation during the collision (Zhao et al., 2016; Huang et al., 2018). We speculate that there could develop a W-E strike slip blind fault zone across the Huatung Ridge between the Lutao and Lanyu volcanic islands to cause uplifting of the middle part of the Huatung Ridge as a bathymetric high ('BHWL') to accommodate a space adjustment due to clockwise rotation of the Lutao and Lanyu volcanic islands (Fig. 13). However, traces of this strike-slip fault line had not been found yet in seismic survey (Hirtzel et al., 2009) presumably due to a poor seismic reflection over the volcanic islands. We consider that it could be a newly-developed blind fault indicated by occurrences of an E-W morphological lineament following the course of the Taitung Canyon (Figs. 2 and 13; Schnűrle et al., 1998; Lehu et al., 2015). Along the lineament of the east-running Taitung Canyon, there occur also some strike-slip earthquakes (Kao and Huang, 2000). This E-W morphotectonic lineament could also extend westward to hit the accretionary prism onshore at a special bend point Y (Figs. 2 and 13) where the trend of accretionary prism changes from a N-S direction of the Hengchun Peninsula to the south to 020° direction of the Central Range to the north (Byrne, 1998).

Syntheses of the modern forearc *syn*-sedimentation deformation and dynamic forearc stratigraphy of the North Luzon Trough offshore SE Taiwan are shown in Fig. 14 (see Section 7).

5.5. Comparisons of various structure models proposed of forearc deformation offshore SE Taiwan

Two contrast structure models have been proposed controversially to interpret forearc deformation offshore SE Taiwan (Fig. 15). However, they all conflict with our results of seismic surveys. Reed et al. (1992) argued that a "tectonic wedge" of accretionary prism materials (Miocene strata of the Hengchun Ridge; Fig. 15A) had been inserted into the space between the North Luzon Trough upper forearc sequence and the volcanic arc by an east-direct blind backthrust fault during the forearc sedimentation (1 in Fig. 15A; Chi et al., 2003). Inserting the 'tectonic wedge' resulted in uplifting and folding the western forearc sequence with divergent seismic reflections above the fold structure in the western forearc basin (2 in Fig. 15A). The 'tectonic wedge' migrated arcward to backthrust the whole forearc sequences as the Huatung Ridge (3 in Fig. 15A). In this model, inserting of the accretionary wedge into the western North Luzon Trough and the arc-directed east-vergent backthrusting play the most important role of forearc deformation, whiles the trench-directed west-vergent thrusting is insignificant during the subduction and collision. The 'tectonic wedge' model claimed that a backthrust domain gets narrow from the Huatung Ridge in the collision zone southward to the subduction zone (Fig. 4 in Reed et al., 1992).

Backthrusting of tectonic wedge over the forearc strata had been documented in the Timor and the Lesser Antilles regions (Reed et al., 1986; Silver and Reed, 1988; Torrini and Speed, 1989). However, our high-resolution seismic profiles show that the east-vergent backthrust fault occurs neither in the subduction zone (Fig. 8; Line 2016-10) nor the subduction/collision transition region (Figs. 9 and 10; Lines 2014-1 and GMGS-973) south of 21°10′N. No 'tectonic wedge'-like block is recognized in our seismic profiles. The so-called "backthrust domain" south of 21°10′N is actually of an east-dipping forearc ridge formed by west-vergent thrusting (EDR in Figs. 2, 14c, d, e) instead of by east-vergent backthrusting. East-vergent backthrust occurs only in the collision zone north of 21°10′N (Figs. 11 and 12) and never happens in the subduction zone (Figs. 8 and 9). Consequently, the width of the east-dipping forearc ridge by west-vergent thrusting in the subduction/collision transition region (FDR in Fig. 2) is much narrow than the bi-vergent thrust Huatung Ridge in the collision zone, and the west-

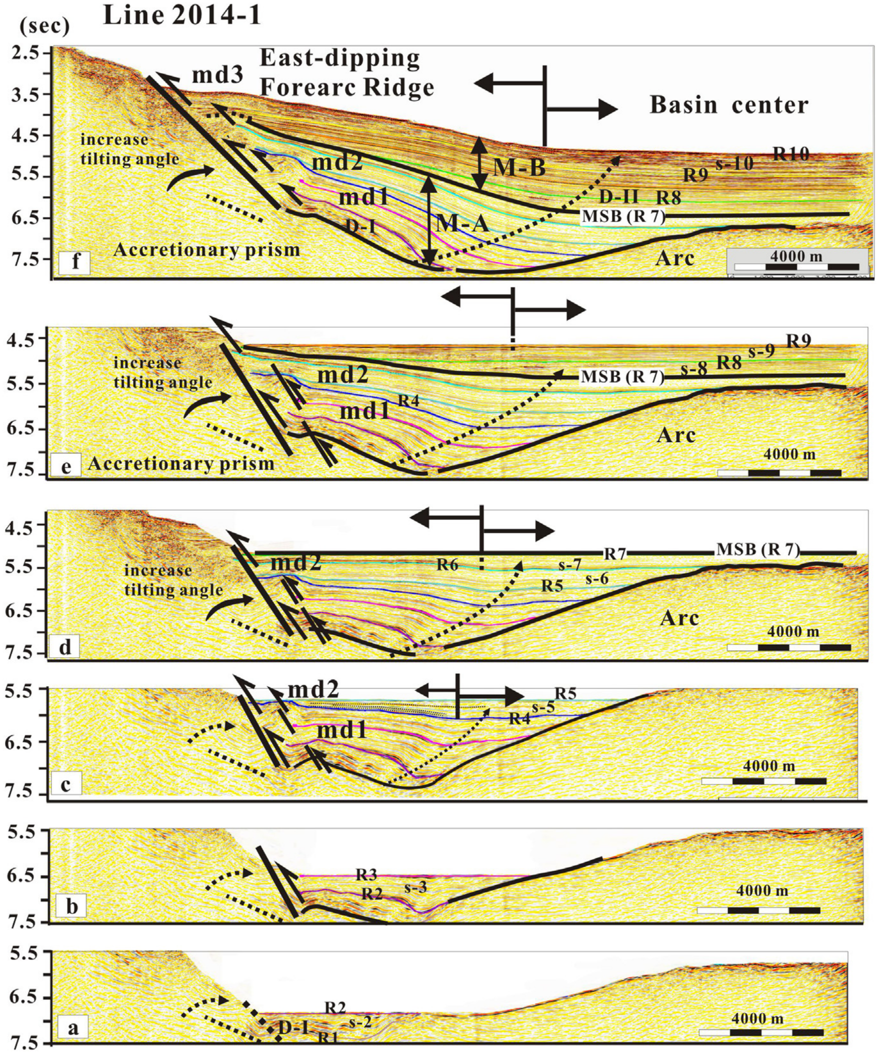

Fig. 10. (a–f) Sequential restoration of each sequence of Line 2014-1 (Fig. 9A) across the subduction/collision transition region off SE Taiwan. West-vergent thrusting along the prism top (or arc-prism boundary) starts as early as the forearc sedimentation of the mega-sequence unit M-A (s-3 in b). Dotted arrow: eastward shifting of forearc depocenter in response to *syn*-sedimentation west-vergent thrusting; md: mud-diapir (after Huang et al., 2018). s: sequence number. Location of seismic line is shown in Fig. 2.

vergent thrust structure event occurs earlier than the east-vergent backthrust structure in the oblique convergent region offshore SE Taiwan (Fig. 14). No definite 'tectonic wedge' is observed in our seismic profiles because subduction is not so active off SE Taiwan north of 20°N where deep seismicity is relatively rare (Kao and Huang, 2000) and tectonics in the Taiwan region had already proceeded to collision in the last 6.5 Ma when the forearc sediments started to deposit in the North Luzon Trough.

On the contrary, by experiments of various sand-box modelling, Malavieille and Trullenique (2009) suggested a "double wedges" to interpret the forearc deformation offshore SE Taiwan (Fig. 15B). Among various experiments, only their experiment 4 can produce significant backthrusting structures. In this experiment "a retro-accretionary wedge" develops by an arcward backthrusting (AW in Fig. 15B). Then another "forearc wedge" (FW in Fig. 15B) occurs in the eastern North Luzon Trough forearc basin (not the western North Luzon Trough as it was claimed by 'tectonic wedge' model) above the volcanic arc before the collision with the accretionary wedge. When tectonics proceeds to the collision, east-dipping thrust faults develop within the forearc wedge and propagates arcward to the center part of the forearc wedge (Fig. 15B-3) which finally collides with the "retro-accretionary wedge" on the west (Fig. 15B-4, 5). Then two wedges combine together as a single large wedge in which the backthrust fault extends from the 'retro-accretionary wedge' into the 'forearc wedge' (Fig. 15B-5). In this model, the east-dipping thrusting plays the most important role within the 'forearc wedge' before the collision with the 'retro-accretionary wedge' (Fig. 15B-3, -4), whereas the arc-direct west-dipping backthrusting is insignificant in the early deformation within the 'forearc wedge'. Results of the sand-box experiments (Malavieille and Trullenique, 2009) are highly contradictory to our seismic profiles which indicate that forearc deformation starts from the western forearc basin then propagate arcward, rather than starting from the eastern forearc basin than propagating westward toward accretionary prism.

Both proposed structural modes can't explain the fundamental character of temporal-spatial variations of a juxtaposition of three forearc sequences as it is observed in our seismic profiles offshore SE Taiwan.

6. Forearc sequence stratigraphy (~6.5–1 Ma) and sedimentation onshore the Coastal Range, eastern Taiwan

To test if similar dynamic sequence stratigraphy, temporal-spatial variations of sedimentation and *syn*-sedimentation deformation that display today in the active collision zone offshore SE Taiwan could

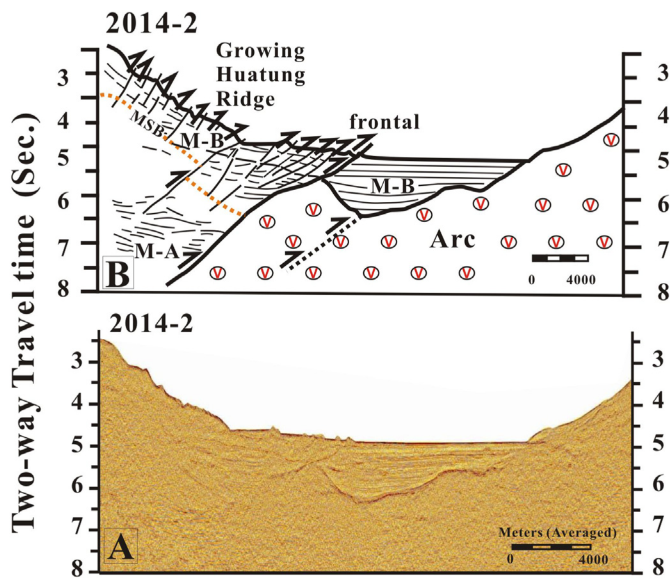

Fig. 11. (A) Seismic profiles and (B) its interpretation of Line 2014-2 in the southernmost collision zone. East-vergent backthrusting structures occur restrictedly in the oblique collision zone. In this profile backthrust propagates eastward to the basin center and divides the entire seismic profile into two contrast parts with different seismic facies (after Huang et al., 2018). Abbreviations are similar to previous ones. Locations of seismic lines are shown in Fig. 2.

occur also in the past, we have conducted detailed field surveys and restudied the forearc stratigraphy onshore the Coastal Range, eastern Taiwan, during the past decade.

6.1. *Characteristics of forearc stratigraphy and structures onshore the Coastal Range*

There are several fundamental features of the forearc stratigraphy, sedimentation and structures onshore the Coastal Range:

(1) The forearc stratigraphy of the Coastal Range includes the old, highly sheared Lichi Mélange in the west and young coherent flysch sequences in the east (Figs. 3 and 5);

(2) The young coherent flysch sequences in the east were deposited in four mildly-deformed remnant forearc troughs east of the old and highly deformed Lichi Mélange (Figs. 3 and 4). They are, from north to south, the Suilien, Loho, Taiyuan and Taitung remnant forearc troughs (Fig. 4). At present, these remnant forearc troughs are separated from each other by east-dipping faults developed during the obduction in the last 1 Ma. The coherent flysch sequences are deformed as south-plunging syncline structures with some portions occurred as broken formation (Fig. 21A). In contrast, the Lichi Mélange in the west are severely deformed and sheared as alternations of mélange (Fig. 16A) and broken formation (Fig. 16B; Huang et al., 2008). Deformations of the broken formation can be weak with discernible stratification or highly sheared without stratification (Hsu, 1968). Mixture of allochthonous blocks are never been found in the broken formation (= α, β and γ grades of shearing in Huang et al., 2008; Raymond, 1984). In contrast, the mélange is featured by intensive shearing and mixture of variable sized (mm to km) blocks of polygenic rock types, including sandstone, volcanic agglomerate, tuff, mafic to ultra-mafic blocks in scaly argillaceous matrices with preferred orientation, showing a block-in-matrix feature (Fig. 16A; δ-grade of Huang et al., 2008);

(3) The basin dimension of the Suilien remnant forearc trough and the Taiyuan remnant forearc trough is much larger than the Loho remnant forearc trough and the Taitung remnant forearc trough due to variations of their paleogeography (Fig. 4). The Loho and Taitung remnant forearc troughs were positioned in the junction area between volcanic islands, whiles the Suilien and Taiyuan remnant forearc troughs were located west of main volcanic island (Fig. 4). Sedimentations of coherent flysch sequences in remnant forearc troughs are also highly variable temporally and spatially. For examples, no sediments younger than 3 Ma were deposited in the Loho remnant forearc trough, but > 3-km-thick coherent flysch sequences younger than 3 Ma were exposed in the Suilien and Taiyuan remnant forearc troughs north and south, respectively, of the Loho remnant forearc trough (Fig. 5). On the other hand, > 2 km thick conglomerates (< 3 Ma) were laid down in the Suilien remnant forearc trough, but no thick conglomerate bed was found in the other three remnant forearc troughs to the south (Fig. 5);

(4) Litho-stratigraphy of the coherent young flysch sequences in four remnant forearc troughs was mapped as the Takangkou Formation (sandy flysch) in the lower part and the Chimei Formation (muddy flysch) in the upper part (Hsu, 1956, 1976). However, the lithological boundary between these two formations is transitional and time transgressive (Chang, 1969). Combining litho- and bio-stratigraphy study, Chang (1969) later revised the sequences as the Late Miocene Fanshuliao Formation with less slate chips in the lower part and the Pliocene Paliwan Formation with more slate chips disconformably in the upper part (Teng, 1979). However, slate contents in both units are also transitional. Whatever the litho-stratigraphy established by Hsu (1956, 1976) or Chang (1967a, 1969), the rock successions of the coherent flysch sequences in the Coastal Range were considered to be in superposition with depositional hiatus or disconformity (Chang, 1967a, 1975). However, superposition of the forearc stratigraphy is highly contradictory to the geology to develop an unusual structure commonly found in the Coastal Range that young sequences in the east thrust over the old strata in the west (Fig. 3B; discussed below). The superposition of litho-stratigraphy also conflicts with the juxtaposed sequence stratigraphy observed in the seismic profiles across the active collision zone offshore (Section 5);

(5) In contrast to what had found commonly in a passive continental margin where old strata thrust over young sequences, an unusual deformation structure (Fig. 3B) that young coherent flysch sequences (Pliocene-Pleistocene age) in the east thrust westward over the old, intensively sheared Lichi Mélange (Late Miocene to Pliocene age) in the west along the Tuluanshan fault (TLF in Fig. 3B) throughout the entire Coastal Range. Such an uncommon thrust structure can be achieved only if the Late Miocene sequence in the west had been deformed before deposition of the young coherent flysch sequences in the east. Consequently there should exist more than one unconformity among these stratigraphic units. This is one of the most critical points to understand the geological nature of the juxtaposed forearc stratigraphy and *syn*-sedimentation deformation onshore the Coastal Range;

(6) Integrating biostratigraphy study of planktonic foraminifera and calcareous nannofossils (Fig. 6) shows that the forearc strata onshore the Coastal Range were deposited in three age intervals of 6.5–5.8 Ma, 5.8–3.0 Ma and < 3.0–1 Ma (Fig. 5). The lower age interval (6.5–5.8 Ma) distributes restrictedly in the footwall side of the Tuluanshan fault in the western Coastal Range, whiles the middle age interval (5.8–3.0 Ma) occurs either in the footwall or the hanging wall sides of the Tuluanshan fault. The youngest age interval (< 3.0–1 Ma) exposes exclusively east of the middle age interval in the eastern Coastal Range (Fig. 3);

(7) Based on temporal-spatial variations of strata distributions and deformation characteristics, these three age intervals onshore the Coastal Range can be recognized as three sequence units (unit S-1, unit S-2 and unit S-3) bounded by two unconformities UA and UB (Fig. 5). These mega-sequences onshore the Coastal Range (blue line square in Fig. 14) are also juxtaposed from the west to the east,

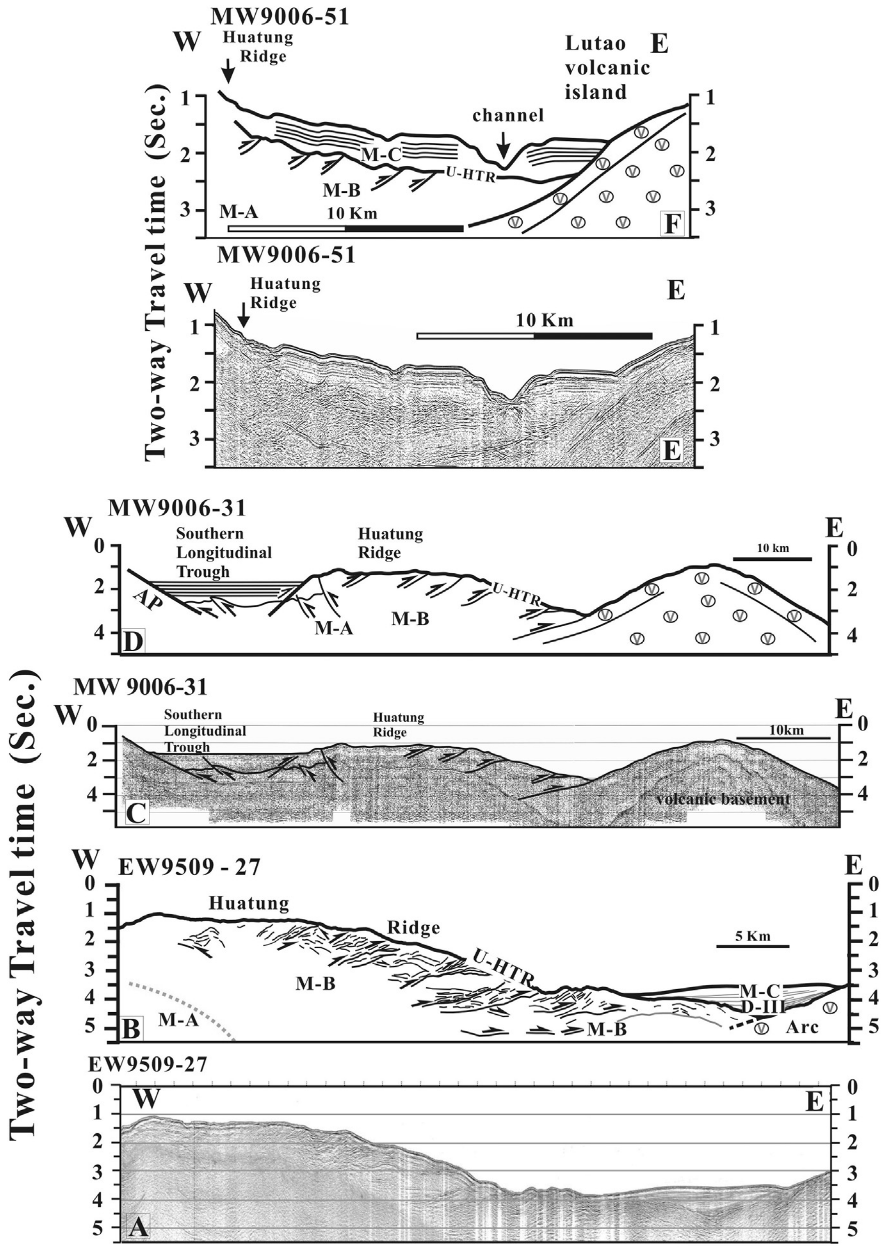

Fig. 12. Seismic profiles of Lines MW9006-51, MW9006-31 and EW9509-27 across the oblique collision zone (Locations of seismic lines are shown in Fig. 2). Three seismic mega-sequenceunits M-A, M-B and M-C bounded by unconformity. Due to intensive deformation by bivergent thrusting, seismic reflections are ambiguous. Profile images are adapted from Reed et al. (1992), Chi et al. (2003, 2014) and Hirtzel et al. (2009). No deposition of the mega-sequence M-C is observed in Line MW9006-31 crossing over the 'BHWL' bathymetric high. U-HTR: unconformity between mega-sequence units M-B and M-C. Locations of seismic lines see Fig. 2.

a scenario analog to those occur today in the active collision zone offshore SE Taiwan (black line square in Fig. 14). Although the forearc stratigraphy onshore and offshore is analog to each other, but the age of the middle and the upper sequence unit S-2 and unit S-3 onshore the Coastal Range is older than the equivalent mega-sequence units M-B and M-C, respectively, in the modern collision zone off SE Taiwan (Fig. 27), confirming a southward propagation of the convergent tectonics in the Taiwan region;

(8) The Lichi Mélange (6.5–3.0 Ma) in the west corresponds to the lower sequence unit S-1 (6.5–5.8 Ma) together with the middle sequence unit S-2 (5.8–3.0 Ma), whiles coherent flysch sequences of the Fanshuliao Formation is equivalent to the middle sequence unit S-2 and the Paliwan Formation represents the upper sequence unit S-3 in the east (Fig. 5). The relationship between this new sequence stratigraphy and the traditional lithostratigraphy onshore the Coastal Range is shown in Fig. 27; and

(9) All these characteristic forearc sequence stratigraphy and structures onshore the Coastal Range can be happenned only in some special conditions (Fig. 14) of: 1) sedimentations of the juxtaposed forearc sequences occurred synchronously with deformation caused by bivergent thrusting; 2) depocenter of the juxtaposed forearc sequences shifted eastward in response to bivergent thrusting structures during the sedimentation; and 3) the forearc strata were deposited in a trough between deformed accretionary prism in the west and the west-dipping volcanic arc basements in the east. The forearc bivergent thrusting structures onshore the Coastal Range (Fig. 14a–d–E–F–G) developed in the processes comparable to what occur today in the active oblique collision zone offshore SE Taiwan (Fig. 14a–d–e–f–g). However, the final westward thrusting of the young flysch sequences over the old Lichi Mélange occurred only in

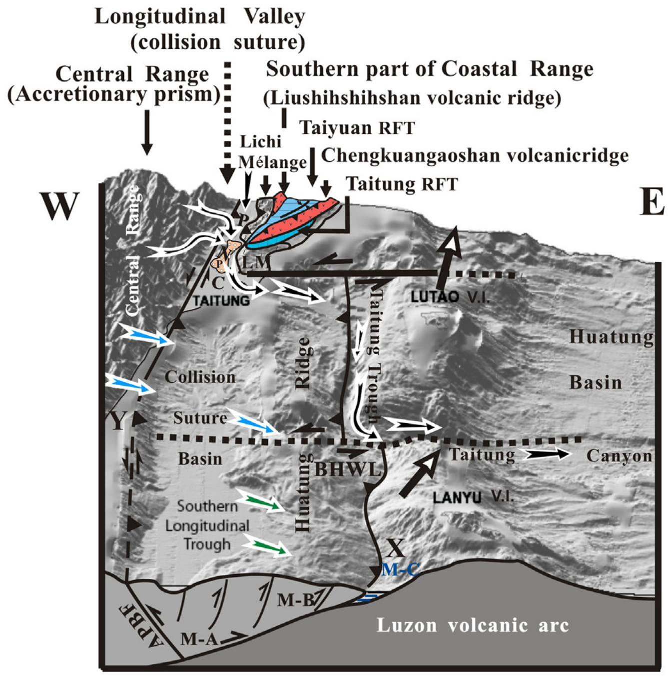

Fig. 13. 3-D image of the North Luzon Trough forearc seafloor in the active collision zone offshore SE Taiwan (adapted from Malavieille et al., 2002 with interpretation modified from Huang et al., 2008). White edged arrows show various transportation routes of modern sediments (mega-sequence unit M-C) into remnant forearc troughs east of the Huatung Ridge. Black arrows: clockwise rotation of the Lutao volcanic island and Lanyu volcanic island (Data from Zhao et al., 2016). BHWL: bathymetric high west of the Lanyu Volcanic Islands. RFT: remnant forearc trough east of the Lichi Mélange. Other abbreviations are similar to previous ones.

the Coastal Range during the obduction in the last 1 Ma (Fig. 14H).

6.2. Key to understand temporal-spatial variations of the dynamic forearc stratigraphy onshore the Coastal Range

Temporal-spatial variations of the forearc stratigraphy onshore the Coastal Range are recognized on the basis of following study: 1) precise age determinations of coherent flysch sequences in some key sections across the structure in four remnant forearc troughs east of the Tuluanshan fault; 2) detailed survey on field occurrences and age determination of the Lichi Mélange west of the Tuluanshan fault; and 3) geological comparisons of the forearc stratigraphy and sedimentation onshore the Coastal Range and the active oblique collision zone offshore SE Taiwan. Among these independent studies, the nature of the Lichi Mélange plays the key role in understanding forearc geology of the Coastal Range.

The Lichi Mélange exposes continuously for 50 km in length from Taitung to Yuli in the western Coastal Range (Fig. 3B; Hsu, 1956, 1976). However, the exposure width of the Lichi Mélange narrows from 5 km west of the Taiyuan remnant forearc trough near Taitung (22°40′N) in the south northward to < 1 km west of the Loho remnant forearc trough near Yuli (23°20′N), and is almost unnoticed west of the Suilien remnant forearc trough in the north near Hualien (24°00′N; Fig. 3A).

6.2.1. Previous study on age of the Lichi Mélange

Chang (1967b, 1968, 1969) systematically studied the stratigraphic distributions of planktonic foraminifera in forearc strata onshore the Coastal Range. He pointed out that the Lichi Mélange in its type locality in the southernmost Coastal Range is Late Miocene age (= *Globigerina nepenthes* Zone; Chang, 1967b). The age could even extend to late Pliocene (= *Sphaeroidinella dehiscens/Globorotalia tosaensis* Subzone of *Sphaeroidinella dehiscens* Zone; Chang, 1968) in other sections north of the type locality. He also noticed that calcareous tests of foraminifera in the highly sheared Late Miocene mélange are poorly preserved or even barren of micro-fossils (marked as "x" in Fig. 20), presumably due to intensive dissolutions of calcareous tests by a high stress caused by compressive tectonics. In contrast, preservation of foraminifera in the broken formation is much better than in the mélange.

6.2.2. Slumping olistostrome model confuses the true depositional age of the Lichi Mélange

In the past four decades various geological models have been proposed for the mechanism responsible for development of the Lichi Mélange in the Coastal Range (see review in Huang et al., 2008). Significance of Late Miocene microfossils in the Lichi Mélange determined by Chang (967b) was thus controversially interpreted. Among these controversial interpretations, the sedimentary olistostrome slumping model challenges the significance of Late Miocene age of the Lichi Mélange (Wang, 1976; Page and Suppe, 1981). The olistostrome model proposed that materials of the Lichi Mélange, including fine particles of argillaceous matrices and large mafic to ultra-mafic blocks, were all transported from the exhumed accretionary prism eastward into the western North Luzon Trough forearc basin by sedimentary slumping processes (Fig. 18A). Therefore, the Lichi Mélange in the west was interpreted to be facies changing with the coherent young flysch sequences in the east stratigraphically. Accordingly, only the youngest microfossils of the Late Pliocene age (~3 Ma) would represent the true indigenous fauna of the Lichi Mélange, whiles the Late Miocene-Early Pliocene microfossils were totally considered as reworked ones (Huang, 1969; Chi et al., 1981; Barrier and Muller, 1984).

However, neither Late Miocene-Early Pliocene strata nor non-metamorphosed Miocene mafic- and ultra-mafic rocks had been ever found in the Central Range (Chang, 1975; Yui et al., 2009). The interpretation of stratigraphic facies changes between the Lichi Mélange and the coherent flysch sequences is nothing else but alternations of different degrees of tectonic thrusting, shearing, disruptions and mixture of the broken formation and the mélange in the footwall side of the Tuluanshan fault (Fig. 16A, B; Huang et al., 2008; Lin et al., 2008). We checked the published fossil data in two key sections (Fengnan section in Fig. 19A, and the Chuiyuanshan section in the northwestern flank of Taiyuan syncline, Fig. 19B) published by Barrier and Muller (1984), and re-draw their sampling locations into the base map we used during field surveys. Fig. 19 shows that their study samples include two distinct age groups of Zone NN11 (Late Miocene) and Zone NN15 (Pliocene), respectively, in different locations with different field occurrences. In the footwall side (or west) of the Tuluanshan fault, the sample group that they dated as the Late Miocene age (Zone NN11) occur always west of the Pliocene sample group (Zone NN15; Fig. 19). Both age intervals are equivalent to our lower sequence unit S-1 and middle sequence unit S-2, respectively (Fig. 19; Significance of the sequence unit S-1 and unit S-2 will be discussed in the following Section 6.3). The Late Miocene samples (for examples, samples no.12O, 13C and 13B in Fig. 19A; and samples no. 19A, 19D, 26 F and 26 G in Fig. 19B) were collected from the intensively sheared mélange (= sequence unit S-1; marked as the dark-gray area in Fig. 19). No any Pliocene calcareous nannoplankton was reported in these Late Miocene samples (see Tables 1 and 2 of Barrier and Muller, 1984). On the other hand, the rock samples of the young Pliocene age group (Zone NN15) were collected either from the basal coherent flysch strata (= sequence unit S-2; samples 69E-U; 70A-C in Fig. 19A) of the Taiyuan remnant forearc trough (marked as dotted pattern in Fig. 19) in the hanging wall side (or east) of the Tuluanshan fault, or were collected from the deformed flysch without stratification of the broken formation of the Lichi Mélange (although they regarded as slumping folding) immediately west of the Tuluanshan fault (= sequence unit S-2; samples 12A-G, 71A-C, 13A, L in light-gray area of Fig. 19A; samples 26A-E, H; 50A-I; 21A-U; 24 and 25 in light-gray area of Fig. 19B). Again, no Miocene indices

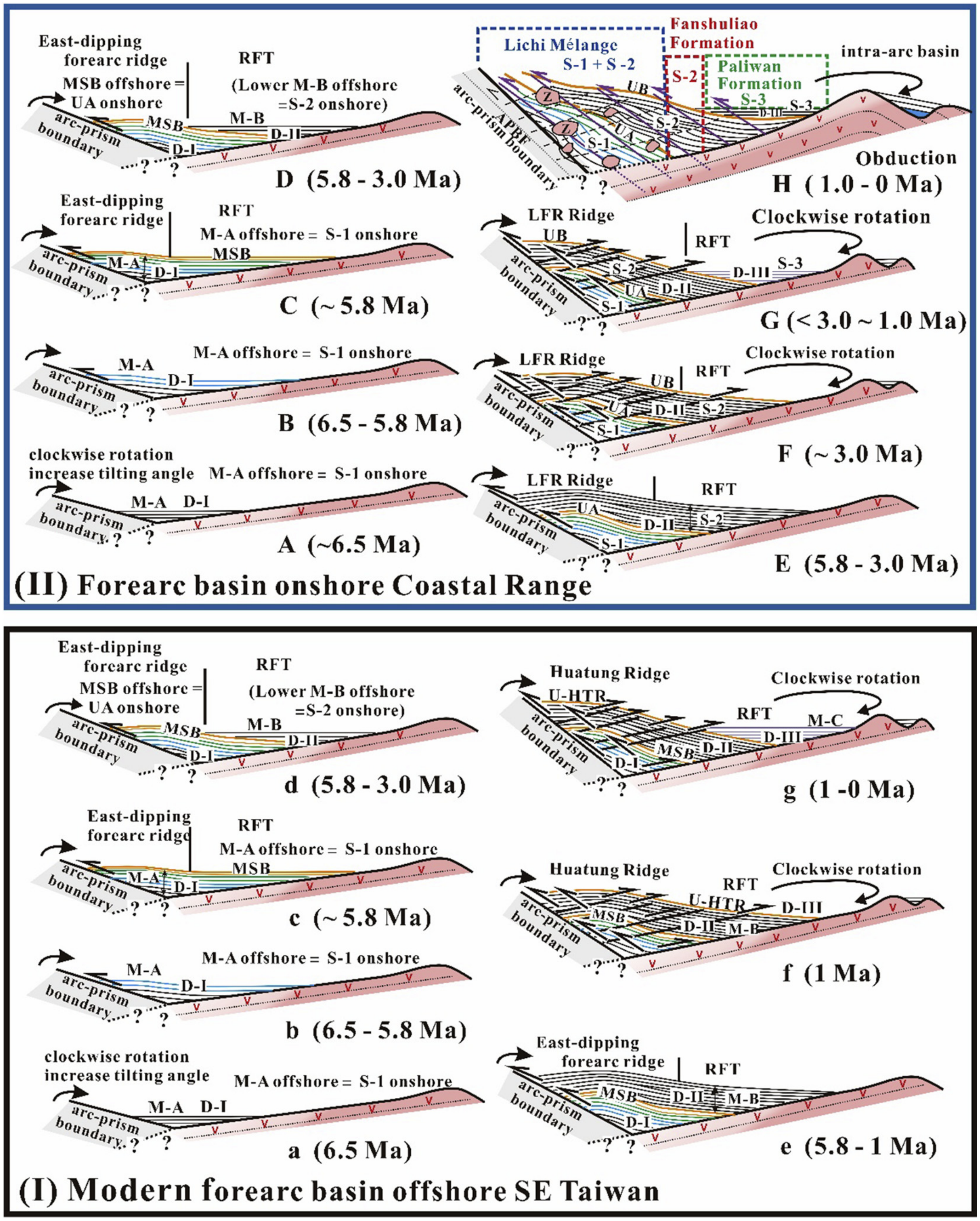

Fig. 14. Processes of forearc sedimentation, juxtaposed stratigraphy and deformation in the modern North Luzon Trough forearc basin offshore SE Taiwan (a–g within black line square I) and onshore the Coastal Range, eastern Taiwan (A–G within blue line square II). Three forearc sequences offshore (units M–A, M–B and M–C) and onshore (units S–1, S–2 and S–3) are all bounded by unconformities (onshore: UA: 5.8 Ma and UB: 3-2 Ma; offshore: MSB: 5.8 Ma and U-HTR: ~1 Ma). Figures are not in scale. Small curved small arrow: clockwise rotation with increase of tilting angle of rear accretionary prism due to frontal accretion along the Manila trench; large curved large arrow: clockwise rotation of forearc and volcanic arc during oblique collision between the volcanic arc and the accretionary prism. Abbreviations are similar to previous ones. Details see Section 7.

were documented in these young Pliocene samples whatever deformed as a broken formation of the Lichi Mélange west of the Tuluanshan fault or the basal thick coherent flysch sequences east of the Tuluanshan fault (Tables 1 and 2 of Barrier and Muller, 1984).

These results indicate that the mapped Lichi Mélange west of the Tuluanshan fault (Hsu, 1976; Wang and Chen, 1993; Lin et al., 2008) includes two different age intervals and field occurrences: Late Miocene (sequence unit S-1, 6.5–5.8 Ma) mélange mixed with igneous mafic- and ultra-mafic blocks and young Pliocene (sequence unit S-2, 3.9–3.7 Ma) broken formation with indiscernible stratification west of the Tuluanshan fault (Fig. 19). However, similar age interval (sequence unit S-2, 3.9–3.7 Ma) might appear as a part of the coherent flysch east of the Tuluanshan fault. They are not in sedimentary facies change, but are contacted by faults tectonically.

The slumping olistostrome interpretation is totally contradictory to the juxtaposed forearc stratigraphy with characteristic temporal-spatial distribution pattern and *syn*-sedimentation deformation of our new study results onshore the Coastal Range (Figs. 3B and 5; discussed below in Sections 6.3 and 6.4) and what had observed in seismic profiles in the active oblique collision zone offshore. The slumping olistostrome model doesn't fit the fact that young Pliocene coherent flysch sequences (sequence units S-2 or S-3) in the east can thrust over the

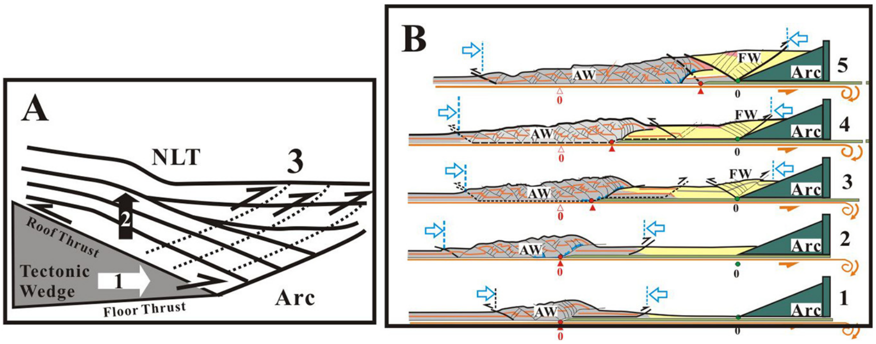

Fig. 15. Two controversial structure models proposed previously to interpret forearc deformation offshore SE Taiwan. A): 'tectonic wedge' model (Reed et al., 1992; Chi et al., 2003); B): "double wedges model" (Malavieille and Trullenique, 2009). AW: accretionary wedge; FW: forearc wedge. For 'tectonic wedge' model, 1: inserting rear accretionary wedge eastward into forearc basin during forearc sedimentation; 2: uplifting and folding in western forearc basin; and 3: backthrusting. Details see Section 5.5.

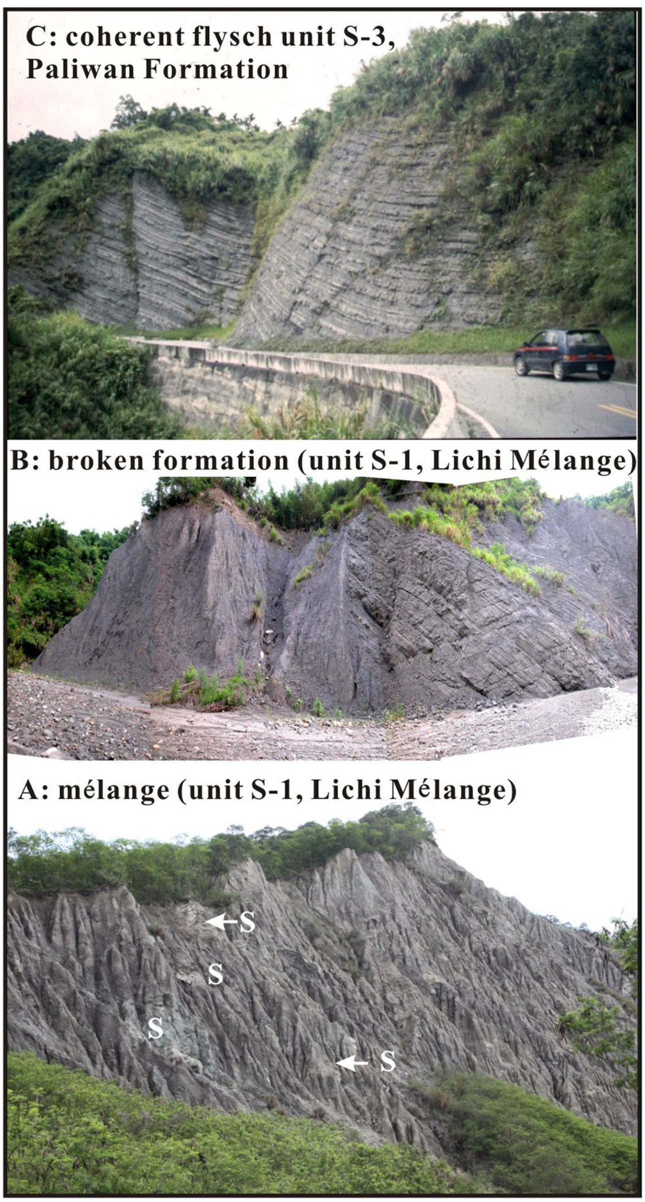

Fig. 16. Field occurrences of the Lichi Mélange (A: mélange; B: broken formation) and coherent flysch sequences (C) onshore the Coastal Range.

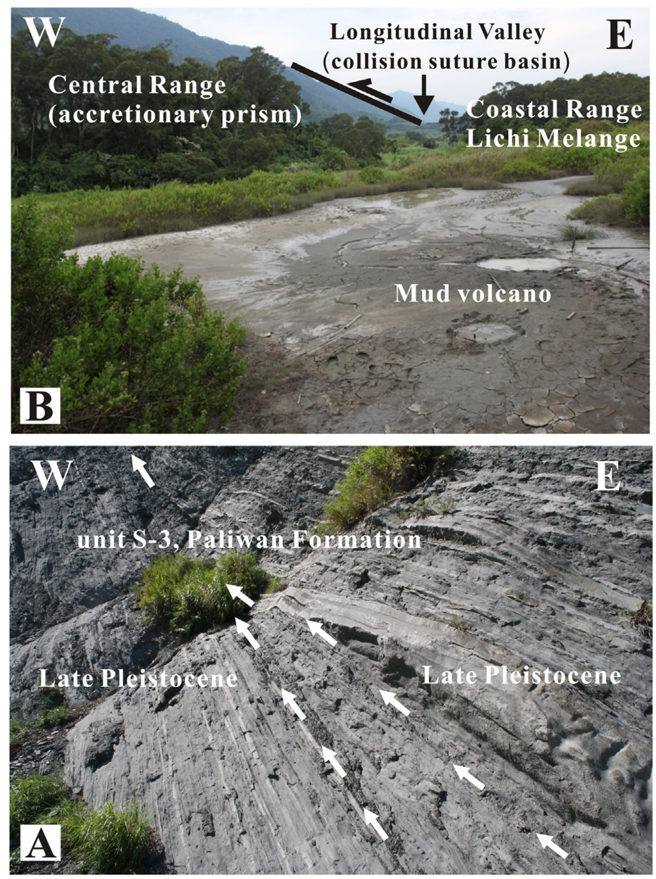

Fig. 17. Field occurrence of A): coherent flysch sequence associated with a westward on-lapping feature exposed along the northern river bank of the Hsiukuluan-Chi River in the southern Suilien remnant forearc trough, northern Coastal Range; B) a modern mud volcano in the Lichi Mélange, western Coastal Range, comparable with seismic profile observed in Line 2014-1 (md in Fig. 9) in the active subduction zone offshore SE Taiwan.

Late Miocene Lichi Mélange (lower sequence unit S-1) in the west (Fig. 3B). Furthermore, if there was any allochthonous block being slumped from the Central Range into the North Luzon Trough forearc basin (Fig. 18A), we should find various-sized angular clasts of the Pre-Cenozoic metamorphic marble, green and black schists, phyllite, gneiss, sandstones and slates in the Lichi Mélange frequently. But none of such metamorphic blocks was ever found in the Lichi Mélange in the last six decades (Hsu, 1956, 1976; Wang and Chen, 1993; Lin et al., 1999; Huang et al., 2000, 2006, 2008; Lin et al., 2008; Lin, YC, 2011b; Lin, CT, 2011a). Instead, Miocene mafic-and ultra-mafic blocks of a SSZ origin and volcanic agglomerate, tuff, andesitic blocks of the Luzon Arc were commonly observed in the Lichi Mélange (Huang et al., 2008). Geochemistry analyses of gabbro blocks in the Lichi Mélange onshore the Coastal Range show signals (for example Nb depleted; Jahn, 1986) similar to SSZ signals from the Mariana forearc igneous rocks (Pearce et al., 1984; Stern, 2004), suggesting a rock assemblage formed in a spreading forearc basin related to initiation subduction of the South China Sea oceanic lithosphere. We regard that these mafic- and ultra-

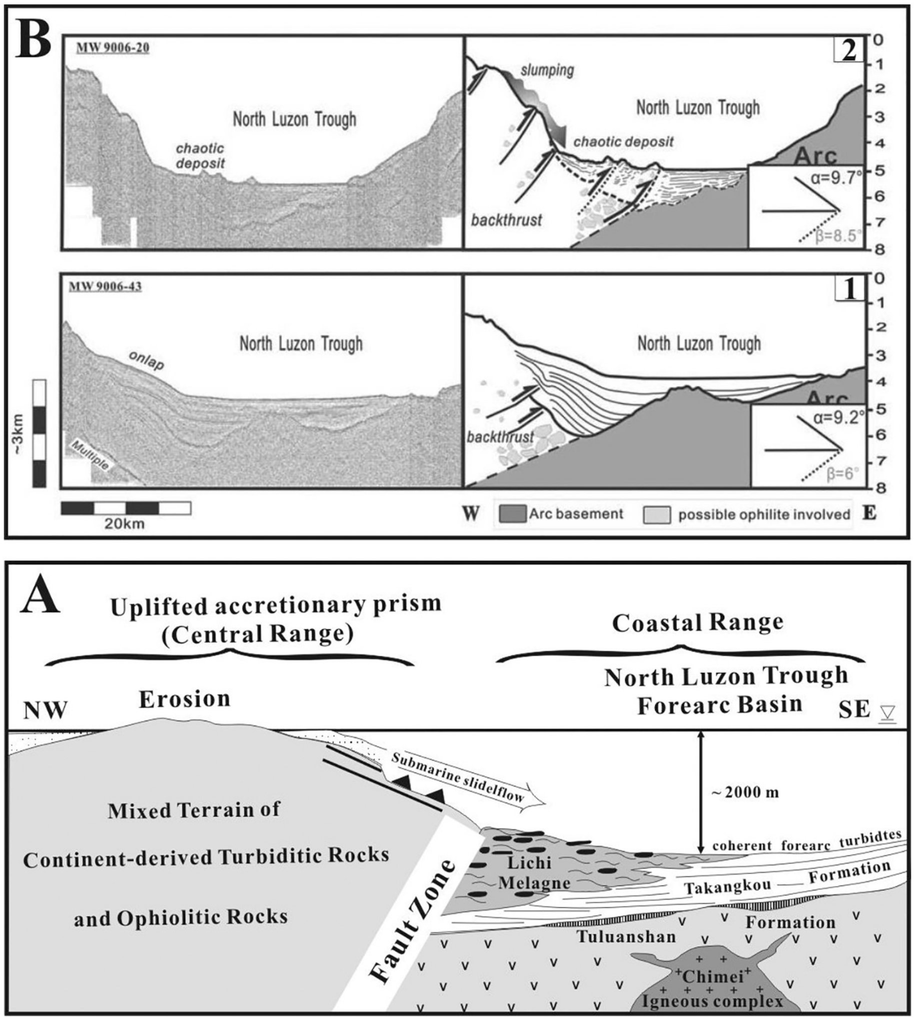

Fig. 18. (A) Sedimentary olistostrome model proposed previously responsible for development of the Lichi Mélange (Page and Suppe, 1981); B) the olistostrome model was followed by Chi et al. (2014) to interpret their seismic profiles offshore SE Taiwan. Details see Section 6.2.2.

mafic blocks were emplaced by westward thrusting tectonically from the forearc and arc off SE Taiwan by obduction in the last 1 Ma (Fig. 14H; Huang et al., 2008; see also Section 8).

Without any field survey on various types of deformation onshore Coastal Range, Chi et al. (2014) followed the olistostrome model to interpret their low-resolution seismic reflections as evidence of mass

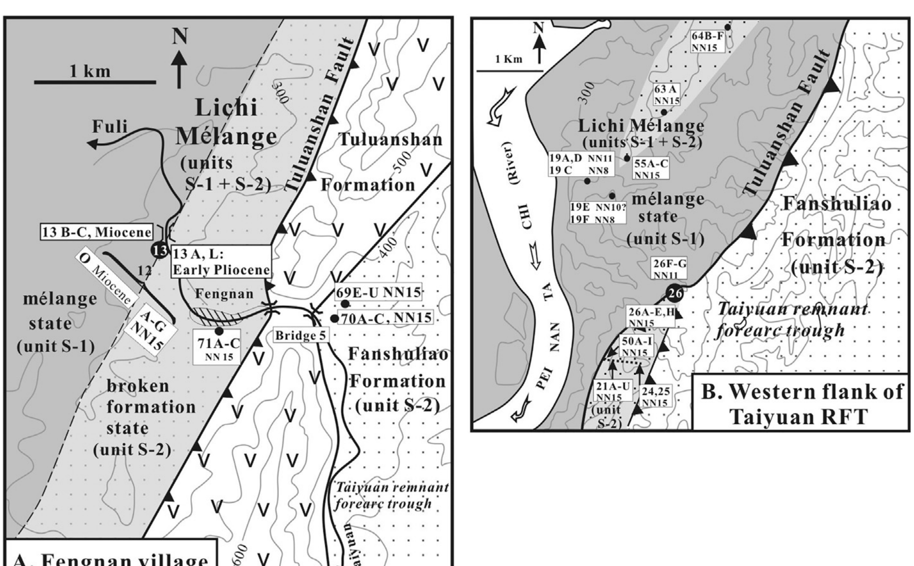

Fig. 19. Geological map of the Lichi Mélange (sequence units S-1 + S-2) and the Fanshuliao Formation (sequence unit S-2) in the Taiyuan remnant forearc trough, southern Coastal Range, with sampling sites and a biostratigraphy study on calcareous nannoplanktons by Barrier and Muller (1984) in (A) Fengnan section and (B) Chuiyuanshan section in western flank of the Taiyuan remnant forearc trough. Mélange and broken formation are shown by dark and light gray area, respectively. Sequence stratigraphy unit S-2 occurs in both sides of the Tuluanshan fault. Details see Section 6.2.2.

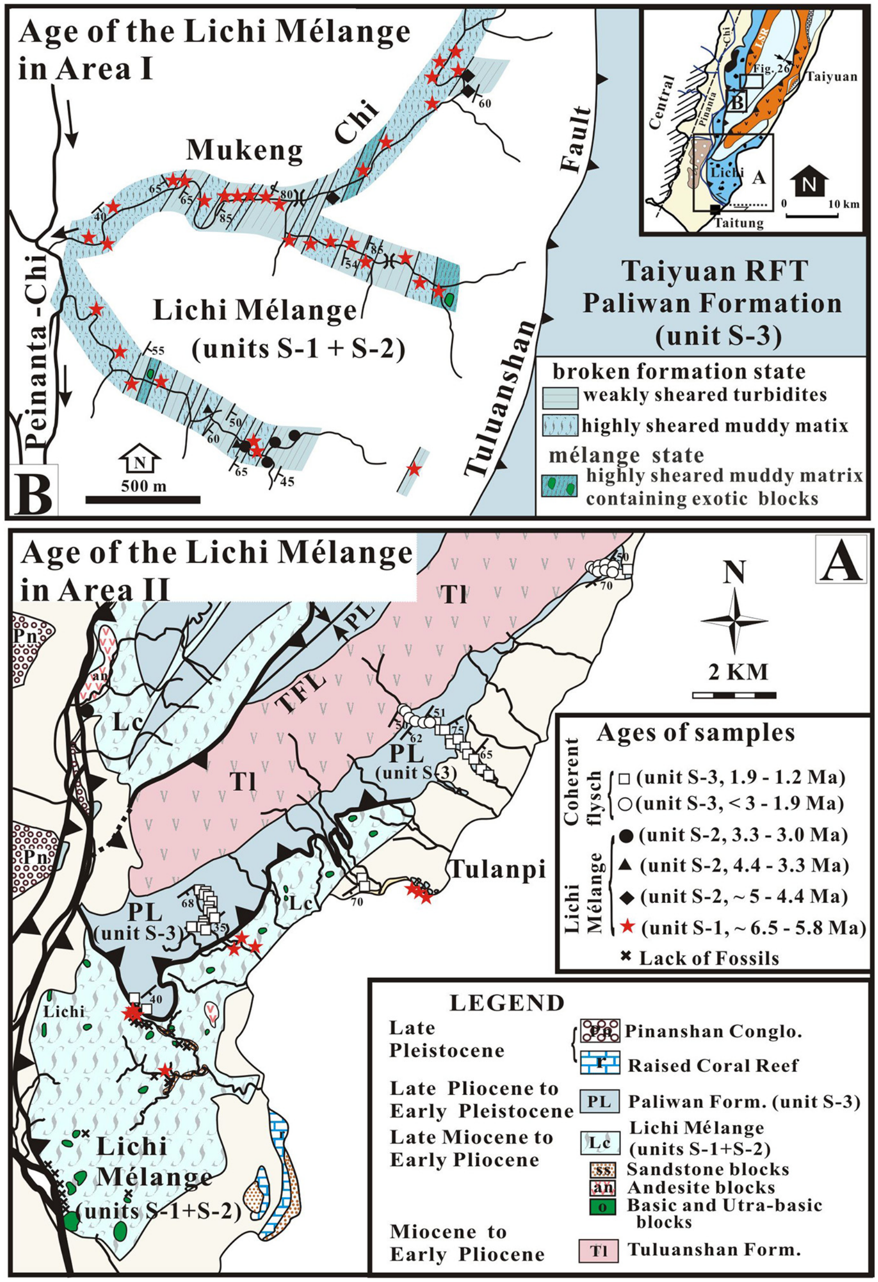

Fig. 20. Sampling locations and depositional age of the Lichi Mélange in the southern Coastal Range (geological map after Lin et al., 2008. Detailed sampling number and fossil content are shown in Chen et al., 2015, 2017). A) Sampling along several short river sections of the Taitung remnant forearc trough in the key area II; B) along the Mukeng-Chi and its southern tributary west of the Taiyuan remnant forearc trough in the study key area I.

slumping in the North Luzon trough forearc basin offshore SE Taiwan (Fig. 18B). They further implied that sedimentary slumping process was the main mechanism to develop the Lichi Mélange onshore the Coastal Range. The main mechanism to produce their mélange is "over-steeping" of the accretionary prism by inserting a 'tectonic wedge' to provide allochthonous blocks eastward into the western part of the North Luzon Trough forearc basin by mass slumping. However, due to intensive deformation in the Hengchun Ridge accretionary prism (Huang et al., 1997), no seismic reflection can be observed in any published seismic profile across the Hengchun Ridge accretionary prism in the last three decades (including *R/V Moana Wave* in 1990, 6-channel; Reed et al., 1992; *R/V Experiment 2* in 1987, China; 24-channels; Huang et al., 2001; *R/V L'Atalante* in 1997, 6-channel; Malavieille et al., 2002; *R/V Maurice Ewing* in 1995, 132-channel; McIntosh et al., 2005; and *R/V Tangbo* of the Guangzhou Marine Geological Survey, China, 480-channels; Li et al., 2007; Huang et al., 2008, 2018). Their slumping interpretation implies that west-vergent thrusting played no role during sedimentation of the forearc sequences. Consequently, only backthrust structures were the main mechanism to deform the forearc strata (Fig. 18B). The thrust-up forearc sequences west of the east-vergent thrust front (Fig. 18B-1, 2) was interpreted as deformed chaotic deposits mixed with slumping materials from the accretionary prism. However, our 480-channel seismic profile of Line 2014-2 clearly demonstrates that seismic reflections of the mega-sequence unit M-B were disturbed by east-vergent backthrusting without any definite evidence of slumping feature. Therefore the basin floor deepens from the western North Luzon Trough eastward fault by fault until the backthrust front in the basin center (Fig. 11). Moreover, no 'tectonic wedge' can be definitely recognizable in any seismic profile over the rear accretionary prism of the Hengchun Ridge offshore

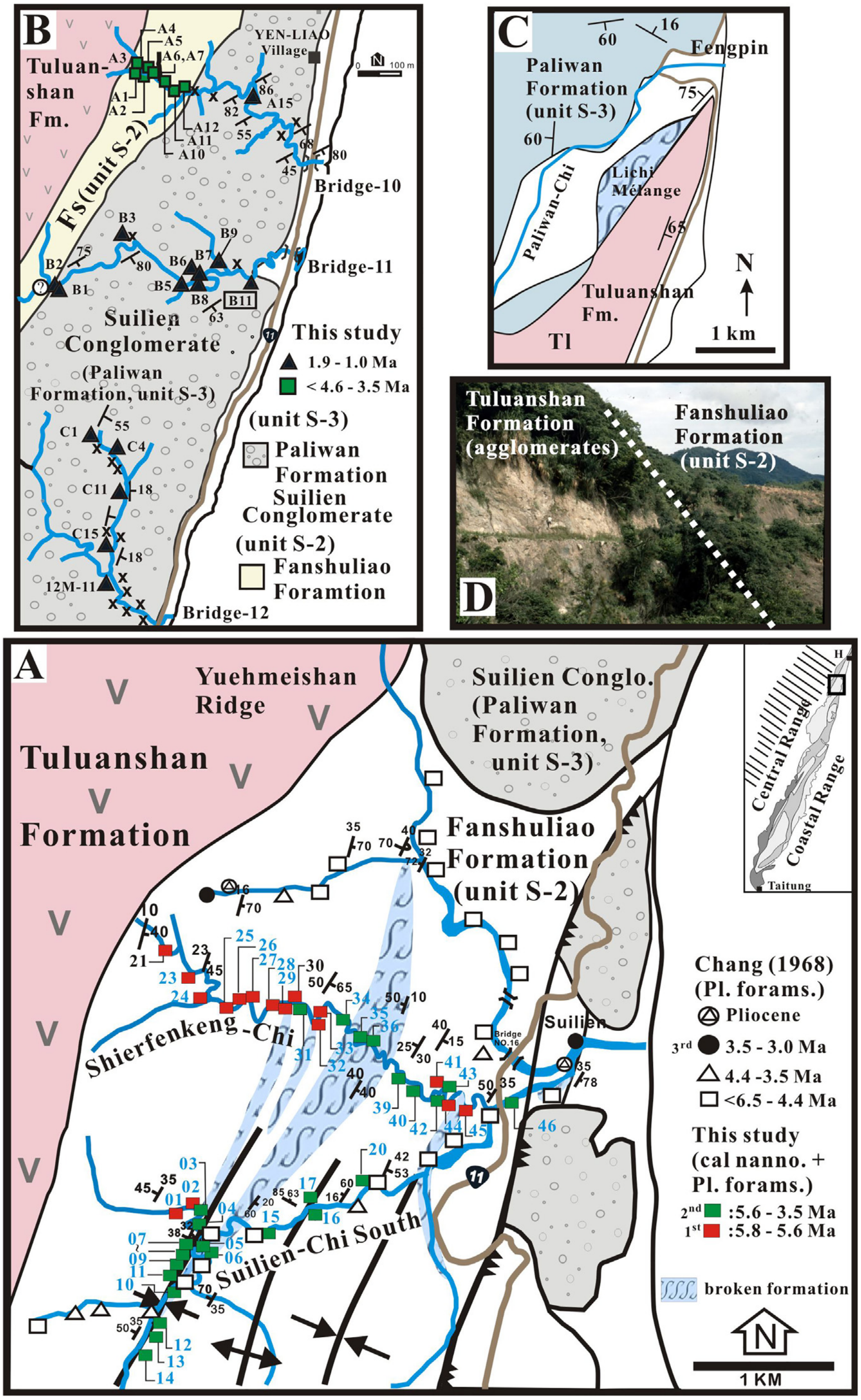

Fig. 21. Geological map and field occurrence of the Suilien remnant forearc trough in the northern Coastal Range. (A) Geological map and sampling locations of key area I along the Suilien-Chi River, Shierfenkeng-Chi River and its distributaries. Sampling locality and biostratigraphy study results by Chang (1968) are integrated in (A); (B) geological map and sampling locations along three creek sections west of Bridge-10, -11 and -12 across the Suilien Conglomerate; (C) a limited exposure of the Lichi Mélange in the eastern Suilien remnant forearc trough south of Fengpin town (after Wang and Chen, 1993); (D) unconformity (white dashed line) between volcanic agglomerates (Tuluanshan Formation) of the Yuehmeishan Volcanic Ridge and the lower coherent flysch sequence (sequence unit S-2, Fanshuliao Formation) in the upper reach of the Suilien-Chi North River.

southern Taiwan. The slumping olistostrome model can neither explain the characteristic temporal-spatial occurrence of three juxtaposed forearc sequence stratigraphy offshore, nor fit the structure characteristics observed onshore the Coastal Range, eastern Taiwan (see Section 5.5 above and Section 7 below).

6.3. Re-study on age of the Lichi Mélange

Our biostratigraphic study on the Lichi Mélange focused on three key areas: 1) along the Mukeng-Chi River and its southern tributary west of the Tuluanshan fault in the southern Coastal Range (Fig. 20B), 2) along the Pinanta-Chi River around the type locality (Lichi Village) and several short east-running river sections across the Taitung remnant forearc trough in the southernmost Coastal Range (Fig. 20A; Chen et al., 2015), and 3) in the Loho remnant forearc trough center of the middle Coastal Range (Fig. 24A; Lin, YC, 2011b; Chen et al., 2015). The age ranges of the Lichi Mélange in these three key areas are discussed below. The details of the faunal list and stratigraphic distributions of planktonic foraminifera along the Mukeng-Chi River (key area I) and along the Pinanta-Chi River (key area II) were published elsewhere (Chen et al., 2017). Stratigraphic distributions of planktonic foraminifera show that the age of the Lichi Mélange ranges from Late Miocene to Late Pliocene or 6.5–3.0 Ma with possibly a short hiatus (Fig. 5).

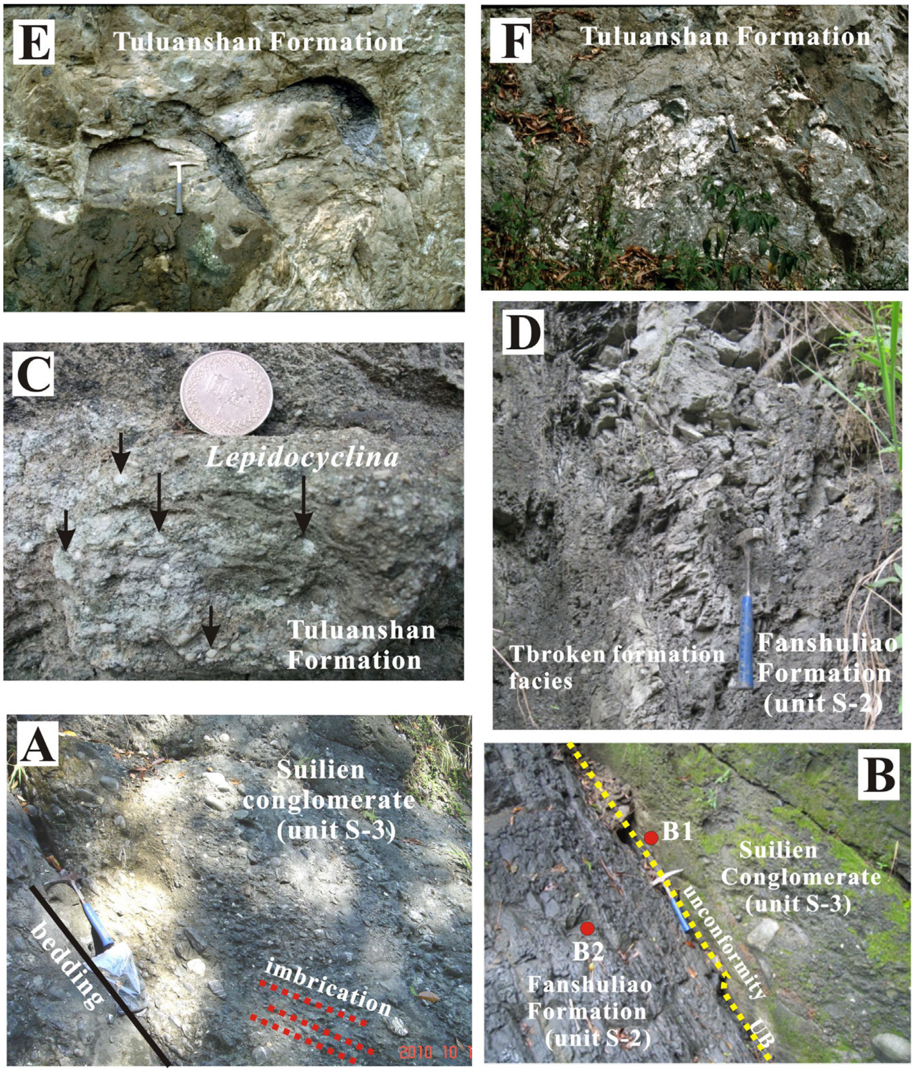

Fig. 22. Field occurrence of the Suilien remnant forearc trough, northern Coastal Range. (A) Elongated pebbles of the Suilien Conglomerate showing imbrication structures (red dotted lines) in the creek section west of Bridge-11; (B) Samples B-2 (Late Pliocene, Fanshuliao Formation, sequence unit S-2, ~3 Ma) and B-1 (Pleistocene, < 1.9 Ma, Suilien Conglomerate, sequence unit S-3) exposed along the creek section west of Bridge-11; (C) larger foraminifera *Lepidocyclina* (white spots) in a limestone block on the top of the Tuluanshan Formation; (D) highly disrupted flysch without stratification of broken formation in the Fanshuliao Formation in the Suilien remnant forearc trough; (E) mudstone with Pliocene foraminifera (~3.0 Ma) deposited on the cavity on the unconformity surface; (F) limestone blocks presumably derived from the Kankou Limestone (a fringing reef caps on the Chimei volcanic island; Huang et al., 1995) on the unconformity surface. (For interpretation of the references to colour in this figure legend, the reader is referred to the web version of this article.)

6.3.1. Key area I

In the key area I along the Mukeng-Chi river sections in the footwall side of the Tuluanshan fault, the majority of the Lichi Mélange contains Late Miocene fauna (sequence unit S-1, 6.5–5.8 Ma marked as red solid star in Fig. 20B) of *Globorotalia plesiotumida* (FO: 8.5 Ma) and *Globoquadrina dehiscens* (LO: 5.8 Ma) with some species extending from Late Miocene to Early Pliocene like *Sphaeroidinellopsis seminulina*, *Dentoglobigerina altispira* and *Globoturborotalita nepenthes* before first appearances of Pliocene indices like *Sphaeroidinella dehiscens* (FO: 5.4 Ma) and *Globorotalia tumida* (FO: 5.5 Ma). Calcareous nannofossils were rare in the Lichi Mélange of the Key area I. However, Late Miocene *Discoaster quinqueramus* (LO: 5.6 Ma) was found in this interval of the key area I (Chen et al., 2017). Therefore the interval was dated as < 8.5–5.8 Ma (Chen et al., 2017), but had better be assigned as 6.5–5.8 Ma, because the sedimentary forearc sequences in the Coastal Range were all laying on the west-dipping volcanic arc basement younger than 6.6 Ma (Fig. 5; Lo et al., 1994).

In addition to the Late Miocene age, there were also some samples contain Pliocene fauna (~30% of the studied samples; equivalent to the sequence unit S-2) with *Sphaeroidinellopsis seminulina* (LO: 3.6 Ma), *Dentoglobigerina altispira* (LO: 3.5 Ma) and *Globoturborotalita nepenthes* (LO: 4.4 Ma), but without *Globoquadrina dehiscens* (LO: 5.8 Ma). Because of rare occurrence to absence of age diagnostic key index of calcareous nannoplankton *Ceratolithus acutus* (Zone NN12, 5.35–5.04 Ma) in the interval between last occurrences of *Globoquadrina dehiscens* (LO: 5.8 Ma) or *Discoaster quinqueramus* (LO: 5.6 Ma) and *Globoturborotalita nepenthes* (LO: 4.4 Ma), there could have various interpretations of the biostratigraphy of either a continuous deposition from the Late Miocene to early Pliocene (5.5–3.4 Ma, Chen et al., 2017) or association with a short hiatus at ~5.8 Ma or in 5.8–5.0 Ma (Fig. 5). Based on structure character and a comparable temporal-spatial distribution feature of the forearc sequence, we prefered that there could have a short hiatus (UA in Fig. 5) at ~5.8 Ma in the Lichi Mélange of the study section.

6.3.2. Key area II

Samples of the Lichi Mélange collected along the Pinanta-Chi river in the key area II were mostly barren of microfossils presumably due to dissolutions by high tectonic stress (marked as x in Fig. 20A; Chang, 1967b). But once microfossils were found, they were of Late Miocene age (6.5–5.8 Ma). However *Globorotalia tosaensis* or/and *G. multicamerata* (LO: 3.0 Ma) were found in samples collected near Lichi Village (sample LM01 in Chen et al., 2017). This suggested an age as young as 3.3–3.0 Ma (Fig. 20A). In conclusion, microfossil study on the Lichi Mélange west of the Tuluanshan fault had an age range from Late Miocene (sequence unit S-1; 6.5–5.8 Ma) to Early Pliocene (unit sequence S-2; 5.8–3 Ma; Figs. 5 and 27).

6.3.3. Key area III

The key area III is located in the Loho remnant forearc trough center

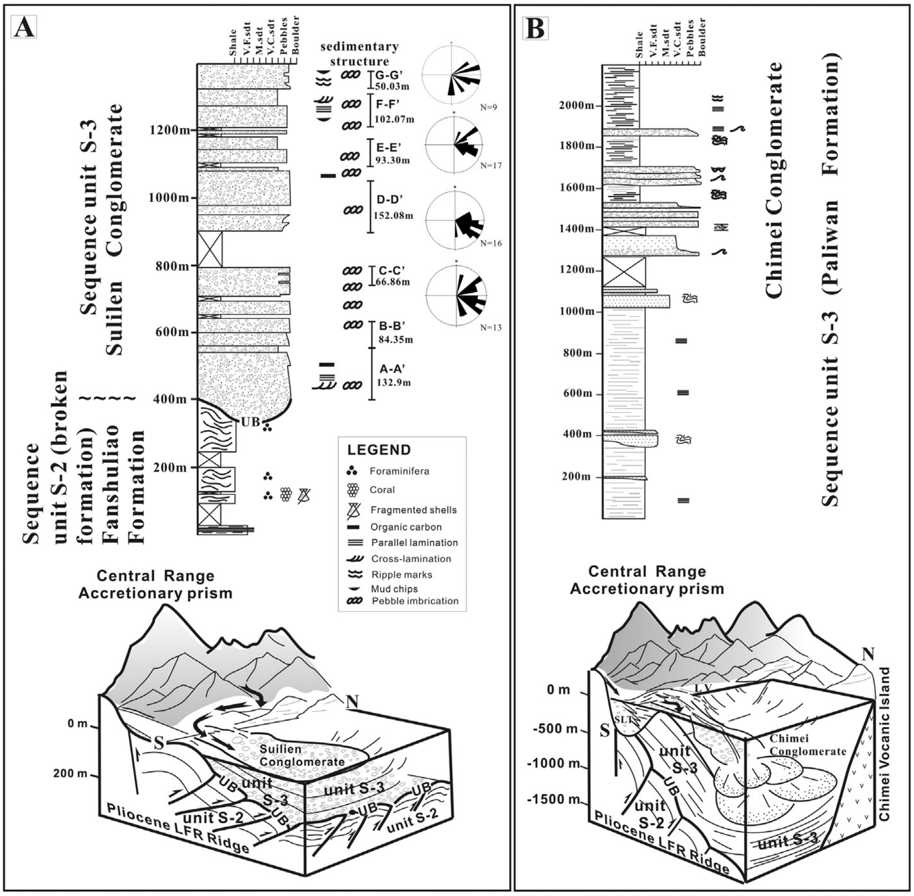

Fig. 23. Lithological column, paleocurrent indicated by imbrications of pebbles in rose diagram and paleo-environment reconstruction of: (A) the Suilien Conglomerate (after Lin, CT, 2011a) and (B) Chimei Conglomerate (after Dorsey and Lundberg, 1988) in the Suilien remnant forearc trough. Black arrows: transportation routes; UB: unconformity (~3–2 Ma) between the Fanshuliao Formation (sequence unit S-2, < 4.6–3.5 Ma) and the overlying Suilien Conglomerate (part of sequence unit S-3, < 1.9–1 Ma). LFR: Pliocene Loho Forearc Ridge deformed at ~3 Ma; SLT: suture basin of the Southern Longitudinal Trough. Details see Sections 6.5.6 and 6.5.7.

(Fig. 24A). The age of the Lichi Mélange was dated as < 4.3–3.4 Ma (Chen et al., 2015). This age was confined within the age range of the type Lichi Mélange in key areas I and II (sequence units S1 + S-2; 6.5–3.0 Ma; Fig. 20). Significance of the Lichi Mélange in the Loho remnant forearc trough center will be discussed in Section 6.6.3.

6.4. How can young strata thrust westward over old sequences?

The most characteristic forearc structure in the Coastal Range is that the young coherent flysch sequences in the east thrust westward over the old and highly sheared Lichi Mélange in the west (Fig. 3B). For examples in the southern Coastal Range, Latest Pliocene-Pleistocene coherent flysch sequences (unit S-3, Paliwan Formation, < 3.0–1 Ma) in the east either thrust over the Late Miocene Lichi Mélange (unit S-1, 6.5–5.8 Ma) along the section G-G′, or thrust over the Late Miocene-Early Pliocene Lichi Mélange (sequence units S-1 + S-2, 6.5–3.0 Ma) along the section F-F′, in the west (Fig. 3B). Along the profile E-E′ the Pliocene coherent young flysch (part of sequence unit S-2, Fanshuliao Formation, 3.9–3.7 Ma; Barrier and Muller, 1984) in the east thrusts westward over the Late Miocene Lichi Mélange in the west (sequence unit S-1, 6.5–5.8 Ma; Figs. 3B). Along the section D-D′ in the Loho remnant forearc trough of the middle Coastal Range, the coherent flysch (upper part of the sequence unit S-2, Fanshuliao Formation, 3.4–3.0 Ma) thrusts over the Lichi Mélange (lower part of the sequence unit S-2, 4.4–3.4 Ma) in the west (Fig. 3B).

Such a characteristic thrust structure that young sequences thrust over old strata, instead of old strata thrust over young sequence as it is commonly observed in the passive continental margin, could be achieved only under two precursory conditions: 1) sedimentation of the Late Miocene mudstones of the Lichi Mélange (sequence unit S-1, 6.5–5.8 Ma in Fig. 14a–d; see discussions Sections 6.3 and 7) must be deposited restrictedly in a depocenter in the western North Luzon Trough before the onset of sedimentation of the young flysch sequences in the east (sequence unit S-2, 5.8–3.0 Ma; Fig. 14d–E–F–G); and 2) the Late Miocene mudstones of the Lichi Mélange (sequence unit S-1) in the west had been deformed (like an east-dipping forearc ridge offshore in Fig. 14c) before it was covered unconformably by the young flysch sequences (sequence unit S-2, Fig. 14d) in the east.

6.5. The Suilien forearc segment in the northern Coastal Range

6.5.1. General geological features

The Suilien forearc segment northwest of the Chimei volcanic island in the northern Coastal Range (Fig. 4) is composed of volcanic agglomerates in the basement unconformably overlain by coherent sedimentary flysch sequences (> 4000 m thick) in the upper part (Figs. 5 and 21). Geology of the Suilien forearc segment is characterized by occurrences of two volcanic ridges, two independent thick conglomerate units, and no significant Lichi Mélange exposed west of the coherent flysch sequence which was either eroded by Hualien-Chi River or covered by modern fluvial deposits (Fig. 3; Hsu, 1956). Coherent flysch sequences in the Suilien remnant forearc trough are deformed as a major asymmetric syncline structure plunging southward (Fig. 3; Hsu, 1956; Chang, 1968; Wang and Chen, 1993).

6.5.2. Volcanic agglomerates in the basement

Volcanic agglomerates expose in both sides of the Suilien remnant forearc trough (Fig. 3). Both volcanic ridges constitute the same Chimei volcanic island accreted in the northern Coastal Range (Fig. 4). The present configuration of both volcanic ridges was resulted from arc-involved deformation during the obduction in the last 1 Ma. The Takangshan volcanic ridge (TVR in Fig. 4) southeast of the syncline axis represents the major part of the accreted Chimei Volcanic Island, whiles the agglomerate sequences of the Yuehmeishan volcanic ridge (YVR in

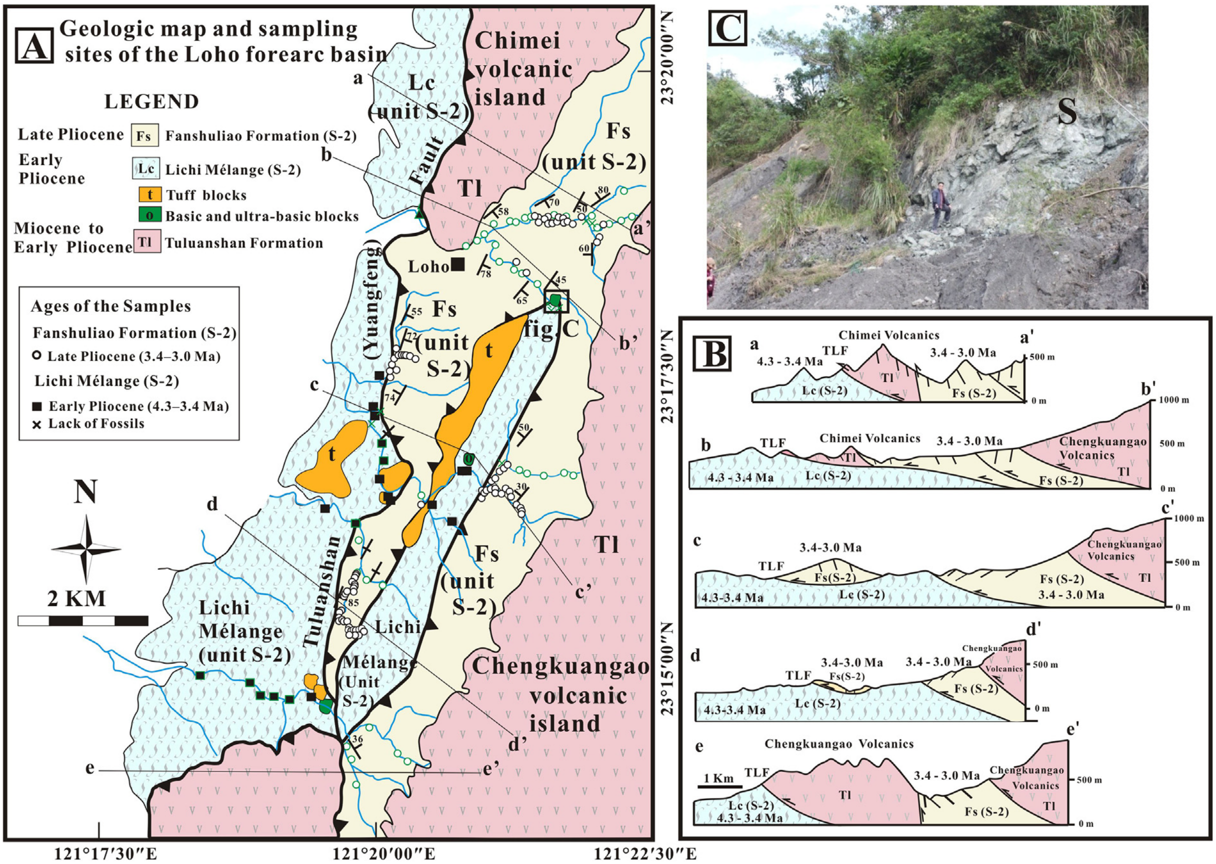

Fig. 24. Geological map of the Loho forearc segment in the middle part of the Coastal Range; (A) biostratigraphy study results (green color: Chang, 1969; black color: Chen et al., 2015; Detailed sample locations and fossil contents see Chen et al., 2015); (B) cross sections of the Loho forearc segment showing that the young coherent flysch sequence (part of sequence unit S-2, Fanshuliao Formation, 3.4–3.0 Ma) thrusts westward onto the old Lichi Mélange (part of sequence unit S-2, 4.3–3.4 Ma) in the west; (C) exposure of the Lichi Mélange with serpentinite blocks (marked as S) in the Loho remnant forearc trough center (location shown in A). TLF: Tuluanshan fault (*s.l.*) or the local Yuangfeng fault. (For interpretation of the references to color in this figure legend, the reader is referred to the web version of this article.)

Fig. 4) northwest of the syncline axis represent the upper part of the Chimei volcanic Island, but they were later thrust westward during the obduction (Z et al., 1995). On the top of the Yuehmeishan agglomerate volcanic ridge, there are some limestone (Fig. 22F) and mudstone blocks (Fig. 22E) filling in concavities along the unconformity surface between the volcanic sequence and the overlying sedimentary flysch sequence (Fig. 21D). The limestone blocks contain larger foraminifera *Lepidocyclina* (Fig. 22C) and corals identical to the fringing-reef fauna in the type Kangkou Limestone exposed along the Hsiukuluan-Chi River near Kangkou Village (Fig. 3A; Yabe and Hanzawa, 1929; Chang, 1969; Huang et al., 1988; Huang and Yuan, 1994; Huang et al., 1995). The Kangkou Limestone represents a fringing reef (~5.2 Ma) developed around the Miocene Chimei Volcanic Island after terminal volcanism at 6.6 Ma (Fig. 4; Huang et al., 1995). Occurrence of these limestone blocks at the unconformity surface (Fig. 22F) suggests that they were derived by slumping from the shallow-marine Kangkou fringing reef in the east. The blocks were then re-deposited into the deep Suilien remnant forearc trough on the west-dipping Chimei volcanic island. The mudstones in the concavities (Fig. 22E) contain Late Pliocene planktonic foraminifera (~3.0 Ma; Chang, 1968) similar to those found in the top of the sequence unit S-2 (Fanshuliao Formation; Fig. 21A).

6.5.3. The Lichi Mélange in the Suilien remnant forearc trough

Unlike other remnant forearc troughs in the middle and southern Coastal Range, no exposure of the Lichi Mélange is observed west of the Suilien remnant forearc trough in the northern Coastal Range (Fig. 3; Hsu, 1956). However, a little Lichi Mélange (0.5 km wide × 1.5 km long) exposes along a fault scarp between the volcanic agglomerate sequences and the coherent young flysch (sequence unit S-3, Paliwan Formation) south of Fengpin town in the southeastern Suilien remnant forearc trough (Fig. 22C; Wang and Chen, 1993). The Lichi Mélange in this little exposure is highly sheared without discernable stratification. Mafic- and ultra-mafic blocks were mixed in scaly argillaceous matrices showing a typical block-in-matrix feature like the type Lichi Mélange in the southern Coastal Range.

Occurrence of this little mélange exposure in the southeastern Suilien remnant forearc trough suggested that the Lichi Mélange can't be developed by the olistostrome slumping processes. If the materials of the Lichi Mélange were interbedded with the coherent flysch sequences as suggested by the olistostrome mass slumping model (Wang, 1976; page and Suppe, 1981), we should commonly find mafic- to ultra-mafic blocks in the main parts of the Suilien remnant forearc trough west of this little mélange exposure. But, no significant mélange exposure was found in the entire Suilien remnant forearc trough in the last six decades (Hsu, 1956, 1976; Wang and Chen, 1993; Lin et al., 1999).

6.5.4. Coherent flysch sequences in the Suilien remnant forearc trough west of the Chimei Volcanic Island

Coherent flysch sequences in the Suilien remnant forearc trough overlie the volcanic agglomerates unconformably (Figs. 3 and 21). Due to a south-plunging syncline deformation, the lower flysch sequences (sequence unit S-2; the Fanshuliao Formation) expose in the north, whereas the upper flysch strata (sequence unit S-3; Paliwan Formation) crop out in the south (Fig. 3).

6.5.4.1. Previous studies of the Fanshuliao Formation (sequence unit S-

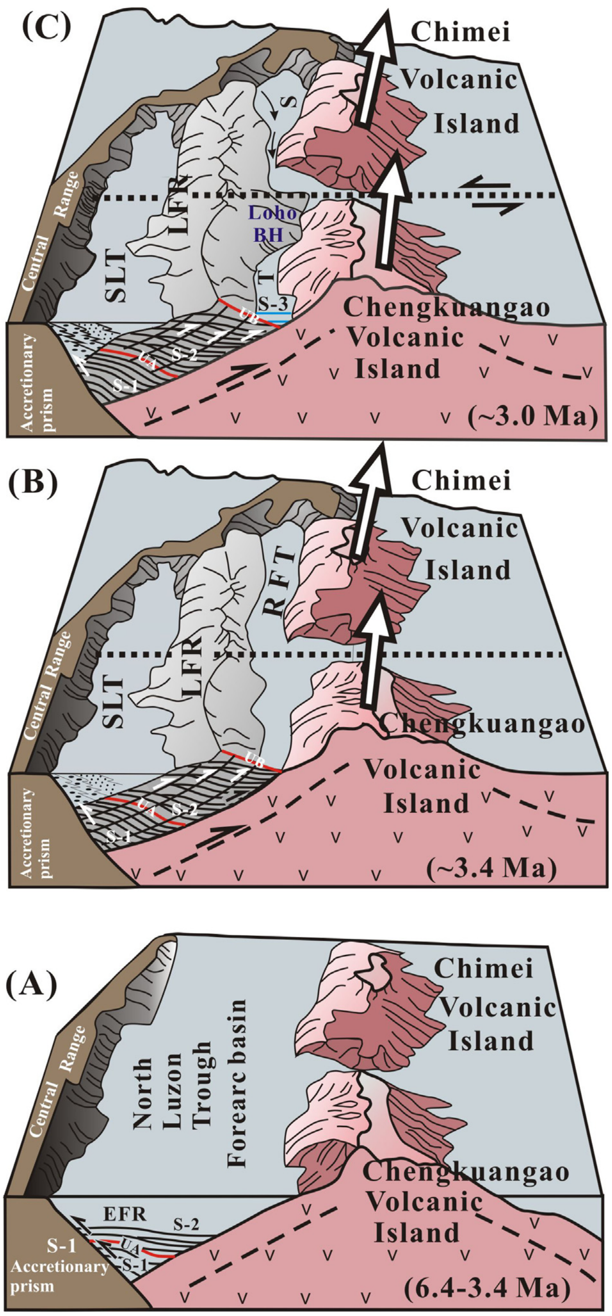

Fig. 25. Tectonic evolution of the Loho forearc segment in the middle Coastal Range. (A) sedimentation of sequence unit S-1 (6.5–5.8 Ma) and sequence unit S-2 bounded by UA unconformity in the North Luzon Trough forearc basin; (B) both sequence units S-1 and S-2 were deformed by bi-vergent thrusting as the Pliocene Loho Forearc Ridge; then (C) the arc basement and the Pliocene Forearc Ridge could have been offset by a left-lateral strike-slip fault to develop the Pliocene Loho bathymetric high west of the Chengkuangao volcanic island at ~3 Ma, like deformation and development of the modern 'BHWL' west of the Lanyu volcanic island offshore. Occurrence of the Pliocene Loho bathymetric high further lead to variations of the sedimentation of the youngest sequence unit S-3. BH: bathymetric high; EFR: east-dipping forearc ridge; LFR: Pliocene Loho Forearc Ridge.

2). The Fanshuliao Formation was primarily determined as Late Miocene (=*Globigerina nepenthes* Zone and *Sphaeroidinellopsis seminulina* Zone; Zones N16–18) with relative thin Late Pliocene interval (=*Sphaeroidinella dehiscence/Globorotalia tosaensis* Zone, N21, Chang, 1968). Similar planktonic foraminiferal assemblage was also found in part of the Lichi Mélange (Chang, 1967b). In addition to Pliocene nannoplankton assemblages of Zones NN12/13-15, Late Miocene calcareous nannofossils (for example *Discoaster quinqueramus*) were also reported from the Fanshuliao Formation. But these Late Miocene nannoplanktons were interpreted as reworked fossils as an evidence of the olistostrome deposits (Chi et al., 1981).

6.5.4.2. Fanshuliao Formation (S-2). To better understand the age of deposition and the spatial distribution of the forearc sequence unit S-2, we re-studied foraminifera and calcareous nannoplanktons in samples collected from the lower coherent flysch sequences exposed along the Suilien-Chi South River and its distributary Shirefenkeng-Chi River across the syncline structure (Fig. 21).

Distributions of microfossils in the Fanshuliao Formation are shown in Tables 1 and 2 for planktonic foraminifera, and Tables 3 and 4 for calcareous nannoplanktons, respectively. Highlights of the previous biostratigraphy study of planktonic foraminifera by Chang (1968) are included also in Fig. 21.

6.5.4.3. Results. Samples collected from both river sections include three age groups (Figs. 21A, B). Samples of the lowest group (I) contain Late Miocene indices of calcareous nannofossils (Tables 3 and 4) of Zone NN11 index *Discoaster quinqueramus* (LO: 5.6 Ma) with some long range species like *Helicosphaera carteri* (NN1–NN21) and *Discoaster variabilis* (NN4–NN16). Late Miocene planktonic foraminifera (Tables 1 and 2) of *Globoturborotalita nepenthes* (LO: 4.4 Ma), *Dentoglobigerina altispira* (LO: 3.5 Ma), *Sphaeroidinellopsis seminulina* (LO: 3.6 Ma) were found in the same samples. However, neither long-ranged Miocene index species of *Globoquadrina dehiscens* (LO: 5.8 Ma) nor Pliocene indices of *Globorotalia tumida* (FO: 5.5 Ma) and *Sphaeroidinella dehiscens* (FO: 5.4 Ma) was recovered in the Group (I) sample. The microplanktons in the group (I) samples suggest a very narrow age range of 5.8–5.6 Ma (marked as solid red solid square in Fig. 21A).

Samples of group (II) contain Pliocene calcareous nannofossils like *Ceratolithus acutus* (5.3–5.0 Ma), *C. rugosus* (NN12–19), *Reticulofenestra pseudoumbilica* (LO: 3.7 Ma) of Zones NN12–15 after extinction of *Discoaster quinqueramus* (LO: 5.6 Ma; Table 2). Early Pliocene planktonic foraminifera of *Globorotalia tumida* (FO: 5.5 Ma), *Dentoglobigerina altispira* (LO: 3.5 Ma), *Sphaeroidinellopsis seminulina* (LO: 3.6 Ma) with or without *Globoturborotalita nepenthes* (LO: 4.4 Ma) were identified from these same samples. Planktonic foraminifera and calcareous nannoplanktons together suggest that the age of the group (II) samples is 5.6–3.5 Ma (marked as solid green square in Fig. 21A).

Samples of group (III) from the lower reach of the Suilien-Chi River where Chang (1968) reported occurrences of *Globorotalia tosaensis* (FO: 3.3 Ma) associated with *Globorotalia tumida* (FO: 5.5 Ma), *G. multicamerata* (LO: 3.0 Ma) and *Sphaeroidinella dehiscens* (FO: 5.4 Ma) after extinction of *Dentoglobigerina altispira* (LO: 3.5 Ma) and *Sphaeroidinellopsis seminulina* (LO: 3.6 Ma). The assemblage indicates an age of 3.5–3.0 Ma (marked as black solid circle in Fig. 21A). The microplankton data (Tables 1–4) thus suggest the deposition age of the lower flysch sequences (unit S-2, Fanshuliao Formation) in the Suilien remnant forearc trough, the northern Coastal Range, is 5.8–3.0 Ma (Fig. 5) equivalent to the sequence unit S-2 of the Lichi Mélange in the southern Coastal Range (see Section 6.3).

6.5.5. Giant tuff blocks in the Suilien remnant forearc trough

Giant tuff blocks for several hundred meters in width and length are found in the eastern part of the Suilien remnant forearc trough (Fig. 3; Hsu, 1956). They are enclosed within the upper part of the lower flysch sequence (unit S-2; Fanshuliao Formation) or in a transition zone from the lower flysch to the upper flysch sequences. Limestone blocks (mm to tens of cm) with corals and shallow-marine reef fauna like mollusks of *Chlamys* and larger foraminifera of *Lepidocyclina* and *Amphistegina* are found in some layers of these giant tuff blocks. The fauna are similar to those found in the Kangkou Limestone capping on volcanic agglomerates of the Tuluanshan Formation of the Chimei volcanic island (Huang

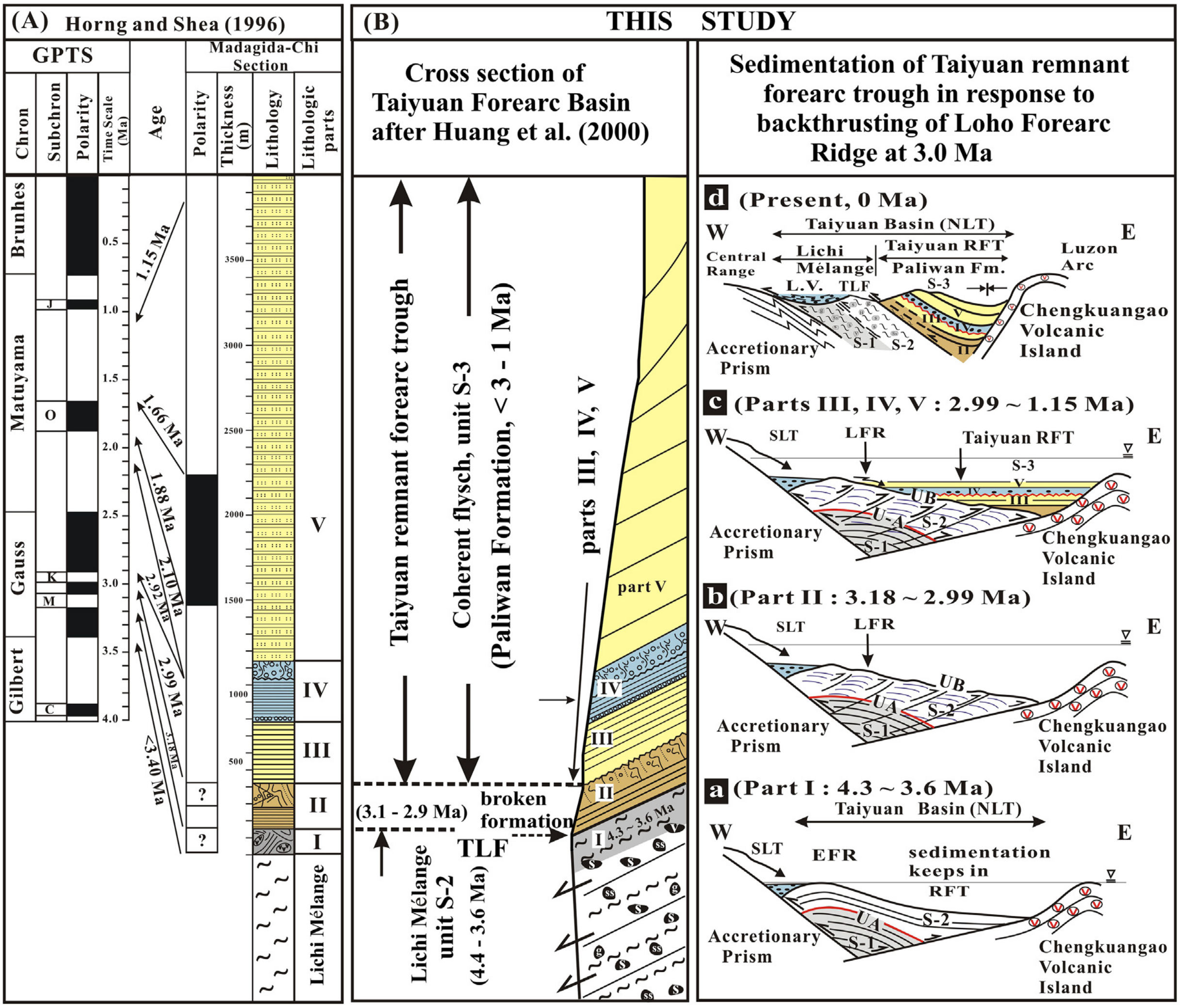

Fig. 26. Sedimentation of coherent flysch sequences in the Taiyuan remnant forearc trough. (A) stratigraphy exposed along the Madagida-Chi River section (adapted from Horng and Shea, 1996); (B) interpretation of the sedimentation and deformation processes of the Taiyuan remnant forearc trough east of the Tuluanshan fault. Abbreviations are same as previous ones. Details of sedimentation see Section 6.7.3.

et al., 1988, 1995; Huang and Yuan, 1994). The occurrence suggests that these giant tuffaceous blocks could slump westward from the Chimei volcanic island into the Suilien remnant forearc trough at ~3 Ma. As the slumping tuff blocks hit the forearc floor, a rapid increase of hydro-pressure and sand dikes (2–20 cm wide) of the low flysch materials were intruded into these giant tuff blocks (Song et al., 1994). These tuff blocks represent the true olistolith derived from the volcanic arc transporting into the Suilien remnant forearc trough by slumping processes like those found in the modern North Luzon Trough off SE Taiwan (seismic line 2016-10, Fig. 8; Huang et al., 2018).

6.5.6. Stratigraphy of two independent thick conglomerate units in the Suilien remnant forearc trough

In the Suilien remnant forearc trough, there are two independent

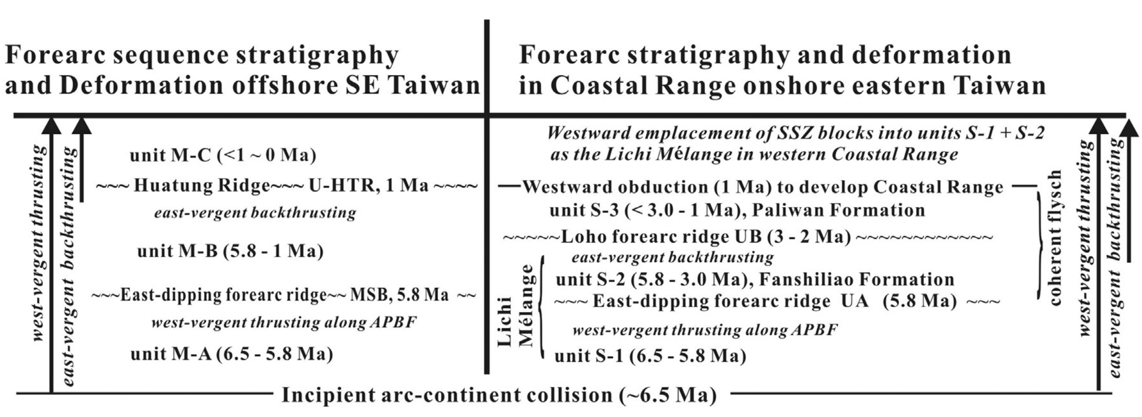

Fig. 27. Correlation of forearc sequence stratigraphy and events of bivergent thrusting onshore and offshore eastern Taiwan.

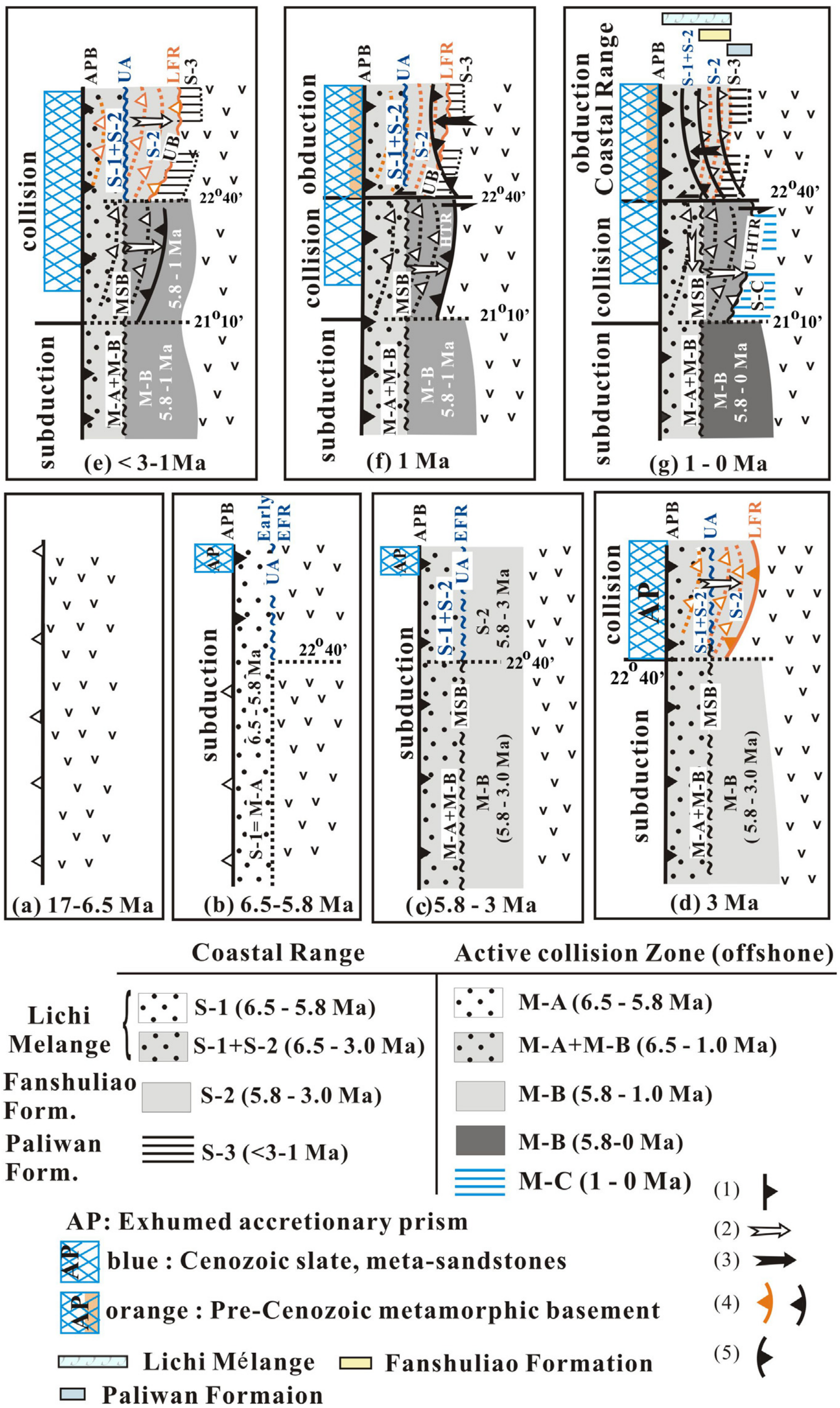

Fig. 28. Correlation and structural evolution of forearc sequences onshore the Coastal Range (sequence units S-1, S-2, and S-3) and offshore active collision zone (mega-sequence units M-A, M-B and M-C); APB: arc-prism boundary; EFR: east-dipping forearc ridge; HTR: Modern forearc Huatung Ridge; LFR: Pliocene Loho Forearc Ridge; UA, UB, U-HTR: unconformity; MSB: mega-sequence boundary; (a-b-c) west-vergent thrusting along arc-prism boundary during subduction; (d): arcward propagation of east-vergent thrust structure during collision; (e): westward propagation of thrusting during obduction; (f): east-vergent backthrust faulting in map view during collision at ~3 Ma (orange-colored fault) and ~1 Ma (black-colored fault), respectively; (g): west-directed thrust faulting in map view during obduction in the last 1 Ma. Details see Section 7.2.

thick conglomerate units intercalated within the upper flysch sequence (unit S-3, Paliwan Formation): Suilien Conglomerate in the north and the Chimei Conglomerate in the south (Fig. 3). Because of a similar composition of pebbles, these two conglomerate units were coined together as the Suilien Conglomerate in previous studies (Usami, 1939; Hsu, 1956; Chang, 1968, 1969; Teng, 1979) and were regarded as feeder channel conglomerates of deep-sea fan depositional system (Teng, 1979). However, detailed stratigraphy and sedimentological study suggests that both conglomerate units are different in stratigraphy age, distribution area and depositional environment. These two thick conglomerates occur only in the Suilien remnant forearc trough but not in the other three remnant forearc troughs to the south (Figs. 3 and 5). Therefore, the occurrence of these two conglomerate units in the Suilien remnant forearc trough plays an important role for understanding temporal-spatial variations of the upper sequence unit S-3 sedimentation during the active oblique collision in < 3–1 Ma. Due to better exposures and easy accessibility, previous field surveys and geological study ware mostly focused on the Suilien Conglomerate in the north (Chang, 1968, 1969; Teng, 1979; Chi et al., 1981; Dorsey and Lundberg, 1988). To understand the significance of temporal-spatial variations of forearc sedimentations in the Coastal Range, we conducted field surveys, sedimentological study and age determinations on

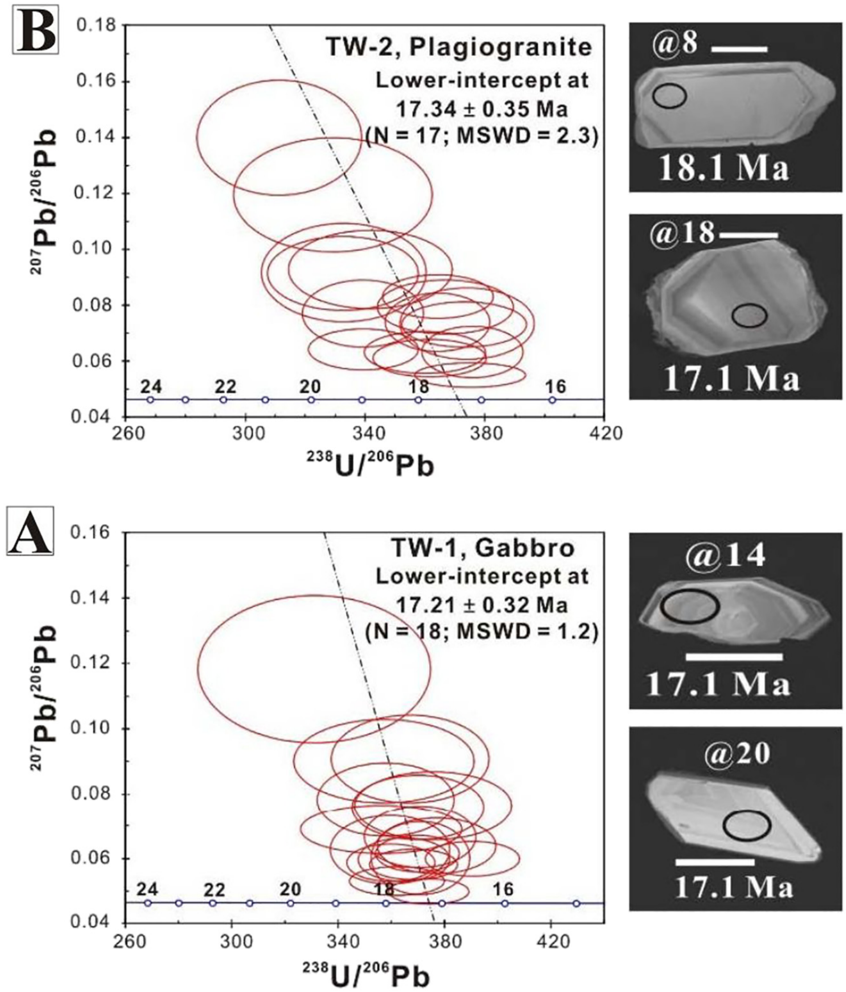

Fig. 29. SIMS age dating on two mafic blocks in the Lichi Mélange. Details see Section 8.2.

these two conglomerate units in the last decade (Lin, CT, 2011a).

6.5.6.1. Result (A), Fanshuliao Formation unconformably beneath the Suilien Conglomerate. Along the creek section west of Bridge-10, the Fanshuliao Formation beneath the Suilien Conglomerate contains Pliocene planktonic foraminiferal fauna of *Sphaeroidinella dehiscens* (FO: 5.4 Ma), *Globorotalia tumida* (FO: 5.5 Ma), *Dentoglobigerina altispira* (LO: 3.5 Ma), *Sphaeroidinellopsis seminulina* (LO: 3.6 Ma) with scattering occurrences of *Globoturborotalita nepenthes* (LO: 4.4 Ma; Table 5). *Globorotalia tosaensis* (FO: 3.3 Ma) did not find in this creek section. The planktonic foraminifera fauna suggest an age of < 5.4–3.5 Ma. However, calcareous nannofossils in this flysch sequence contain Pliocene indices of *Reticulofenestra pseudoumbilica* (LO; 3.7 Ma), *Sphenolithus abies* (LO: 3.6 Ma) and *Pseudoemiliania lacunose* (FO: 4.6 or 4.2 Ma) (Table 5) of Zones NN14–15 or an age of 4.6–3.6 Ma. Along the creek section of Bridge-11, a sample (B-2) collected from the siltstone of the Fanshuliao Formation (sequence unit S-2) unconformably beneath the Suilien Conglomerate contains similar planktonic foraminiferal fauna (Fig. 21B; Table 6) as those found along the creek section of Bridge-10 (Table 5). Therefore, planktonic foraminifers and calcareous nannoplanktons reveal the age of the Fanshuliao Formation (part of the sequence unit S-2) unconformably beneath the Suilien Conglomerate is < 4.6–3.5 Ma (Fig. 21B). This age is confined within the age range of the Fanshuliao Formation (5.8–3.0 Ma) along the Suilien-Chi South River and its distributary sections discussed above (Fig. 21A).

6.5.6.2. Result (B), deposition age of the Suilien Conglomerate. Due to a dilution by tremendous debris flow deposits of sands and pebbles, micro-fossils in most parts of the Suilien Conglomerate are rare (< 20–3 specimens/200 g of sands) or even barren (Fig. 21B, Table 6). Therefore, Chang (1968) did not collect any rock sample for study, whiles Chi et al. (1981) collected only four samples for nannoplankton study. But the later failed to find any nannofossil within the Suilien Conglomerate. We fortunately got foraminifera in 15 out of 40 samples collected from the Suilien Conglomerate in three creek sections (Fig. 21B). Samples collected along the creek section west of Bridge-10 in the north are mostly barren of foraminifera. Only 5 specimens of three long age range species of planktonic foraminifera (Late Miocene-Recent; Table 5) and three specimens of agglutinated benthics of *Haplopragmoides* sp. were found in the sample A-15 (Fig. 21B). On the other hand, along creek sections of Bridge-11 and 12 in the south we found foraminifera in 9 and 5 samples, respectively, of some thin sandstone-siltstone layers intercalating within thick disordered conglomerate beds (Fig. 21B). Pleistocene index microfossils of planktonic foraminifera *Globorotalia truncatulinoides* (LO: 1.9 Ma) were found in the base of the thick Suilien Conglomerate along the creek section west of Bridge-11 (sample B1, Figs. 21B and 22B; Table 6), whereas Pleistocene calcareous nannofossils *Gephyrocapsa oceanic* (FO: < 1.6 Ma) was recovered in the very upper part of the Suilien Conglomerate exposed along the creek section beneath Bridge-11 (sample B11 in Fig. 21B; Lin, CT, 2011a). Planktonic foraminifera in the creek section of Bridge-12 in the south are all long-ranged young fauna with *Globorotalia crassaformis*

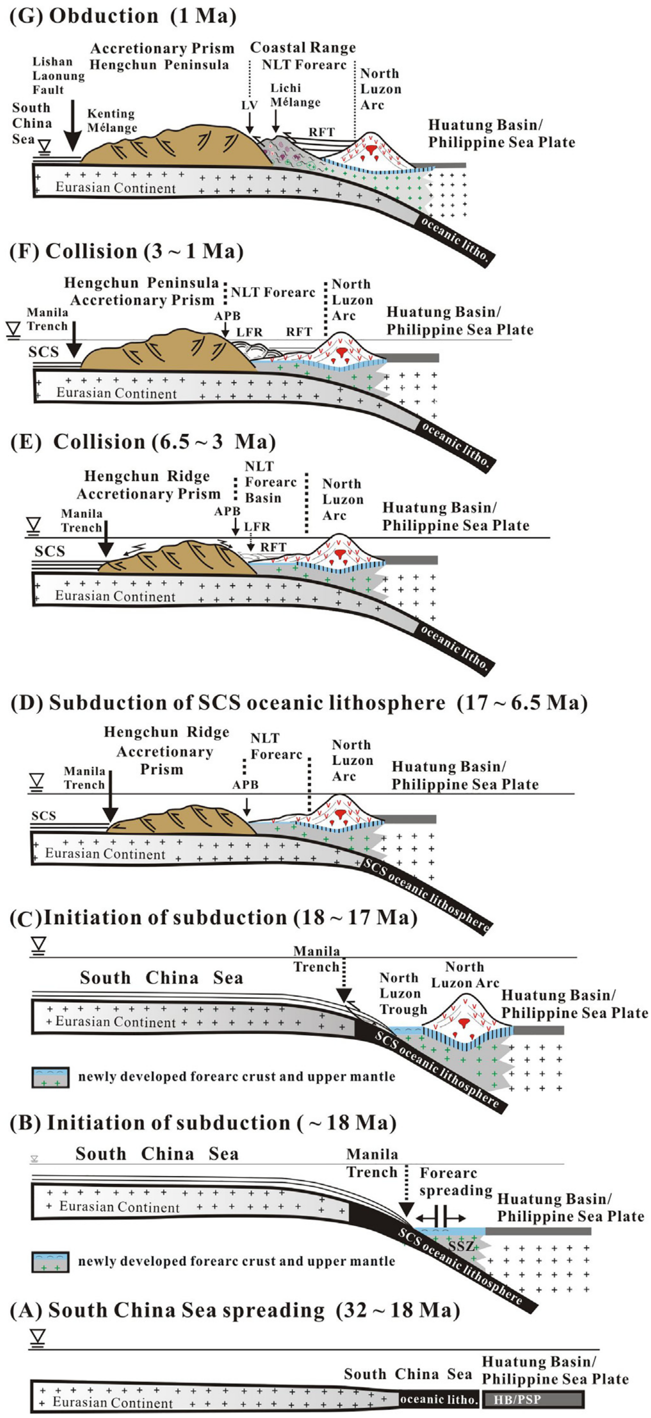

Fig. 30. Tectonic evolution of the North Luzon Trough forearc stratigraphy onshore Coastal Range since Early Miocene from subduction through collision to obduction in the oblique convergent region, eastern Taiwan. The tectonic evolution is reconstructed based on data obtained from seismic profiles in the modern oblique subduction-collision zones offshore SE Taiwan and detailed forearc stratigraphy onshore the Coastal Range. APB: arc-prism boundary; LFR: Pliocene Loho Forearc Ridge; LV: Longitudinal valley; NLT: North Luzon Trough forearc basin; RFT: remnant forearc trough east of the Pliocene Loho Forearc Ridge; SSZ: supra-subduction zone. Details see Section 9.

(FO: 4.3 Ma; Table 7). Fossil data thus suggest that the Suilien Conglomerate in the type area were deposited in Early Pleistocene (< 1.9–1 Ma; Figs. 5 and 21B).

6.5.6.3. Result (C), deposition environment of the Suilien Conglomerate. The Suilien Conglomerate in the north is ~1000 m thick debris flow sequences predominant of poorly-sorted, ordered-to-disordered, amalgamated matrix-supported cobbles and sandstones (Fig. 23A). No typical turbidite Bouma sequence can be recognized throughout the whole sequence of the Suilien Conglomerate. Although marine microfossil are barren in the most parts of the Suilien Conglomerate (Fig. 21A), very rare shallow-marine fauna benthic fauna like Genera *Heterolepa*, *Ammonia*, *Elphidium* and terrestrial plant seeds were recovered in some siltstone or fine sandstone beds (Tables 5–7) within the thick dis-ordered coarse-grained to pebbles of the Suilien Conglomerate. No younger stratigraphic unit rests on the Suilien Conglomerate (Fig. 3). This indicates that the Suilien Conglomerate would represent the youngest lithostratigraphic unit in the northern Suilien remnant forearc trough. In some intervals, imbrications of elongate pebbles show paleocurrent directions from the west to the northeast or southeast (Figs. 22A and 23A-1). All these sedimentological and paleontological features indicate that the debris deposits of the Suilien Conglomerate were primarily eroded from the upper sequences of the Central Range accretionary prism in the west via some east-flowing rivers to a fluvial fan delta environment (Fig. 23A; Lin, CT, 2011a).

6.5.6.4. Result (D), deep-sea fan deposition environment of the Chimei Conglomerate. The upper flysch sequences (unit S-3, the Paliwan Formation; Fig. 5) exposes widely in the southeastern part of the Suilien remnant forearc trough along the Hsiukuluan-Chi River (Fig. 3). Previous studies have documented that the Paliwan Formation contains planktonic foraminifera (Chang and Chen, 1970) of *Globorotalia tosaensis* (3.3–0.6 Ma) and Pleistocene calcareous nannofossils *Gephyrocapsa* spp. of Upper Zone NN 19 (< 1.6 Ma; Chi et al., 1981). These studies suggest a Pleistocene age for the Chimei Conglomerate (< 1.6–1 Ma; Fig. 5).

The Chimei Conglomerate (~1000 m thick; Fig. 23B) in the southern Suilien remnant forearc trough is intercalated within the upper flysch sequences (unit S-3, Paliwan Formation) of a Pleistocene age (Figs. 3 and 5). The Chimei Conglomerate is composed of deep-sea fan sequences. Each sequence of ~25–40 m thick includes a thick feeder channel conglomerate bed in the base (5–10 m), thick middle fan sandstone lobe in the middle (3–10 m), and muddy to sandy turbidite layers of a lower fan deposition in the upper part (10–20 m; Fig. 23B-1; Dorsey and Lundberg, 1988). The sequences represent migrations of deep-sea fan deposition in a middle-lower slope environment (Walker, 1978). The spatial distribution pattern of the Chimei Conglomerate and paleocurrent measurements suggests that the fan apex could locate in the west (Fig. 23B; Teng, 1982). Based on lithological column and sedimentary structures exposed along the Hsiukuluan-Chi River section, the debris of the Chimei fan could be transported from the Central Range accretionary prism into the southern Suilien remnant forearc trough via deep-sea submarine canyons in the southern Suilien remnant trough (Fig. 23B).

6.5.7. Deformation of sequence unit S-2 (Fanshuliao Formation) before sedimentation of sequence unit S-3 (Suilien Conglomerate)

The lower flysch sequence (unit S-2; Fanshuliao Formation) unconformably underlies the fluvial fan debris deposits of the Suilien Conglomerate (Fig. 21B). However, the lower flysch sequences contain deep-sea benthic foraminiferal fauna, like *Oridosalis umbonatus* (Reuss), *Gyroidinoides* spp., *Melonis pompilioides* (Fichtel and Moll), *Hoeglundina elegans* (d'Orbigny), *Globocassidulina favus* (Brady) and *Planulina wuellerstorfi* (Schwager) associated with some upper-slope fauna Genera of *Uvigerina*, *Bulimina*, *Lenticulina* and *Praeglobobulimina* (Chang, 1968). These fauna suggest that the lower flysch sequence was deposited in low-middle slope environments. But these low-middle slope deposits of the lower flysch sequences (unit S-2, Fanshuliao Formation) are unconformably covered by the fluvial-fan delta debris flow deposits along a distinct erosive surface made by channel cutting (Figs. 22B and 23A).

Table 1
Stratigraphic distributions of planktonic foraminifera along the Suilien-Chi South River section.

Formation	Fanshuliao Formation (Suilien-Chi South River section)															
Sample number	1	2	3	14	13	12	11	10	9	8	7	6	5	15	17	20
Species																
Globigerinoides trilobus (Reuss)	10	28	96	4	45	130		3	10	2	42	70	88	21	105	94
G. conglobatus (Brady)			7		1	3	8				8	16	4			6
G. obliqus Bolli		2			2	1					7	6	10	3	30	2
G. ruber (d'Orbigny)		2														
Globortalia meandrii (d'Orbigny)		5	44	48	58	120	15	3	2	6	25	78	25	1	12	80
G. tumida (Brady)			10		3	2	1			1	4	22	8		1?	2
G. multicamerata Cushman and Jarvis			5		7						3	8	4			
Globoturborotalita nepenthes (Todd)					22	2)	4				2	1	23	3	26	3
Dentoglobigerina altispira (Cushman & Jarvis)			38		28	30	6				38	75	20	2		40
Orbulina universa d'Orbigny			92		21	30	42			1	41	74	16		2	60
Neogloboquadrina humerosa (Takayanagi & Saito)			20	2	2						9	9	8	4	7	28
Sphaeroidinellopsis seminulina Schwager		2	66	7	70	64	36		8	6	26	59	68		5	
Sphaeroidinella dehiscens (Parker & Jones)			2		3		2	1?					4			
Biorbulina bilobata (d'orbigny)			10		2	1						5				
Hastigerina siphonifera (d'Orbigny)					1						2	1				

Table 2
Stratigraphic distributions of planktonic foraminifera along the Shierfenkeng-Chi River section.

Formation	Fanshuliao Formation (Shierfenkeng-Chi River section)							
Sample number	21	27	30	35	43	44	45	46
Species								
Globigerinoides trilobus (Reuss)	72	33	44	10	4	6	2	61
G. conglobatus (Brady)			10					3
G. obliqus Bolli	18	10	6					7
G. ruber (d'Orbigny)			1					
Globortalia meandrii (d'Orbigny)	42	14	27					76
G. tumida (Brady)	2	4						2
Globoturborotalita nepenthes (Todd)	5		12					2
Dentoglobigerina altispira (Cushman & Jarvis)	2	8	2					26
Orbulina universa d'Orbigny	60	12	49					60
Neogloboquadrina humerosa (Takayanagi & Saito)	9		22					16
Sphaeroidinellopsis seminulina Schwager	13	18	16					40
Pulleniatina obliquiloculata (Parker & Jones)		8						5
Hastigerina siphonifera (d'Orbigny)	2							

This infers that there was a significant geological break of age and paleo-bathymetry of depositional environments between the Suilien Conglomerate (sequence unit S-3) and the underlying Fanshuliao Formation (sequence unit S-2). Some intervals (each 300–500 m in width) of the lower flysch sequences (unit S-2, Fanshuliao Formation) in the Suilien remnant forearc trough were intensively sheared without discernible stratification like a broken formation (Figs. 21A and 22D). Based on sedimentology features, benthic foraminiferal fauna and age study, it appears that there is a significant stratigraphic time gap associated with a remarkable change of depositional environment between the lower flysch sequences with a broken formation deformation feature (sequence unit S-2, Fanshuliao Formation, 5.8–3.0 Ma; upper-middle slope, ~ − 1000 m water depth) and the overlying young fluvial-shelf fan delta Suilien Conglomerate (sequence unit S-3, < 1.9–1 Ma; 0– < 50 m water depth; Fig. 23A).

More than 2 km-thick Pleistocene conglomerates of the Suilien Conglomerate and the Chimei Conglomerate (within sequence unit S-3 of the Paliwan Formation) occur only in the Suilien remnant forearc trough of the northern Coastal Range, but no equivalent thick conglomerate unit crops out in the other three remnant forearc troughs to the south (Figs. 3 and 5). Variation of conglomerate sedimentations onshore the Coastal Range indicates that the transportation routes of these conglomerates in the north were blocked by a topography high in the south. Such a spatial variation of the sequence unit S-3 sedimentation onshore the Coastal Range is similar to what observes today in the active collision zone offshore where the fluxoturbidite sedimentations of the mega-sequence unit M-C in the north are blocked by a bathymetric high of the middle Huatung Ridge in the south ('BHWL' in Fig. 13; see Section 5).

This raises questions of: 1) what had happened in the time window of 3–2 Ma that > 2 km thick conglomerates younger than 3 Ma were dumped only in the Suilien remnant forearc trough but not in other remnant forearc troughs to the south? 2) what is the main mechanism responsible for such a distinct N-S temporal-spatial variations of forearc sedimentations of the sequence unit S-3? and 3) was this mechanism similar to that occurs today in the active collision zone offshore SE Taiwan?

The key to understand the mechanism to cause such a temporal-spatial variation of forearc sedimentation of conglomerates within the Paliwan Formation (sequence unit S-3) onshore the Coastal Range relies upon a detailed geological study on the stratigraphy and structure of the Pliocene Loho remnant forearc trough (Fig. 24; Loho Forearc Ridge, LFR, in Fig. 25) in the middle part of the Coastal Range (Section 6.6 reviewed and discussed below).

6.6. Loho forearc segment in the middle Coastal Range

6.6.1. General geological features

Paleogeographic reconstruction suggests that the Loho forearc segment in the middle Coastal Range was located in the junction region between the accreted Chimei volcanic island in the north and the Chengkuangao volcanic island in the south (Fig. 4). The Loho forearc

Table 3
Stratigraphic distributions of calcareous nannoplanktons along the Suilien-Chi South River section.

Formation		Fanshuliao Formation (Suilien-Chi South River section)																						
Sample number		1	2	3	4	14	14	13	13	12	12	12	11	10	10	9	8	7	6	5	15	16	17	20
Calcareous nanno-planktons																								
Taxa	Zonation	11	11	12–15	12	12	12	12–15	13–15	13–14	13–14	13–14	13–15	12	12	13–15	13–15	13–15	13–15	13–15	13–15	13–15	13–15	13–15
Amaurolithus amplificus	NN11–NN12				P	P	P																	
A. ninae	NN11–14									P	P	P												
Calcidiscus leptoporus	Mio.-NN21	R	R	R	R	R	R	R	R	R	R	R	R	R	R	R	R	R	R	R		R	R	R
C. macintyrei	NN4–NN19																				R			
C. armatus	NN12													P	P									
C. rugosus	NN12–NN19							P							P									
Cyclicargolithus floridanus	NP20–NN6																							
Discoaster productus	Pliocene.	F	F	F	R	R	R	R	R	R	R	R	C	R	R	R	R	R	R	R	R	F	R	R
D. brouweri	NN8–NN18		P			R	R	P	P	P	P	P	FR								R	R	R	
D. challengeri	NN8–NN15				P																			
D. pentaradiatus	NN9–NN17					R	R	P	FR	P	P		FR	R	R					FR	R			
D. quinqueramus	NN11	R	R																					
D. surculus	NN11–16				P	R		P	R	P	P										P		R	R
D. variabilis	NN4–NN16		P	P	F	R	R	P	R	P	P	P	FR	R	R	R	R	R	FR	R	R	R	R	R
Gephyrocapsa spp.	NN13–NN21																							
Helicosphaera carteri	NN1–NN21	R	R	R	R	R	R	R	R	R	P		R	R			R	R	R	R	R	R	R	
Pseudoemiliania lacunosa	NN13–NN19								P										P		P		R	P
Reticulofenestra spp.	Eo.-NN16	F	F	C	F	C	F	FC	FC	FC	F	F	FC	R	R	R	R	R	F	F	F	C	R	R
R. minutula	NN3–NN16	R	R	F	FR	F	FR	FC	F	FC	F	F	F	R	R	R	FR	R	FR	FR	FR	F	R	F
R. pseudoumbilica	NN7–NN15	R	R	R	R	R	R	R	R	R	R	R	R				R		R	R	R	R	R	R
Sphenolithus abies	NN9–NN15	R	R	F	R	FR	FR	F	R	F	R	R	R	R	R	R	R	A	A	R	R	R	R	R
S. neoabies	NN7–NN15																							
Umbilicosphaera sibogae	M.Mio-NN21			R	R				R				R							R				

Table 4
Stratigraphic distributions of calcareous nannoplanktons along the Shierfenkeng-Chi River section.

Formation		Fanshuliao Formation (Shierfenkeng-Chi River section)																						
Sample number		21	23	24	25	26	27	28	29	30	31	32	33	34	35	36	39	40	41	42	43	44	45	46
Calcareous nanno-planktons																								
Taxa	Zonation	11	11	11	11	11	?	11	11	11	13–15	11	11	13–15	13–15	13–15	13–15	13–15	11	13–15	13–15	11	11	13–15
Amaurolithus amplificus	NN11–NN12																							
A. ninae	NN11–14																							
Calcidiscus leptoporus	Mio.-NN21	R	R	R		R		R	R			R	R	R	R	R	F	F	R	R			P	R
C. macintyrei	NN4–NN19																							
C. armatus	NN12																							
C. rugosus	NN12–NN19																							
Cyclicargolithus floridanus	NP20–NN6											P											P	
Discoasters. productus	Pliocene	F	F	F	F			F	F	R	R	R	R	F	F	R	R	R	R		R	R	R	
D. brouweri	NN8–NN18										R	P												
D. challengeri	NN8–NN15																							
D. pentaradiatus	NN9–NN17	P												P	R	P	FR	R	R	R		R	R	
D. quinqueramus	NN11	R	R	R	P	R		R	R	P		R	R						P			R	R	
D. surculus	NN11–16																							
D. variabilis	NN4–NN16		R	R		R		R	R		R				R	R	R	R	R	R	R	R	R	R
Gephyrocapsa spp.	NN13–NN21																							
Helicosphaera carteri	NN1–NN21												R	R	R	R	R	R	R	R	R	R	R	
Pseudoemiliania lacunosa	NN13–NN19														?		P			P	?			
Reticulofenestra spp.	Eo.-NN16	F	F	F	F	F		F	F	F		F		F	C					R				
R. minutula	NN3–NN16	R	R	R				R	R	R	R	R	R	R	F	F	C	FC	FC	F	F	R	R	
R. pseudoumbilica	NN7–NN15	R	R	R	R	R	R	R	R	R	R	R	R	R	R	R	R	R	F	R	R	R	R	
Sphenolithus abies	NN9–NN15	R	R	R	R	R		R	R	R	R	R	R	R	R	R	F	F	F	F	R	R	F	
S. neoabies	NN7–NN15										R		F	FC	FC									
Umbilicosphaera sibogae	M.Mio-NN21							R	R				R	R	R									

Table 5
Stratigraphic distributions of planktonic foraminifera along the Bridge-10 creek section.

Formation	Fanshuliao Formation (Bridge-10 creek section)										Suilien Conglo.
Sample number	A1	A2	A3	A4	A5	A6	A7	A10	A11	A12	A15
Species											
Globoturborotalita nepenthes (Todd)		4	10	5		8	2	14			
Globigerina druryi Akers			36	10		25					
Globigerinatina glutinata Egger				4							
Globigerinoides conglobatus (Brady)		7	11	4	3	19	4	15			
G. obliquus Bolli	3	2	2		1	5	8	3			
G. ruber (d'Orbigny)		1							8	1	
G. trilobus (Reuss)	2	70	35	58	3	201		166	32	4	1
Globortalia meandrii (d'Orbigny)	3	72	2	43	26	103	65	32	3		1
G. multicamerata Cushman and Jarvis		2		1			3	1			
G. ungulata Bermudez			1		3		1				
G. tumida (Brady)		5				3	2	1			
Dentoglobigerina altispira (Cushman & Jarvis)		11	18	7		8	12	8	3		
Neogloboquadrina humerosa (Takayanagi & Saito)	2	19	13	21	1	57	15	15	15	4	3
Orbulina universa d'Orbigny	1	26	5	13		37	22	47	7		
Pulleniatina obliquiloculata (Parker & Jones)		12	2	4				3	8	7	
Sphaeroidinellopsis seminulina Schwager	5	65	9	8	23	46	16	77	7	1	
Sphaeroidinella dehiscens (Parker & Jones)	38	10		6	2	56	14		4	12	

segment is composed of volcanic agglomerates (the Tuluanshan Formation) in the lower part overlain unconformably by the deep-sea sedimentary strata in the upper part (Fig. 3). The sedimentary strata include the Lichi Mélange in the west and lower coherent flysch sequence (sequence unit S-2; Fanshuliao Formation) in the east (Fig. 24; Lin, YC, 2011b).

Comparing with the Suilien and Taiyuan forearc segments to the north and south, respectively, geology of the Loho forearc segment in the middle Coastal Range is characterized by its relative small basin size, occurrences of the Lichi Mélange in west of the Tuluanshan fault and the remnant forearc trough center (Fig. 24A), lack of thick conglomerate unit and absence of the Late Pliocene-Pleistocene upper coherent flysch sequence (sequence unit S-3, Paliwan Formation; Fig. 5). In structure geology, the Loho forearc segment is also featured by an unusual structure that the young coherent lower flysch sequence (3.3–3.0 Ma) thrust westward over the relatively old Lichi Mélange (4.3–3.4 Ma) in the trough center along a low angle detachment fault. This detachment fault may connect to the Tuluanshan fault (or the local

Table 6
Stratigraphic distributions of planktonic foraminifera along the Bridge-11 creek section.

Formation	Fanshuliao Formation	Suilien Conglomerate (Bridge-11 creek section)								
Sample number	B2	B1	B3	B5	B6	B7	B8	B9	B10	B11
Species										
Globoturborotalita nepenthes (Todd)										1*
Globigerinoides conglobatus (Brady)	10					1	1	2		2
G. trilobus (Reuss)	162	111	1	1	26	34	35	52		32
G. obliquus Bolli	11	3		1	2		2			3
G. ruber (d'Orbigny)	8	16								
Globorotalia tosaensis Takayanagi & Saito		10								
G. fluxosa (Koch)					1*					
G. meandrii (d'Orbigny)	31				14	12	6	30		7
G. multicamerata Cushman and Jarvis					2*					
G. tumida (Brady)	1				1	4		1		1
G. truncatulinoides (d'Orbigny)		8								
G. inflata (d'Orbigny)	10									
G. crassaformis (Galloway & Wissler)	9	34			8	33	34	92		40
Dentoglobigerina altispira (Cushman & Jarvis)					2*	2*	1*			2*
Neogloboquadrina humerosa (Takayanagi & Saito)	227	132		4	19	57	18	88	1	25
Orbulina universa d'Orbigny	25	7			5	1	4	10		1
Pulleniatina obliquiloculata (Parker & Jones)	152	99			28	24	17	45		4
Sphaeroidinellopsis seminulina Schwager	1*	17*			6*	1*				
Sphaeroidinella dehiscens (Parker & Jones)	43	134	1	2		5	1	11		9

Table 7
Stratigraphic distributions of planktonic foraminifera along the Bridge-12 creek section.

Formation	Suilien Conglomerate (Bridge-12 creek section)				
Sample number	C1	C4	C11	12M-11	C15
Species					
Globigerina druryi Akers					1
Globigerinoides trilobus (Reuss)	8	1	2	6	4
G. ruber (d'Orbigny)		1	1		
Globorotalia meandrii (d'Orbigny)				2	2
G. tumida (Brady)				1	
G. crassaformis (Galloway & Wissler)			2	1	
Neogloboquadrina humerosa (Takayanagi & Saiteo)	2	1	1	3	
Pulleniatina obliquiloculata (Parker and Jones)	1 (2)			3	

Yuangfeng fault; Fig. 24A). Consequently, the Lichi Mélange is thus exposed like a tectonic window in the Loho remnant forearc trough center (sections C-C′ and D-D′ in Fig. 24B; Hsu, 1976). The NE-SW-striking Tuluanshan fault extends southward to the west of the Taiyuan remnant forearc trough in the southern Coastal Range (Fig. 3; Hsu, 1956, 1976).

6.6.2. Volcanic agglomerates in the lower part

The volcanic agglomerates appear as two topographic ridges running in NW and SE sides, respectively, of the Loho remnant forearc trough (Fig. 24A). Volcanic agglomerates of the NW ridge dip to the southeast and can be traced continuously northeastward to the Takangshan volcanic ridge of the Chimei Volcanic Island, whereas the agglomerates of the SE ridge dip to the northwest and extends southeastward to the Chengkuangaoshan volcanic ridge of the Chengkuangao Volcanic Island (Fig. 4).

6.6.3. Forearc stratigraphy of the Lichi Mélange

The Lichi Mélange occurs as alternations of broken formation and mélange in both sides of the Tuluanshan fault (Hsu, 1976; Lin YC, 2011b). The intensively-sheared mélange contains variable-sized polygenic blocks of serpentinite (Fig. 24C) and huge tuff blocks (hundred meters wide and thick; Fig. 24A) embedded in scaly argillaceous matrices showing a block-in-matrix feature. Although microfossils in the mélange are rare, we are fortunately to find enough planktonic foraminifera and calcareous nannoplanktons for a precise age dating. Our study shows that most parts of pervasively sheared mudstones of the Lichi Mélange are mainly within an age range of 4.3–3.4 Ma (Chen et al., 2015). But *Globorotalia tosaensis* was also found in some limited samples collected from the sheared mélange near the Antung Hot Spring site. This suggests that the age of the Lichi Mélange in the Loho remnant forearc trough center could be of 4.3–3.4 Ma (Fig. 24A) confined within age range of the sequence unit S-2 in the type Lichi Mélange (5.8–3.0 Ma) of the southern Coastal Range (Fig. 5).

6.6.4. Stratigraphy age of the lower flysch sequences

The lower flysch sequences (part of the sequence unit S-2, Fanshuliao Formation) in the elongated Lobo remnant forearc trough east of the Tuluanshan fault show different degrees of strata disruptions from a weak deformation with stratification to broken formation facies without stratification. Fig. 24A shows results of the stratigraphy ages of these lower flysch sequences determined by integrated biostratigraphy of planktonic foraminifera and calcareous nannofossils (Chang, 1969; Chen et al., 2015) in 81 samples collected from three transects across the Loho remnant forearc trough. Based on occurrences of the diagnostic planktonic foraminifera, the lower flysch sequences in the Loho remnant forearc trough (sequence unit S-2, part of the Fanshuliao Formation in Fig. 24) were deposited in a limited age range of 3.3–3.0 Ma (Chen et al., 2015) despite of their field occurrences in coherent strata or broken formation.

6.6.5. Why no strata younger than 3 Ma in the Loho remnant forearc trough?

Biostratigraphic study shows that there is no sequence younger than 3 Ma in the Loho remnant forearc trough (Fig. 5). However, > 3 km thick coherent upper sequences (including 2-km-thick conglomerates) younger than 3 Ma crop out in the Suilien remnant forearc trough to the north and the Taiyuan remnant forearc trough to the south (Fig. 5). The absence of the younger strata in the Loho remnant forearc trough could be either no deposition in the last 3 Ma or being removed away from the Loho remnant forearc trough by river erosions after the obduction of the Coastal Range in the last 1 Ma.

The entire Coastal Range (22°40′–24°00′N) is located in the same subtropical climate zone with comparable morphological relief. If the absence of younger sediments (< 3 Ma) in the Loho remnant forearc trough was caused by river erosions, the rivers running through the Loho remnant forearc trough should have a much larger drainage area, thus have a higher annual river discharge to cause a higher erosion rate, than those in the Suilien and Taiyuan Remnant forearc troughs. However, the river drainage area of the Loho remnant forearc trough ($52\,km^2$) is much smaller than in the Suilien ($> 200\,km^2$) and the Taiyuan remnant forearc troughs ($112\,km^2$). Accordingly, the absence of upper flysch sequences (< 3 Ma) in the Loho remnant forearc trough is unlikely due to river erosions after obduction tectonics. Instead, it must be due to a lack of deposition of the young strata in the last 3 Ma. But why there was no deposition in the Loho remnant forearc trough of the last 3 Ma?

6.6.6. Comparison with modern analog offshore SE Taiwan

Paleogeographic and tectonostratigraphic reconstructions show that the Loho remnant forearc trough was located in the junction area between the Chimei Volcanic Island to the northeast and the Chengkuangao Volcanic Island to the southeast (Figs. 4 and 24; Huang et al., 1995, 2000). This special paleogeography of the Loho forearc segment is similar to the modern 'BHWL' (Fig. 2) in the middle segment of the modern Huatung Ridge south of the junction area between the Lutao Volcanic Island to the northeast and the Lanyu Volcanic Island to the southeast offshore SE Taiwan (Fig. 13). Taking the following geological features into consideration: 1) thick conglomerates occur only in the over-filling Suilien remnant forearc trough to the north but not in the Loho remnant forearc trough; 2) absence of < 3 Ma flysch in the Loho remnant forearc trough due to no deposition; and 3) a similar geography between the Loho remnant forearc trough and the modern 'BHWL' of the middle Huatung Ridge between two volcanic islands, we regard that the absence of young upper flysch sequence (< 3 Ma) in the Loho remnant forearc trough could be due to occurrence of a Loho bathymetric high in the middle part of the Pliocene Loho Forearc Ridge (LFR in Fig. 25) west of the Chengkuangao volcanic island at ~3 Ma before deposition of the sequence unit S-3, a scenario analog to what happens today that the modern bathymetric high 'BHWL' in the middle part of the Huatung Ridge west of the Lanyu volcanic island before sedimentation of the mega-sequence unit M-C in the active oblique collision zone offshore SE Taiwan (Fig. 13). This Pliocene Loho Forearc Ridge could also be deformed and uplifted by bivergent thrusting similar to the Huatung Ridge in the active collision zone offshore SE Taiwan (Fig. 25; see Section 7).

6.6.7. Why the Lichi Mélange exposes like a window in the Loho remnant forearc trough center?

Due to an absence of the young coherent flysch sequence (< 3 Ma) in the Loho remnant forearc trough, it is likely that after obduction of the Loho forearc segment in the last 1 Ma, local rivers could erode away part of the relatively thin lower forearc flysch sequences (sequence unit S-2, Fanshuliao Formation, estimated to be no > 1 km thick) to expose the Lichi Mélange beneath the low-angle decollement thrust fault. Consequently, the Lichi Mélange exposes like a tectonic window in the Loho remnant forearc trough center (Fig. 24). However, there are > 3 km thick young coherent flysch sequences (sequence unit S-3, Paliwan Formation) in the Suilien and Taiyuan Remnant forearc troughs, they are too thick to be eroded away by rivers in a short time of the last 1 Ma. Therefore the Lichi Mélange beneath the Tuluanshan decollement fault is still covered by the thick upper flysch (sequence unit S-3) and thus has not been exposed yet in the Suilien and Taiyuan remnant forearc trough centers.

6.7. Taiyuan forearc segment in the southern Coastal Range

6.7.1. General geological features

The Taiyuan forearc segment in the southern Coastal Range includes volcanic agglomerates (Tuluanshan Formation) in the basement and the overlying sedimentary rocks of the Lichi Mélange in the west and coherent flysch sequences in the east (Figs. 3 and 5). The Taiyuan forearc segment has been deformed as an asymmetry south-plunging syncline structure (Fig. 3; Hsu, 1956) during obduction in the last 1 Ma. The syncline deformation also leads to an occurrence of volcanic agglomerates in both sides of the Taiyuan remnant forearc trough: the Liushihshihshan volcanic ridge on the northwest and the Chengkuangaoshan volcanic ridge on the east (Fig. 3). Both volcanic ridges merge together along an N-S-running fault north of the Taiyuan remnant forearc trough (Fig. 3). The young coherent flysch sequences (sequence unit S-2, 3.9–3.7 Ma and unit S-3, < 2.0–1 Ma) and volcanic agglomerates of the Liushihshihshan volcanic ridge thrust westward over the old Lichi Mélange (sequence unit S-1, 6.5–5.8 Ma) along the east-dipping Tuluanshan fault (cross-sections E-E′ and F-F′, Fig. 3B). Geology of the Lichi Mélange in the west has been thoroughly studied before (see Sections 6.2–6.3), but stratigraphic significance of the thick coherent young flysch sequences in the Taiyuan remnant forearc trough has not been well explored before yet. We reconstruct the sedimentation and deformation of the sequences in the Taiyuan remnant forearc trough east of the Tuluanshan fault as right panel of Fig. 24.

6.7.2. Volcanic agglomerate basement

The Chengkuangaoshan volcanic ridge east of the Taiyuan remnant forearc trough represents the main part of the Chengkuangao Volcanic Island before it was accreted onto the southern Coastal Range (Figs. 3 and 4). Like the Chimei Volcanic Island to the north, a Late Pliocene fringing reef of the Tungho Limestone (2.9 Ma) caps unconformably on the Miocene–Pliocene Chengkuangao Volcanic Island (Figs. 3 and 4). The top of the Liushihshihshan volcanic basement (~3.3 Ma; Lo et al., 1994) in the NW contains some limestone blocks with corals, larger foraminifera *Amphistegina* and rhodolith algae identical to those found in the fringing reef of the Latest Pliocene Tungho Limestone. This suggests that the volcanic basement of Liushihshihshan volcanic ridge represents part of the Chengkuangao Volcanic Island before the syncline deformation during obduction.

6.7.3. Stratigraphic age of coherent flysch sequences east of Tuluanshan fault

Stratigraphy of the coherent flysch sequences (sequence unit S-2, Fanshuliao Formation and sequence unit S-3, Paliwan Formation) in the Taiyuan remnant forearc trough east of the Tuluanshan fault has been studied before (Chang, 1967b; Chi et al., 1981). Combing litho-, bio- and magneto-stratigraphy along the Madagida-Chi River section, Horng and Shea (1996) divided the sequence into 5 units (I–V) from the Tuluanshan fault zone eastward (parts I–V in the left panel of Fig. 26). Stratigraphic ages of these five parts are followed in this study. However to retain a consistency of the datum ages of key planktonic microfossil, the age of part I is modified from < 3.3–3.18 Ma by Horng and Shea (1996) to < 4.4–3.6 Ma in this study (Fig. 26). We regard part II (3.1–2.9 Ma) as a broken formation interval, instead of a slumping interval with reworked Late Miocene microfossils as it was interpreted by Horng and Shea (1996), in which sequence unit S-2 of either the Lichi Mélange or the lower coherent flysch sequence were involved into thrusting deformation. Sedimentation and deformation processes of these five parts are interpreted in the right panel of Fig. 26.

Part I (> 150 m) is a sheared and chaotic unit containing exotic serpentinite and volcanic blocks showing a block-in-matrix feature without discernible stratification (Horng and Shea, 1996). The field occurrence suggests that part I represents a part of the Lichi Mélange (sequence unit S-2; Fig. 26). Sheared mudstones of part I contain planktonic foraminifera *Sphaeroidinella dehiscens* (FO: 5.4 Ma), *Globorotalia tumida* (FO: 5.5 Ma) and *Dentoglobigerina altispira* (LO: 3.5 Ma), but without *Globoturborotalita nepenthes* (LO: 4.4 Ma). Calcareous nannoplanktons *Reticulofenestra pseudoumbilica* (LO: 3.7 Ma), *Discoaster pentaradiatus* (9.37–2.39 Ma) and *Discoaster surculus* (7.7–2.5 Ma) were also found in the part I. Microplanktons indicate that part I was deposited in < 4.4–3.5 Ma, similar to the age of the sequence unit S-2 of the type Lichi Mélange west of the Taiyuan remnant forearc trough (see Section 6.3).

Part II (270 m) consists of the coherent flysch sequence in the lower part and sheared, deformed mudstone in the upper part (left panel of Fig. 26). No exotic mafic or ultra-mafic block was observed in part II, suggesting a typical broken formation of either part of the Lichi Mélange or of the coherent flysch sequence within the Tuluanshan fault zone (right panel of Fig. 26). In a same rock sample of part II, Pliocene indigenous microfossils like *Sphaeroidinella dehiscens* (FO: 5.4 Ma), *Dentoglobigerina altispira* (LO: 3.5 Ma) and *Globorotalia tumida* (FO: 5.5 Ma) occur with Late Miocene microfossils, such as *Globoquadrina dehiscens* (LO: 5.8 Ma) (planktonic foraminifera) and calcareous nannofossil of Late Miocene assemblage of *Discoaster quinqueramus* (LO: 5.6 Ma), *D. berggrenii*, *D. deflandrei*, *Cyclicargolithus floridanus and Sphenolithus heteromorphus*. However, *Globorotalia tosaensis* (FO at 3.3 Ma) was not found in part II. Occurrences of these Late Miocene and Early Pliocene fossils lead to a conclusion that the interval of part II was either a broken formation interval or a fault zone in which the Lichi Mélange (6.5–3.0 Ma) was involved into fault deformation (Fig. 26d). However, Horng and Shea (1996) regarded interval of part II as a slumping zone in which the Late Miocene fossils were reworked. According to Horng and Shea (1996) part II was deposited in a narrow time interval of 3.18–2.99 Ma.

Parts III, IV and V are well-bedded coherent sandy young flysch sequences (sequence unit S-3 or the Paliwan Formation; Fig. 26). The age spans from 3 Ma (above FO of *Globorotalia tosaensis*) upward to 1.15 Ma (Horng and Shea, 1996) or < 3–1 Ma consistent with the sequence unit S-3 or the Paliwan Formation exposed in the Suilien remnant forearc trough in the northern Coastal Range (Fig. 21). More than 90% area of the Taiyuan remnant forearc trough are the exposures of parts III–V (Fig. 3).

6.8. The Taitung forearc segment in the southernmost Coastal Range

6.8.1. General geological features

The Taitung forearc segment in the southernmost part of the Coastal Range represents the latest obducted arc-forearc geological unit in eastern Taiwan (Fig. 4). Therefore, geology of the Taitung forearm segment would connect well southward to the active collision zone offshore SE Taiwan (Fig. 1). However, deformation in the southernmost Coastal Range is mostly of westward thrusting structures developed during obduction in the last 1 Ma (Figs. 3 and 20; Chang et al., 2000), whiles prominent structures in offshore SE Taiwan are eastward back-thrusting developed in the modern active collision zone (Fig. 2). Consequently, there is an E-W left-lateral strike-slip fault between onshore the southernmost Coastal Range of the obduction zone and the active collision zone offshore (Figs. 3A and 13). The east-running Pinanta-Chi River follows this strike-slip fault line in the southernmost Coastal Range (Fig. 13).

Stratigraphy of the Taitung forearc segment includes the old Lichi Mélange (sequence units S-1 and S-2) in the footwall side of the Tuluanshan fault and the coherent young flysch sequences (sequence unit S-3, Paliwan Formation, Fig. 5) in the hanging wall side of the fault (Fig. 20). Paleogeography of the Taitung forearc segment is comparable to the Loho forearc segment in the middle Coastal Range. Basin size of both remnant forearc troughs are all relatively small, and are located between two accreted volcanic islands. The Loho remnant forearc trough was positioned between the Chimei volcanic island and the Chengkuangao volcanic island (Figs. 4 and 24), whiles the Taitung remnant forearc trough was located between the Chengkuangao volcanic island onshore and the Lutao volcanic island offshore (Fig. 4). However, all the Loho forearc strata and part of the arc basement (Chengkuangao volcanic island) had been thrust westward onto the middle Coastal Range. Due to a southward propagation of tectonics, only part of the Taitung remnant forearc trough is exposed onshore the southernmost Coastal Range. The Lutao volcanic island east of the Taitung remnant forearc trough still retains offshore and has not been accreted onto the southernmost Coastal Range yet.

The coherent young flysch sequences (< 3.0–1 Ma; Chen et al., 2015) in the east thrust westward over the old and intensively sheared Lichi Mélange (6.5–3.0 Ma) along a low-angle decollement fault connecting to the N-S-striking Tuluanshan fault (F-F′ section in Fig. 3B). However, due to erosions by the east-running Pinanta-Chi River along the left-lateral strike slip fault line, a significant part of young stratified flysch strata above the decollement fault has been eroded away like what occurs in the Loho remnant forearc trough. Consequently, the Lichi Mélange beneath the low-angle Tuluanshan decollement fault was exposed widely (5 km) in the southernmost Coastal Range (Figs. 3 and 20). Geological significance and age of the Lichi Mélange (6.5–3.0 Ma) of the Taitung forearc segment have been discussed in Section 6.3.

6.8.2. Stratigraphic age of coherent young flysch sequences

Coherent upper flysch sequences (sequence unit S-3, or the Paliwan Formation, Fig. 5) in the Taitung remnant forearc trough dip to SE. Several thin tuff layers intercalate within the lower part and a thick pebbly siltstone bed (~200 m) occurs in the upper part. The pebbles are mostly of sub-rounded volcanic andesite, tuff or tuffaceous limestone and mudstone presumably derived from the Chengkuangao Volcanic Island and its fringing reef to the northwest.

Stratigraphy distributions of planktonic foraminifers and calcareous nannofossils in the upper coherent flysch sequences expose along four creek sections of the Taitung remnant forearc trough were studied (Fig. 20A; Chen et al., 2015). Results show that the age of the upper flysch sequences (unit S-3, Paliwan Formation) in the Taitung remnant forearc trough spans from Late Pliocene to Early Pleistocene (< 3.3–1.2 Ma, most probably < 3.0–1 Ma) in the north and early Pleistocene (< 1.9–1 Ma) in the south (Fig. 20A) in agreement with a SE-dipping structure of the Taitung remnant forearc trough.

7. Discussions: Analog comparisons of forearc sedimentation, stratigraphy and structure onshore and offshore eastern Taiwan

7.1. Characteristic distribution pattern of forearc stratigraphy onshore the Coastal Range

Detailed study on biostratigraphy show that the lower sequence unit S-1 (6.5–5.8 Ma) can only be found in the Lichi Mélange west of the Tuluanshan fault, whiles the middle sequence unit S-2 (5.8–3.0 Ma) can be found either in the Lichi Mélange west of the Tuluanshan fault or in the remnant forearc troughs (the lower coherent flysch sequences of the Fanshuliao Formation) east of the Tuluanshan fault (Fig. 5). However in the both sides of the Tuluanshan fault, filed occurrences of the middle sequence unit S-2 are highly contrast in spatial distribution. For example, the width of the Lichi Mélange exposures (sequence units S-1 + S-2; 6.5–3.0 Ma) in the footwall side of the Tuluanshan fault system decreases northward from 5 km wide in the southernmost Coastal Range, to < 2 km wide (only part of the sequence unit S-2; 4.4–3.4 Ma) in the middle Coastal Range, and is almost unnoticed in the northern Coastal Range (Fig. 3). In contrast, the sequence unit S-2 (5.8–3.0 Ma; coherent Fanshuliao Formation) in the hanging wall side of the Tuluanshan fault system exposed widely in the Suilien remnant forearc trough of the northern Coastal Range (section B-B′, Fig. 3), but only upper part of the same sequence unit S-2 was mapped in the middle (3.4–3.0 Ma; Loho remnant forearc trough; section D-D′ in Fig. 3B) and southern (Taiyuan remnant forearc trough; 3.9–3.7 Ma; section F-F′ in Fig. 3B) Coastal Range, and was almost insignificantly in the Taitung remnant forearc trough of the southernmost Coastal Range (section F-F′ in Fig. 3B). This suggests that the sequence unit S-2 in remnant forearc troughs represents the deformation relicts of the sequence unit S-2 of the Lichi Mélange. Consequently, the wider Lichi Mélange exposes west of the Tuluanshan fault, while the narrower the sequence unit S-2 of the Fanshuliao Formation occurs in the remnant forearc troughs east of the

Tuluanshan fault (Fig. 14H).

The youngest sequence unit S-3 (Paliwan Formation, < 3–1 Ma) is only exposed in remnant forearc troughs east of, and unconformably overlying, the middle sequence unit S-2 (Fanshuliao Formation). Such a characteristic distribution pattern suggests that the youngest sequence unit S-3 was juxtaposed unconformably east of the deformed middle sequence unit S-2, presumably by east-vergent backthrusting to develop as the Pliocene Loho Forearc Ridge analog to the modern Huatung Ridge offshore (Fig. 14F–G). Therefore, the youngest sequence unit S-3 overlies upon the middle unit S-2 unconformably along UB (Fig. 14F–G). This unconformity is clearly shown by the age gap, paleobathymetric change and the channel cutting between the Fanshuliao Formation (sequence unit S-2) and the overlying Suilien Conglomerate (sequence unit S-3) of the Paliwan Formation (section A-A′ in Fig. 3B). However, the unconformity UB could have been disturbed by the westward thrusting during the development of the highly sheared Lichi Mélange when the forearc sequences were obducted in the last 1 Ma.

The temporal-spatial variations of strata distribution together with unusual deformation of young-thrust-old character result in the fundamental features of forearc geology onshore the Coastal Range: The oldest stratigraphic unit with the most intensive deformation occur restrictedly in the western Coastal Range, whiles the middle and the youngest stratigraphic units with mild deformation crop out in the center and eastern part of the Coastal Range, respectively, a scenario analog to the modern oblique collision zone offshore SE Taiwan (Fig. 14).

7.2. Comparable forearc sedimentation, stratigraphy and deformation onshore and offshore eastern Taiwan

Forearc geology onshore the Coastal Range reviewed and discussed above demonstrates that the sedimentation, deformation processes and stratigraphy onshore the obduction zone (green line square in Fig. 14a–d–E–G) are analog to what presently occur in the active oblique collision zone (black line square in Fig. 14a–d–e–g) offshore SE Taiwan (Fig. 14). They are all characterized by *syn*-sedimentation deformation, shifting of depocenter from west to east in response to the active bivergent thrusting during the collision, juxtaposition of three mega-sequences bounded by two unconformities, and occurrence of a deformed forearc ridge pop-up as a bathymetric high in the junction between two clockwise-rotated volcanic islands to cause temporal-spatial variations of the sedimentation of the younger sequence. The similarity of forearc sedimentation and deformation processes allows us to construct the structural evolution of the entire North Luzon Trough forearc basin north of 20°N in the last 6.5 Ma from subduction to collision and obduction (Fig. 28). However, due to a southward propagation of the oblique convergent tectonics in the Taiwan region (Suppe, 1984), the tectonic processes are diachronously, early in the north but late in south (Fig. 28). In the following discussion, the sequence units S-1, S-2, and S-3 stand for the respective forearc succession accreted onshore the Coastal Range north of 22°40′N, whiles mega-sequence units M-A, M-B and M-C are the forearc stratigraphy revealed in seismic profiles across the active oblique convergent region offshore SE Taiwan (Fig. 28):

(1) Forearc basin was floored by eruptive volcanic agglomerates in 17–6.5 Ma. A west-dipping backthrust fault might develop in the rear accretionary pris along the arc-prism boundary (Fig. 28a);
(2) Forearc sedimentation of sequence unit S-1 started from 6.5 Ma when accretionary prism exposed above sea-level (Fig. 28b). Sequence unit S-1 spreads over the whole forearc basin. Therefore sequence unit S-1 (in the northern subduction zone) north of 22°40′N is equivalent to the mega-sequence unit M-A (in the southern subduction zone) south of 22°40′N. When the sequence unit S-1 (6.5–5.8 Ma) was deposited in the western forearc basin of the subduction zone, it was deformed simutaneously by west-vergent thrusting along arc-prism boundary as an early east-dipping forearc ridge (Fig. 28b), while sedimentation continued in the southern subduction zone without significant west-vergent thrusting (Fig. 28b);
(3) Sequence unit S-2 (6.5–3.0 Ma) laps westward upon the deformed early east-dipping ridge of the sequence unit S-1 along the unconformity UA in the north (Fig. 28c). During the late sedimentation of the mega-sequence unit M-A (~5.8 Ma) south of 22°40′N, forearc strata were deformed as an east-dipping ridge by west-vergent thrusting along arc-prism boundary (Fig. 28c). It was then lapped by the overlying the mega-sequence unit M-B lapping westward upon the deformed the mega-sequence unit M-A along MSB south of 22°40′N (Fig. 18c);
(4) When the volcanic arc collided with the accretionary prism, forearc strata of the sequence units S-1 and S-2 were deformed by east-vergent thrusting (Fig. 28d) to develop the Loho Forearc Ridge pop-up as a bathymetric high in the collision zone north of 22°40′N at ~3 Ma (LFR in Fig. 28d). In the meantime, sedimentation of the mega-sequence unit M-B (5.8–1 Ma) continued in the subduction zone south of 22°40′N;
(5) When the collision tectonics propagated southward, the sequence unit S-3 (< 3.0–1 Ma) covered the deformed Loho Forearc Ridge along unconformity UB in the northern collision zone north of 22°40′N (< 3–1 Ma; Fig. 28e). A new phase of east-vergent backthrusting started to cut through the mega-sequence units M-A and M-B in the southern collision zone (22°40′N-21°210′N) during late sediment of the sequence unit M-B (Fig. 28e). Sedimentation continued in the subduction zone south of 21°210′N (Fig. 28e);
(6) During the obduction in the last 1 Ma, forearc strata (S-1, S-2 and S-3) and their arc basement in the north were thrusted westward onto the accretionary prism to form the modern Coastal Range in eastern Taiwan north of 22°40′N (Fig. 28f and g);
(7) Bivergent thrusting of forearc mega-sequence units M-A and M-B led to the development of the modern Huatung Ridge in the collision zone (22°40′N-21°210′N) at ~1 Ma (Fig. 28f), and then covered by the youngest mega-sequence unit M-C unconformably along U-HTR (Fig. 28g). South of 21°20′N sedimentation of the mega-sequence unit M-B continued in the modern subduction zone (Fig. 28g).

8. Development of the modern-forming forearc Lichi Mélange

8.1. The mechanism and processes responsible for development of the Lichi Mélange

Any model proposed to interpret the mechanism and processes responsible for the formation of the Lichi Mélange onshore the Coastal Range, eastern Taiwan, should not ignore the basic and fundament issues of temporal-spatial pattern of the forearc stratigraphy and the processes of bivergent thrusting discussed in Section 7. Based on our understanding of the forearc deformation and dynamic stratigraphy of the North Luzon Trough in the last 6.5 Ma, we prefer a tectonic collision mechanism responsible for developments of the Lichi Mélange as shown in Figs. 14H and 28g.

During the obduction in the last 1 Ma the deep-sea forearc strata (6.5–1 Ma) and their arc basements offshore were thrust westward along the east-dipping thrust faults onto the accretionary prism to give the birth of the Coastal Range in eastern Taiwan north of 22°40′N (Fig. 28g). These east-dipping thrust faults propagated westward (Fig. 14H). The Longitudinal Valley fault marks the frontal obduction fault (Fig. 5). The obduction in the last 1 Ma also results in the development of uncommon thrust structure that the young sequence mega-sequence unit S-3 (< 3–1 Ma, Paliwan Formation) in the east thrusts westward over the old and bivergent thrust sequences units S-1 and S-2 (Lichi Mélange, 6.5–3.0 Ma) in the west (Fig. 3B).

Consequently, the deformation processes of the forearc strata onshore the Coastal Range have experienced multiple stages of thrusting processes. The western forearc strata were first deformed by west-vergent thrusting over the accretionary prism since the early sedimentation during late subduction in 6.5–5.8 Ma. It was then followed by bivergent thrusting in 5.8–3.0 Ma during the collision ad finally westward thrusting again during the obduction in the last 1 Ma (Fig. 28). Due to multiple stages of deformation with contrast vergence of thrusting from subduction through collision to obduction, the sequence units S-1 and S-2 north of 22°40′N in the western forearc basin were intensively thrust and sheared with emplacements of SSZ blocks as the Lichi Mélange in the western Coastal Range (Figs. 14H, 28g).

The analog comparison between onshore and offshore forearc geology (Fig. 14) also predicts that the modern Huatung Ridge in the active collision zone offshore would become the next extension of the Lichi Mélange in the future when the obduction tectonics propagates further southward to the modern collision zone in the next million years.

8.2. Age and origin of the mafic- and ultra-mafic blocks in the Lichi Mélange inferring the initiation of the South China Sea subduction

The origin of the mafic- to ultra-mafic blocks in the Lichi Mélange has long been interpreted controversially as either of the South China Sea (Suppe, 1984; Jahn, 1986; Chung and Sun, 1992) or the Luzon arc (Juan et al., 1980; Chen, 1988). Whatever geochemistry tools used to interpret the origin of these mafic- and ultra-mafic blocks in the Lichi Mélange, they are not of a huge oceanic crust-mantle block with complete ophiolite sequence, but pieces (cm to tens meter wide) of highly sheared dismembered blocks of oceanic crust and upper mantel rocks together with andesitic agglomerates and tuff blocks of the arc origin (Hsu, 1956, 1976; Liou et al., 1977; Juan et al., 1980; Page and Suppe, 1981; Barrier and Muller, 1984; Chen, 1988). These blocks are enclosed in highly sheared scaly argillaceous matrix (mélange facies) with preferred orientation of the forearc sequence units S-1 (6.5–5.8 Ma) or S-2 (6.5–3.0 Ma). Significance of these andesite and giant tuff blocks of the Luzon arc origin, which occurred with the mafic- and ultra-mafic blocks in nearby outcrops in the Lichi Mélange, was ignored by olistostromal geologists. If the mafic- and ultra-mafic blocks were of the South China Sea origin, how could the South China Sea oceanic blocks west of the accretionary prism together with the andesitic agglomerate and tuff blocks of the Luzon arc east of the accretionary prism be emplaced into the forearc Lichi Mélange in a same geologic event (~1 Ma) by a same geological process? Intensive geological surveys including petroleum explorations of hundreds of industry wells and ODP-IODP drillings (Legs 184; Wang et al., 2000; IODP Expedition 349 Scientists, 2014) in the last 6 decades did not find any andesite rocks from the South China Sea. They were neither find in the Central Range accretionary prism onshore Taiwan. Thus, they could only be emplaced tectonically from the arc or arc-related oceanic environment (Huang et al., 2008).

Various ages of the mafic blocks in the Lichi Mélange have been dated previously. By using K-Ar dating method, Jahn (1986) confirmed Miocene age for the mafic blocks in the Lichi Mélange (plagiogranite: 33 ± 5 Ma; gabbro: 11 ± 4 Ma; glassy basalt: 14.6 ± 0.4 Ma) collected from the Kuanshan district in the western Coastal Range (Fig. 3). We determine ages of zircon grains separated from a plagiogranite and a gabbro block in the Lichi Mélange along the Chiawu-Chi section east of Kuanshan village to be 17.21 ± 0.32 Ma and 17.34 ± 0.35 Ma, respectively (Fig. 29) using SIMS mechanism installed in the Institute of Geology and Geophysics, Chinese Academy of Sciences, in Beijing. The age is close to the earliest volcanism age recorded in the Lanyu volcanic island of the North Luzon arc by a study of calcareous nannoplanktons (NN3, 18–17 Ma, Chi and Suppe, 1985) in the red matrix of volcanic agglomerates. In the Lichi Mélange the plagiogranite and gabbro blocks are believed to be underlying the "red shale" in which calcareous nannoplanktons of Zone NN5 (14.3–13.5 Ma; Anthonissen and Ogg, 2012) were found (Huang et al., 1979). We regard the mafic- to ultra-mafic blocks in the Lichi Mélange are of subduction-related SSZ blocks (Pearce et al., 1984; Dilek and Furnes, 2011) originated from the North Luzon arc or from of a short-lived spreading oceanic rocks of the North Luzon Trough forearc basin, like the Mariana basin (Pearce, 2003), when the South China Sea subducted initially beneath the Huatung Basin/Philippine Sea Plate in Late Early Miocene at ~18 Ma (Fig. 30).

8.3. Why no backthrust fault was mapped in the Coastal Range?

According the analog comparisons between onshore and offshore forearc geology, east-vergent backthrust faults should commonly be observed in the sequence unit S-2 (the Lichi Mélange or the Fanshuliao Formation in the Suilien remnant forearc trough; Fig. 14E–H). Backthrust faults had been documented within the Lichi Mélange (Fig. 3 in Chang et al., 2000; Figs. 6 and 8 in Chang et al., 2001). But they were never recognized in the Suilien remnant forearc trough where the middle sequence unit S-2 (the Fanshuliao Formation) is widely exposed (Hsu, 1956; Wang and Chen, 1993). The failure to recognize backthrust faults in the Fanshuliao Formation of the Suilien remnant forearc trough could either be re-activated as west-dipping thrust faults during the obduction in the last 1 Ma, or be further disturbed as broken formation without discernible stratification during the obduction. Our surveys in the Suilien remnant forearc trough did find wide intervals of broken formation repeatedly in the Fanshuliao Formation of the northern Coastal Range (each 50–300 m wide; Figs. 21A and 22B).

9. Conclusions and 2-D tectonic evolution of the North Luzon Trough forearc basin since Early Miocene

Integrating marine geology off southern Taiwan and the North Luzon Trough forearc sedimentation and structure development, tectonic evolution onshore and offshore eastern Taiwan since the early Miocene can be depicted as follows (Fig. 30):

1) The SCS oceanic lithosphere spreaded in Late Oligocene-Early Miocene (33 Ma–16 Ma; Taylor and Hayes, 1983; Li et al., 2014). The SCS oceanic lithosphere contacted the Huatung Basin/Philippine Sea Plate oceanic lithosphere along a transform fault (Fig. 30A);
2) Initial subduction of the South China Sea oceanic lithosphere beneath the Huatung Basin/Philippine Sea Plate started from Late Early Miocene (18 Ma; Fig. 29B). The subduction might lead to formation of a new small oceanic lithosphere by forearc spreading in the upper plate like the modern Mariana forearc basin (Fig. 29B; Bloomer et al., 1995; Pearce, 2003; Stern, 2004);
3) New forearc spreading was followed by the earliest volcanism of the North Luzon Arc (18–17 Ma) recorded in the Lanyu Volcanic Island (Chi and Suppe, 1985). The Eurasian continental margin sequences were scraped off into the Hengchun Ridge accretionary prism in Early Middle Miocene (Fig. 29C; Huang et al., 1997);
4) The subduction and volcanism continued until the incipient oblique collision between the Luzon Arc and the eastward-subducting Eurasian continent in Late Miocene at ~6.5 Ma (Huang et al., 1997, 2000; Lin et al., 2003). Between 18 and 6.5 Ma the North Luzon Trough forearc basin was floored by eruptive volcanic agglomerates (Tuluanshan Formation) during intra-oceanic subduction (Fig. 29D);
5) The accretion of the SCS sediments into the accretionary prism together with an oblique arc-continent collision starting from 6.5 Ma led to an initiation of exhumation (0.65–1.28 mm/year) of the Central Range accretionary prism above sea-level as the proto-Taiwan Island (Fig. 29E; Lee et al., 2006). Sub-aerial erosions of the proto-Taiwan Island provided sediments transporting eastward to the North Luzon Trough forearc basin and westward to the foreland basin (Fig. 29E; Chen et al., 2017);
6) The forearc sequences (6.5–1 Ma) were deformed by bivergent thrusting during the sedimentation. Syn-sedimentation deformation

by bivergent thrusting gave rise to a juxtaposition of forearc sequence stratigraphy bounded by unconformity (Fig. 29F);

7) During obduction in the last 1 Ma, various blocks including SSZ mafic (17 Ma) and ultra-mafic rocks of forearc spreading oceanic crust-mantle origin or crust-mantle arc origin, and agglomerates with tuff of the Luzon arc origin were emplaced tectonically westward into the deformed forearc ridge to become the modern-forming collision forearc Lichi Mélange (6.5–3.0 Ma) in the western Coastal Range (Fig. 29g). The obduction in the last 1 Ma led to unexpected high exhumation rate of the Central Range accretionary prism (up to 10 mm/year; Lee et al., 2006);
8) Physical erosions by rivers and coastal waves and currents further eroded the relative thin coherent flysch sequences and exposed the Lichi Mélange below the decollement fault west of the Tuluanshan fault in the southern Coastal Range (Fig. 29g) and as tectonic windows east of the Tuluanshan fault in the middle and southernmost Coastal Range (Figs. 20 and 24).

Acknowledgements

The authors thank PinXian Wang of the Tongji University, Shanghai, Chengshan Wang of the China University of Geosciences, Beijing, and Dou-Fu Chen of the Shanghai Ocean University in Shanghai, China, for their constructive discussions during the study. We also appreciate two reviewers for constructive comments. This study is supported by grants from the National Natural Science Foundation of China (41472093, U1505231, 91528301) and from the Guangzhou Marine Geological Survey, China (20161972, DD20160138-01) to C.Y. Huang.

References

Anthonissen, D.E., Ogg, J.G., 2012. Cenozoic and Cretaceous biochronology of planktonic foraminifera and calcareous nannofossils. In: Gradstein, F.M. (Ed.), (Appendix 3) The Geological Time Scale, 2012. Elsevier, Boston, Mass, pp. 1083–1127.
Barrier, E., Muller, C., 1984. New observations and discussion on the origin and age of the Lichi Mélange. Mem. Geol. Soc. China 6, 303–325.
Beaumont, C., Ellis, S., Hamilton, J., Fullsck, P., 1996. Mechanical model for subduction-collision tectonics of alpine-type compressional orogens. Geology 24, 675–678.
Berggren, W.A., Hilgen, F.J., Langereis, C.G., Kent, D.V., Obradovich, J.D., Raffi, I., Raymo, M.E., Shackleton, N.J., 1995. Late Neogene chronology: new perspectives in high-resolution stratigraphy. Geol. Soc. Am. Bull. 107, 1272–1287.
Bloomer, S.H., Taylor, B., MacLeod, C.J., Stern, R.J., Fryer, P., Hawkins, J.W., Johnsoon, L., 1995. Early arc volcanism and the ophiolite problem: a perspective from drilling in the Western Pacific. Am. Geophys. Union Geophys. Monogr. 88, 1–30.
Blow, W.H., 1969. Late Middle Eocene to Recent planktonic foraminiferal biostratigraphy. In: Bronnimann, P., Renz, H. (Eds.), The First International Conference on Planktonic Microfossils, Geneva 1967. 1. pp. 199–421.
Brink, U.S.T., Marshak, S., Bruña, J.G., 2009. Bivergent thrust wedges surrounding oceanic island arc: insight from observations and sandbox models of the northeastern Caribbean plate. Geol. Soc. Am. Bull. 121, 1522–1536. http://dx.doi.org/10.1130/b26512.1.
Byrne, T., 1998. Pre-collision kinematics and a possible modern analog for the Lichi and Kenting Mélanges, Taiwan. J. Geol. Soc. China 41, 535–550.
Chang, L.S., 1967a. Tertiary biostratigraphy of Taiwan and its correlation. In: Kotora, Hatai (Ed.), Tertiary Correlations and Climatic Changes in the Pacific. Tokyo, pp. 57–65.
Chang, L.S., 1967b. A biostratigraphic study of the Tertiary in the Coastal Range, eastern Taiwan, based on smaller foraminifera (I: Southern part). Proc. Geol. Soc. China 10, 64–76.
Chang, L.S., 1968. A biostratigraphic study of the Tertiary in the Coastal Range, eastern Taiwan, based on smaller foraminifera (II. Northern part). Proc. Geol. Soc. China 11, 19–33.
Chang, L.S., 1969. A biostratigraphic study of the Tertiary in the Coastal Range, eastern Taiwan, based on smaller foraminifera (III: Middle part). Proc. Geol. Soc. China 12, 89–101.
Chang, L.S., 1975. Biostratigraphy of Taiwan. Geol. Paleontol. SE Asia 15, 337–361.
Chang, L.S., Chen, T.H., 1970. A biostratigraphic study of the Tertiary along the Hsiukuluan-Chi in the Coastal Range, eastern Taiwan, based on smaller foraminifera. Proc. Geol. Soc. China 13, 115–128.
Chang, C.P., Angelier, J., Huang, C.Y., 2000. Origin and evolution of a mélange: the active plate boundary and suture zone of the Longitudinal Valley, Taiwan. Tectonophysics 325, 43–62.
Chang, C.P., Angelier, J., Huang, C.Y., Liu, C.S., 2001. Structural evolution and significance of a mélange in a collision belt: the Lichi Mélange and the Taiwan arc-continent collision. Geol. Mag. 138, 633–651.
Chen, C.H., 1988. Mineral compositions of primary phases in ultramafic rocks in the Coastal Range and implication of source region of these rocks. Acta Geol. Taiwan. 26, 193–222.
Chen, M.P., Juang, W.S., 1986. Seafloor physiography off southeastern Taiwan. Acta Oceanogr. Taiwan. 16, 1–7.
Chen, C.H., Shieh, Y.C., Lee, T., Chen, C.H., Mertzman, S.A., 1990. Nd-Sr-O isotopic evidence for source contamination and an unusual mantle component under Luzon Arc. Geochim. Cosmochim. Acta 54, 2473–2483.
Chen, W.H., Huang, C.Y., Lin, Y.J., Zhao, Q., Yan, Y., Chen, D., Zhang, X., Lan, Q., Yu, M., 2015. Depleted deep South China Sea $\delta^{13}C$ paleoceanographic events in response to tectonic evolution in Taiwan–Luzon Strait since Middle Miocene. Deep-Sea Res. II. http://dx.doi.org/10.1016/j.dsr2.2015.02.005.
Chen, W.H., Huang, C.Y., Yan, Y., 2017. Stratigraphy and provenance of forearc sequences in the Lichi Mélange, Coastal Range: geological records of active Taiwan oblique arc-continent collision. J. Geophys. Res. Solid Earth 122. http://dx.doi.org/10.1002/2017JBO14378.
Cheng, W.B., Wang, C., 2001. Seismogenic zones in the convergent margin, eastern Taiwan and its implications in the Luzon forearc deformation. Terr. Atmos. Ocean. Sci. 12, 269–286.
Chi, W.R., Suppe, J., 1985. Tectonic implications of Miocene sediments of Lan-Hsu Island, North Luzon arc. Pet. Geol. Taiwan 21, 93–106.
Chi, W.R., Namson, J., Suppe, J., 1981. Stratigraphic record of plate interactions in the Coastal Range of eastern Taiwan. Mem. Geol. Soc. China 4, 155–194.
Chi, W.C., Reed, D.L., Moore, G., Nguyen, T., Liu, C.S., Lundberg, N., 2003. Tectonic wedging along the rear of the offshore Taiwan accretionary prism. Tectonophysics 374, 199–217. http://dx.doi.org/10.1016/j.tecto.2003.08.004.
Chi, W.C., Chen, L., Liu, C.S., Brookfield, M., 2014. Development of arc-continent collision mélanges: linking onshore geological and offshore geophysical observation of the Pliocene Lichi Mélange, southern Taiwan and northern Luzon arc, western Pacific. Tectonophysics 636, 70–82. http://dx.doi.org/10.1016/j.tecto.2014.08.009.
Chung, S.L., Sun, S.S., 1992. A new genetic model for the East Taiwan Ophiolite and its implications for dual domains in the Northern Hemisphere. Earth Planet. Sci. Lett. 109, 133–145.
Dilek, Y., Furnes, H., 2011. Ophiolite genesis and global tectonics: geochemical and tectonic fingerprinting of ancient oceanic lithosphere. Bull. Geol. Soc. Am. 123, 387–411. http://dx.doi.org/10.1130/B30446.1.
Dorsey, R.J., 1988. Provenance evolution and un-roofing history of a modern arc-continent collision: evidence from petrography of Plio-Pleistocene sandstones, eastern Taiwan. J. Sediment. Petrol. 58, 208–218.
Dorsey, R.J., Lundberg, N., 1988. Lithofacies analysis and basin reconstruction of the Plio-Pleistocene collisional basin, Coastal Range of eastern Taiwan. Acta Geol. Taiwan. 26, 57–132.
Harris, R.A., 1991. Temporal distribution of strain in the active Banda orogen: a reconciliation of rival hypothesis. In: Hall, R., Nichols, G., Rangin, C. (Eds.), Orogensis in Action. J. Southeast Asian Earth Sci. 6. pp. 373–386.
Harris, R.A., 2011. The nature of the Banda Arc-continent collision in the Timor region. In: Brown, D., Ryan, P.D. (Eds.), Arc Continent Collision, Frontiers in Earth Sciences. Springer Verlag, Berlin Heidelberg. http://dx.doi.org/10.1007/97835408855807.
Harris, R.A., Huang, C.Y., 2008. Linking Mélange Types and Occurrences With Active Mélange-forming Process in Timor and Taiwan. 2010 Abstracts With Programs, Tectonic Crossroads: Evolving Orogens of Eurasia-Africa-Arabia, Ankara, Turkey. pp. 84–85.
Harris, R.A., Sawyer, R.K., Audley-Charles, M.G., 1998. Collisional mélange development: geologic associations of active mélange-forming processes with exhumed mélange facies in the western Banda orogen: Indonesia. Tectonics 17, 458–480.
Hirtzel, J., Chi, W.C., Reed, D., Chen, L., Liu, C.S., Lundberg, N., 2009. Destruction of Luzon forearc basin from subduction to Taiwan arc-continent collision. Tectonophysics 479, 43–51. http://dx.doi.org/10.1016/j.tecto.2009.01.032.
Horng, C.S., Shea, K.S., 1996. Dating of the Plio-Pleistocene rapidly deposited sequence based on integrated magneto-biostratigraphy: a case study of the Madagida-Chi section, Coastal Range, eastern Taiwan. J. Geol. Soc. China 39, 31–58.
Hsu, T.L., 1956. Geology of the Coastal Range, eastern Taiwan. Bull. Geol. Surv. Taiwan 8, 39–64.
Hsu, K.J., 1968. Principles of mélanges and their bearing on the Franciscan-Knoxville paradox. Geol. Soc. Am. Bull. 79, 1063–1074.
Hsu, T.L., 1976. The Lichi Mélange in the Coastal Range framework. Bull. Geol. Surv. Taiwan 25, 87–95.
Huang, T., 1969. Some planktonic foraminiferous from a bore at Shihshan, near Taitung, Taiwan. Proc. Geol. Soc. China 12, 103–119.
Huang, C.Y., 1988. Evidence of the Pliocene Arc Subsidence in the Coastal Range, Eastern Taiwan. Proceedings of the Second Symposium on Geophysics, Taipei. pp. 364–373.
Huang, C.Y., 1993. Bathymetric ridges and troughs in the active arc-continent collision region off southeastern Taiwan: reply and discussions. J. Geol. Soc. China 36, 91–109.
Huang, C.Y., 2008. Mechanism and consequence of forearc back-thrusting in formation of Lichi Mélange in Coastal Range, eastern Taiwan. In: 2010 Abstracts with Programs, Tectonic Crossroads: Evolving Orogens of Eurasia-Africa-Arabia, Ankara, Turkey, pp. 84–85.
Huang, C.Y., Yin, Y.C., 1990. Bathymetric ridges and troughs in the active arc-continent collision region off southeastern Taiwan. Proc. Geol. Soc. China 33, 351–372.
Huang, C.Y., Yuan, P.B., 1994. Stratigraphy of the Kangkou Limestone in the Coastal Range, eastern Taiwan. J. Geol. Soc. China 37, 585–605.
Huang, T.C., Chen, M.P., Chi, W.R., 1979. Calcareous nannofossils from the red shale of the ophiolite-mélange complex, eastern Taiwan. Mem. Geol. Soc. China 3, 131–138.
Huang, C.Y., Yuan, P.B., Teng, L.S., 1988. Paleontology of the Kangkou Limestone in the middle Coastal Range, eastern Taiwan. Acta Geol. Taiwan. 26, 133–160.
Huang, C.Y., Shyu, C.T., Lin, S.B., Lee, T.Q., Sheu, D.D., 1992. Marine geology in the arc-

continent collision zone off southeastern Taiwan: implications for late Neogene evolution of the Coastal Range. Mar. Geol. 107, 183–212.
Huang, C.Y., Yuan, P.B., Song, S.R., Lin, C.W., Wang, C., Chen, M.T., Shyu, C.T., Karp, B., 1995. Tectonics of short-lived intra-arc basins in the arc-continent collision terrane of the Coastal Range, eastern Taiwan. Tectonics 14, 19–38.
Huang, C.Y., Wu, W.Y., Chang, C.P., Tsao, S., Yuan, P.B., Lin, C.W., Xia, K.Y., 1997. Tectonic evolution of accretionary prism in the arc-continent collision terrane of Taiwan. Tectonophysics 281, 31–51.
Huang, C.Y., Yuan, P.B., Lin, C.W., Wang, T.K., 2000. Geodynamic processes of Taiwan arc-continent collision and comparison with analogs in Timor, Papua New Guinea, Urals and Corsica. Tectonophysics 325, 1–21.
Huang, C.Y., Xia, K., Yuan, P.B., Chen, P.Y., 2001. Structural evolution from Paleogene extension to Latest Miocene-Recent arc-continent collision offshore Taiwan: comparison with on land geology. J. Asian Earth Sci. 19, 619–639.
Huang, C.Y., Yuan, P.B., Tsao, S.J., 2006. Temporal and spatial records of active arc-continent in Taiwan: a synthesis. Geol. Soc. Am. Bull. 118, 274–288.
Huang, C.Y., Chien, C.W., Yao, B., Chang, C.P., 2008. The Lichi Mélange: a collision mélange formation along early arcward backthrusts during forearc basin closure, Taiwan arc-continent collision. In: Draut, A.E., Clift, P.D., Scholl, D.W. (Eds.), Formation and Applications of the Sedimentary Record in Arc Continent Collision Zone. Geol. Soc. Amer., Spec. Paper 436, pp. 127–154. http://dx.doi.org/10.1130/2008.2436(06).
Huang, C.Y., Yen, Y., Zhao, Q., Lin, C.T., 2012. Cenozoic stratigraphy of Taiwan: window into rifting, stratigraphy and paleoceanography of South China Sea. Chin. Sci. Bull. 57, 3130–3149. http://dx.doi.org/10.1007/s11434-012-5349-y.
Huang, C.Y., Li, X., Zhao, X., Yang, K.M., Yang, S., 2018. Syn-sedimentation bivergent deformation and dynamic stratigraphy of the North Trough forearc basin in active oblique convergent region offshore SE Taiwan. (Submitted to *Mari.Geol.*).
Jahn, B.M., 1986. Mid-ocean ridge or marginal basin origin of the East Taiwan Ophiolite: chemical and isotopic evidence. Contrib. Mineral. Petrol. 92, 194–206.
Juan, V.C., Lo, H.J., Chen, C.H., 1980. Genetic relationship and the emplacement of the exotic basic rocks enclosed in the Lichi mélange, Coastal Range, east Taiwan. Proc. Geol. Soc. China 23, 56–68.
Kao, H., Huang, G.C., 2000. Transition from oblique subduction to collision in the northern Luzon arc-Taiwan region: constraints from bathymetry and seismic observations. J. Geophys. Res. 105, 3059–3079.
Lallemand, S.E., Liu, C.S., Font, Y., 1997. A tear fault boundary between the Taiwan orogen and the Ryukyu subduction zone. Tectonophysics 274, 171–190.
Lee, T.Q., 1991. Paleomagnetic evidence for a diachronic clockwise rotation of the Coastal Range, eastern Taiwan. Earth Planet. Sci. Lett. 104, 245–257.
Lee, Y.H., Chen, C.C., Liu, T.K., Ho, H.C., Lu, H.Y., Lo, W., 2006. Mountain building mechanisms in the southern Central Range of the Taiwan orogenic belt – from accretionary wedge deformation to arc-continent collision. Earth Planet. Sci. Lett. 252, 413–422. http://dx.doi.org/10.1016/j.epsl.2006.09.047.
Lehu, R., Lallemand, S., Hsu, S.K., Baronneau, N., Ratzov, G., Lin, A.T., Dezileau, L., 2015. Deep-sea sedimentation offshore eastern Taiwan: facies and processes characterization. Mar. Geol. 369, 1–15. http://dx.doi.org/10.1016/j.margeo.2015.05.013.
Lewis, J.C., O'Hara, D.J., Rau, R.-J., 2015. Seismogenic strain across the transition from fore-arc slivering to collision in southern Taiwan. J. Geophys. Res. Solid Earth 120, 4539–4555. http://dx.doi.org/10.1002/2015JB011906.
Li, C.F., Xu, X., Lin, J., Sun, Z., Zhu, J., Yao, Y., Zhao, X., Liu, Q., Kulhanek, D., Wang, J., Song, T., Zhao, J., Qiu, N., Guan, Y., Zhou, Z., Expedition 349 Scientists, 2014. Ages and magnetic structures of the South China Sea basin constrained by deep to magnetic surveys and IODP Expedition 349. Geochem. Geophys. Geosyst. 15, 4958–4983. http://dx.doi.org/10.1002/2014GC005567.
Li, C.F., Zhou, Z.Y., Li, J.B., Chen, H.J., Geng, J.H., Li, H., 2007. Precollisional tectonics and terrain amalgamation offshore southern Taiwan: Characterizations from reflection seismic and potential field data. Sci. China Ser. D Earth Sci. 50, 897–908. http://dx.doi.org/10.1007/s11430-007-0025-9.
Lin, C.T., 2011a. Sedimentological Study on Pliocene Fan Delta and Pleistocene Deep-sea Fan Conglomerates in Forearc Basin of Coastal Range, Eastern Taiwan, During Active Arc-continent Collision. Mater Thesis. Institute of Earth Sciences, National Cheng Kung University, pp. 1–58 (in Chinese).
Lin, Y.C., 2011b. Evolution of the Loho Remnant Forearc Trough and Origin of the Lichi Mélange of the Coastal Range: Micropaleontological and Clay Mineral Evidences. Master Thesis. Institute of Earth Sciences, National Cheng Kung University, Tainan, Taiwan, pp. 1–72 (in Chinese).
Lin, C.W., Liu, Y.C., Lai, W.C., Cheng, W.H., 1999. Fault tectonics of the Coastal Range, eastern Taiwan. J. Geol. Soc. China 42, 429–446.
Lin, A.T., Watts, W., Hesselbo, S.P., 2003. Cenozoic stratigraphy and subsidence history of the South China Sea margin in the Taiwan region. Basin Res. 15, 453–478.
Lin, W.H., Lin, C.W., Liu, Y.C., Chen, P.T., 2008. Geological Map of Taitung and Jhihben, Sheet Map 59 and 64 (Scale 1:50,000). Central Geological Survey, MOEA, ROC.
Liou, J.G., Lan, C.Y., Ernst, W.G., 1977. The East Taiwan Ophiolite. Mining Res. Servi. Organ. (Taipei) Special Publication. 1. pp. 1–212.
Liu, C.S., Liu, S.Y., Lundberg, S.E.N., Reed, D.L., 1998. Digital elevation model offshore Taiwan and its tectonic implications. Terr. Atmos. Ocean. Sci. 9, 705–738.
Lo, C.H., Onstott, T.C., Chen, C.H., Lee, T., 1994. An assessment of $^{40}Ar/^{39}Ar$ dating for the whole-rock volcanic samples from the Luzon Arc near Taiwan. Chem. Geol. 114, 157–178.
Lundberg, N., Reed, D.L., Liu, C.S., Lieske Jr., J., 1992. Structural controls on orogenic sedimentation, submarine Taiwan collision. Acta Geol. Taiwan. 30, 131–140.
Lundberg, N., Reed, D.L., Liu, C.S., Lieske, J., 1997. Forearc-basin closure and arc accretion in the submarine suture zone south of Taiwan. Tectonophysics 274, 5–23.
Malavieille, J., Trullenique, G., 2009. Consequence of continental subduction on forearc basin and accretionary wedge deformation in SE Taiwan: insights from analogue modeling. Tectonophysics 466, 377–394. http://dx.doi.org/10.1016/j.tecto.2007.11.016.
Malavieille, J., Lallemand, S.E., Dominguez, S., Deschamps, A., Lu, C.Y., Liu, C.S., Schnürle, P., The ACT Scientific Crew, 2002. Arc-continent collision in Taiwan: New marine observations and tectonic evolution. In: Byrne, T.B., Liu, C.S. (Eds.), Geology and Geophysics of an Arc-continent Collision, Taiwan. Geol. Soc. Amer., Spec. Paper 358, pp. 187–211.
Martini, E., 1971. Standard Tertiary and Quaternary Calcareous Nannoplankton Zonation. Proceedings of 2nd International Planktonic Conference, Rome. pp. 739–785.
McIntosh, K., Nakamura, Y., Wang, T.K., Shih, R.C., Chen, A., Liu, C.S., 2005. Crustal-scale seismic profiles across Taiwan and the western Philippine Sea. Tectonophysics 401, 23–54.
Page, B.M., Suppe, J., 1981. The Pliocene Lichi Mélange of Taiwan: its plate-tectonic and olistostromal origin. Am. J. Sci. 281, 193–227.
Pearce, J.A., 2003. Subduction zone ophiolites. In: Dilek, Y., Newcomb, S. (Eds.), Ophiolite Concept and the Evolution of Geological Thought. Special Paper, Geol. Soc. Amer., Boulder. 2003. pp. 269–294.
Pearce, J.A., Lippard, S.J., Robert, S., 1984. Characteristics and tectonic significance of suprasubduction zone ophiolites. In: Kokelaar, B.P., Howell, M.F. (Eds.), Marginal Basin Geology. Geological Society (London) Special Publication. 16. pp. 77–94.
Raffi, I., Backman, J., Fornaciari, E., Palike, H., Rio, D., Lourens, L., Hilgen, F., 2006. A review of calcareous nannofossils astrobiochronology encompassing the past 25 million years. Quat. Sci. Rev. 25, 3113–3137. http://dx.doi.org/10.1016/j.quascirev.2006.07.007.
Raymond, L.A., 1984. Classification of mélanges. In: Raymond, L.A. (Ed.), Mélanges: Their Nature and Significance. Geological Society of America, Special Paper 198, pp. 7–20.
Reed, D.L., Silver, E.A., Prasetyo, H., Meyer, A.W., 1986. Deformation and sedimentation along a developing terrane suture: Sunda forearc, Indonesia. Geology 14, 1000–1003.
Reed, D.L., Lundberg, N., Liu, C.S., Kuok, B.Y., 1992. Structural relations along the margins of the offshore Taiwan accretionary wedge: implications for accretion and crustal kinematics. Acta Geol. Taiwan. 30, 105–122.
Sarkarinejad, K., Alizadeh, A., 2009. Dynamic model for the exhumation of the Tutak gneiss dome within a bivergent wedge in the Zagros thrust system of Iran. J. Geodyn. 47, 201–209.
Schnűrle, P., Liu, C.S., Lallemand, S., Reed, D., 1998. Structural controls of the Taitung Canyon in the Huatung Basin east of Taiwan. Terr. Atmos. Ocean. Sci. 9, 453–472.
Shyu, C.T., Chen, S.C., 1991. A topographic and magnetic analysis off southeastern Taiwan. Acta Oceanogr. Taiwan. 27, 1–20.
Silver, E.A., Reed, D.L., 1988. Backthrusting in accretionary wedges. J. Geophys. Res. 93, 3116–3126.
Song, S.R., Lo, H.J., Chen, W.S., 1994. Origin of clastic dikes in the Coastal Range, eastern Taiwan with implications for sedimentary processes during the arc-continent collision. J. Geol. Soc. China 37, 407–424.
Stern, R.J., 2004. Subduction initiation: spontaneous and induced. Earth Planet. Sci. Lett. 226, 275–292. http://dx.doi.org/10.1016/j.espi.2004.08.007.
Suppe, J., 1984. Kinematics of arc-continent collision, flipping of subduction, and back-arc spreading near Taiwan. Mem. Geol. Soc. China 6, 21–33.
Susilohadi, S., Gaedicke, C., Ehrhardt, A., 2005. Neogene structures and sedimentation history along the Sunda forearc basins off southwest Sumatra and southwest Java. Mar. Geol. 219, 133–154. http://dx.doi.org/10.1016/j.margeo.2005.05.001.
Taylor, B., Hayes, D.E., 1983. Origin and history of the South China Sea. In: Hayes, D.E. (Ed.), The Tectonic and Geologic Evolution of Southeast Seas and Islands (Pt. 2). Amer. Geophy. Union, Geophy. Monogr., 27, pp. 23–56.
Teng, L.S., 1979. Petrographical study of the Neogene sandstones of the Coastal Range, eastern Taiwan. Acta Geol. Taiwan. 20, 129–156.
Teng, L.S., 1982. Stratigraphy and sedimentation of the Suilien Conglomerate, northern Coastal Range, eastern Taiwan. Acta Geol. Taiwan. 21, 201–220.
Teng, L.S., Wang, Y., 1981. Island arc system of the Coastal Range, eastern Taiwan. Proc. Geol. Soc. China 24, 99–112.
Tian, J., Yang, Q., Liang, X., Xie, L., Hu, D., Wang, F., Qu, T., 2006. Observation of Luzon Strait transport. Geophys. Res. Lett. 33, L1960. http://dx.doi.org/10.1029/2006GL026272.
Torrini Jr., R., Speed, R., 1989. Tectonic wedging in the forearc basin-accretionary prism transition, Antilles forearc. J. Geophys. Res. 94, 10,549–10,584.
Tsai, Y.B., 1986. Seismotectonics of Taiwan. Tectonophysics 125, 17–37.
Tsai, Y.B., Liaw, Z.S., Lee, T.Q., Lin, M.T., Yeh, Y.H., 1981. Seismological evidence of an active plate boundary in the Taiwan area. Mem. Geol. Soc. China 4, 143–154.
Usami, M., 1939. Explanatory Text of the Geological Map of Taiwan, Karenko Sheet. Government General of Taiwan (no. 862).
Wade, B.S., Pearson, P.N., Berggren, W.A., Pälike, H., 2011. Review and revision of Cenozoic tropical planktonic foraminiferal biostratigraphy and calibration to the geomagnetic polarity and astronomical time scale. Earth-Sci. Rev. 104, 111–142. http://dx.doi.org/10.1016/j.earscirev.2010.09.003.
Walker, R.G., 1978. Deep-water sandstone facies and ancient submarine fans: models for exploration for stratigraphic traps. Am. Assoc. Pet. Geol. Bull. 62, 932–966.
Wang, C.S., 1976. The Lichi Formation of the Coastal Range and arc-continent collision in eastern Taiwan. Bull. Geol. Surv. Taiwan 25, 73–86.
Wang, C.S., Chen, T.T., 1966. Turbidite formations around the southern plunge of the Coastal Range near Taitung. Proc. Geol. Soc. China 9, 46–54.
Wang, Y., Chen, W.S., 1993. Geological Map of Eastern Coastal Range (Scale 1:100,000). Central Geological Survey, MOEA, Taiwan.
Wang, W.H., Davis, D.M., 1996. Sandbox model simulation of forearc evolution and noncritical wedges. J. Geophys. Res. *101*, 11,329–11,339.
Wang, C., Shao, X., Liu, Z., Lippert, P.C., Graham, S.A., Coe, R.S., Yi, H., 2008. Constraints

on the early uplift history of the Tibetan Plateau. Proc. Natl. Acad. Sci. U. S. A. 105, 4987–4992. http://dx.doi.org/10.1073/pnas.0703595105.
Wang, C., Li, X., Liu, Z., Li, Y., Jansa, L., Dai, J., Wei, Y., 2011. Revision of the Cretaceous–Paleogene stratigraphic framework, facies architecture and provenance of the Xigaze forearc basin along the Yarlung Zangbo suture zone. Gondwana Res. http://dx.doi.org/10.1016/j.gr.2011.09.014.
Wang, P., Prell, L., Blum, P. (Eds.), 2000. Proceeding ODP, Initial Reports, vol. 184 (CD-ROM). Ocean Drilling Program. Texas A&M University, College Station TX 77845-9547, USA.
Willet, S., Beaumont, C., Fullsack, P., 1993. Mechanical model for the tectonics of doubly vergent compressional orogens. Geology 21, 371–374.
Yabe, H., Hanzawa, S., 1929. Tertiary foraminiferal rocks of Taiwan (Formosa). Sci. Rep. Tohoku Imp. Univ. Ser. 2 (14), 1–46.
Yang, K.M., Wang, Y., Tsai, Y.B., Hsu, V., 1983. Paleomagnetic studies of the Coastal Range, Lutao and Lanhsu in eastern Taiwan and their tectonic implications. Academia Sinica, Inst. Earth. Sci. Bull. 3, 173–189.
Yang, T.F., Yeh, G.H., Fu, C.C., Wang, C.C., Lan, T.F., Lee, H.F., Chen, C.H., Walia, V., Sung, Q.C., 2004. Composition and exhalation flux of gases from mud volcanoes in Taiwan. Environ. Geol. 46, 1003–1011. http://dx.doi.org/10.1007/s00254-004-1086-0.
Yen, J.Y., Lundberg, N., 2006. Sediment compositions in offshore southern Taiwan and their relations to the source rocks in modern arc-continent collision zone. Mar. Geol. 225, 247–263. http://dx.doi.org/10.1016/j.margeo.2005.09.003.
Yu, S.B., Chen, H.K., Kuo, L.C., 1997. Velocity field GPS stations in Taiwan area. Tectonophysics 274, 41–59.
Yui, T.F., Okamoto, K., Usuko, T., Lan, C.Y., Chu, H.T., Liou, J.G., 2009. Late Triassic-Late Cretaceous accretion/subduction in the Taiwan region along the eastern margin of South China- evidence from zircon SHRIMP dating. Int. Geol. Rev. 51, 304–328. http://dx.doi.org/10.1080/00206810802636369.
Zhao, X., Huang, C.Y., Ren, H., Guo, J., Chen, W., Yuan, W., 2016. Paleomagnetic Evidence of Clockwise Rotation of the Lanyu Island of SE Taiwan Since the Late Pliocene: Abstract OS51C-2075 Presented at 2016 Fall Meeting, AGU, San Francisco, California, 12–16, December.